

SANDIA REPORT

SAND90-1206 • UC-721

Unlimited Release

Printed June 1991

Mechanical Compaction of Waste Isolation Pilot Plant Simulated Waste

B. M. Butcher, T. W. Thompson, R. G. VanBuskirk, N. C. Patti

Prepared by
Sandia National Laboratories
Albuquerque, New Mexico 87185 and Livermore, California 94550
for the United States Department of Energy
under Contract DE-AC04-76DP00789

Issued by Sandia National Laboratories, operated for the United States Department of Energy by Sandia Corporation.

NOTICE: This report was prepared as an account of work sponsored by an agency of the United States Government. Neither the United States Government nor any agency thereof, nor any of their employees, nor any of their contractors, subcontractors, or their employees, makes any warranty, express or implied, or assumes any legal liability or responsibility for the accuracy, completeness, or usefulness of any information, apparatus, product, or process disclosed, or represents that its use would not infringe privately owned rights. Reference herein to any specific commercial product, process, or service by trade name, trademark, manufacturer, or otherwise, does not necessarily constitute or imply its endorsement, recommendation, or favoring by the United States Government, any agency thereof or any of their contractors or subcontractors. The views and opinions expressed herein do not necessarily state or reflect those of the United States Government, any agency thereof or any of their contractors.

Printed in the United States of America. This report has been reproduced directly from the best available copy.

Available to DOE and DOE contractors from
Office of Scientific and Technical Information
PO Box 62
Oak Ridge, TN 37831
Prices available from (615) 576-8401, FTS 626-8401

Available to the public from
National Technical Information Service
US Department of Commerce
5285 Port Royal Rd
Springfield, VA 22161
NTIS price codes
Printed copy: A05
Microfiche copy: A01

SAND90-1206
Unlimited Release
Printed June 1991

Distribution
Category UC-721

MECHANICAL COMPACTION OF WASTE ISOLATION PILOT PLANT SIMULATED WASTE

B. M. Butcher
Sandia National Laboratories
Albuquerque, New Mexico 87185

T. W. Thompson, R. G. VanBuskirk, and N. C. Patti
Science Applications International Corporation,
Golden, Colorado

ABSTRACT

The investigation described in this report acquired experimental information about how materials simulating transuranic (TRU) waste compact under axial compressive stress, and used these data to define a model for use in the Waste Isolation Pilot Plant (WIPP) disposal room analyses. The first step was to determine compaction curves for various simulant materials characteristic of TRU waste. Stress-volume compaction curves for various combinations of these materials were then derived to represent the combustible, metallic, and sludge waste categories. Prediction of compaction response in this manner is considered essential for the WIPP program because of the difficulties inherent in working with real (radioactive) waste.

Next, full-sized 55-gallon drums of simulated combustible, metallic, and sludge waste were axially compacted. These results provided data that can be directly applied to room consolidation and data for comparison with the predictions obtained in Part I of the investigation. Good agreement was obtained between prediction and test results.

Finally, compaction curves, which represent the combustible, metallic, and sludge waste categories, were determined, and a curve for the averaged waste inventory of the entire repository was derived. The results for axial compaction of combustible and metallic waste were found to be consistent with the assumptions used to estimate the final mechanical state of a typical disposal room, initially made as supporting information for the Draft Supplemental Environmental Impact Statement for WIPP.

CONTENTS

1.0	INTRODUCTION	1
2.0	MATERIAL COMPACTION STUDIES	3
2.1	Objectives	3
2.2	Apparatus.....	4
2.3	Methods of Analysis.....	7
2.3.1	Analytic Representation of Compaction Curves	7
2.3.2	Estimation of Solid Densities.....	8
2.3.3	Correction for Time-Dependent Compaction.....	8
2.3.4	Composite Curves	12
2.4	Results.....	14
2.4.1	Cellulosics (Wood and Cloth)	14
2.4.2	Plastics	40
2.4.3	Metals.....	41
2.4.4	Sorbents.....	42
2.4.4.1	Dry Portland Cement	42
2.4.4.2	Vermiculite.....	43
2.4.4.3	Oil Dri.....	43
2.5	Moist Sand and Dry Cement	44
2.6	Composite Curve for Metallic and Combustible Waste	44
3.0	DRUM COMPACTION MEASUREMENTS	49
3.1	Objectives	49
3.2	Materials.....	49
3.3	Description of Analysis.....	50
3.3.1	Method of Interpretation of Results.....	50
3.3.2	Ring Formation in the Drums During Collapse.....	52
3.3.3	Drum Compaction Curves.....	53
3.4	Definition of Waste Material for the Drum Tests	55
3.5	Results.....	56
4.0	REPOSITORY COMPACTIBILITY	65
4.1	Method of Analysis.....	65
4.2	Repository Inventory.....	65
4.2.1	Metals Inventory.....	65
4.2.2	Combustibles Inventory.....	67
4.2.3	Sludge Inventory	67
4.2.4	Container Materials	67
4.2.5	Inventory Discrepancies	68
4.3	Repository Curves for Axial Drum Compaction.....	68

4.4	Repository Curves for Lateral Compaction of the Waste	71
4.4.1	The Influence of Shear Stress on Compaction.....	71
4.4.2	Closure of a Room Entirely Filled with Waste and Salt/Bentonite Backfill	72
4.4.3	Lateral Compaction of Drums	74
5.0	SUMMARY	77
6.0	REFERENCES	79
	APPENDIX A: The Average Initial Density of Waste in the Repository.....	A-1
	DISTRIBUTION.....	Dist-1

FIGURES

2-1	Oedometer set up for compaction testing	6
2-2	An example of the application of the power law relationship for sample consolidation with time, Equation 2.3.3.1, to data representing the change in density with time of a mixture of PVC, polyethylene parts, and surgical gloves under a constant axial stress of 13.8 MPa	11
2-3	An example of the application of the exponential relationship for sample consolidation with time, Equation 2.3.3.3, to data representing the change in density of a mixture of PVC, polyethylene parts, and surgical gloves under a constant axial stress of 13.8 MPa	13
2-4	Wood cubes and rags stress versus density curves	20
2-5	Wood cubes and rags stress versus porosity curves	21
2-6	Cellulosic compaction curve variability	22
2-7	PVC, polyethylene parts, and surgical gloves stress versus density curves	23
2-8	PVC, polyethylene parts, and surgical gloves stress versus porosity curves	24
2-9	Plastics compaction curve variability	25
2-10	Metal parts stress versus density curves	26
2-11	2.5 cm (1 inch) metal-parts stress versus porosity curves	27
2-12	7.6 cm (3 inch) metal-parts stress versus porosity curves	28
2-13	Metal parts compaction curves	29
2-14	Dry Portland cement stress versus density curves	30
2-15	Dry Portland cement stress versus porosity curves	31
2-16	Vermiculite stress versus density curves	32
2-17	Modified vermiculite stress versus density curves	33
2-18	Oil Dri [®] stress versus density curves	34
2-19	Modified Oil Dri [®] stress versus density curves	35

FIGURES

2-20	Compaction curves for sorbents	36
2-21	Moist sand and dry cement (sludge simulant) stress versus density curves	37
2-22	Modified moist sand and dry cement (sludge simulant) stress versus density curves	38
2-23	Composite compaction curve for combustible waste	46
2-24	Composite compaction curve for metallic waste.....	48
3-1	A comparison between experimental results showing the relationship between applied load and state of collapse of simulated combustible waste drums (4 tests) and predictions either assuming that the drum material is part of the waste or ignoring the drum completely	57
3-2	A comparison between experimental results showing the relationship between applied load and state of collapse of simulated metallic waste drums (4 tests) and predictions either assuming that the drum material is part of the waste or ignoring the drum completely	58
3-3	Recommended drum collapse curves for combustible, metallic, and simulated sludge wastes.....	60
3-4	Simulated sludge drum collapse curves	63
4-1	A comparison between the predicted compaction curve for all the waste in the WIPP repository and the recommended compaction curves for combustible, metallic, and simulated sludge wastes	70
4-2	Plane strain-finite element model of a TRU storage room.....	73
4-3	Predicted average void fraction-time history for waste in a room filled with TRU waste and 70% salt/30% bentonite backfill	75

TABLES

2-1	Simulated Waste Materials.....	5
2-2	Waste Solid Densities.....	9
2-3	Waste Densification with Time.....	12
2-4	Test Parameters and Results for Combustibles.....	15
2-5	Test Parameters and Results for Plastics.....	16
2-6	Test Parameters and Results for Metals.....	17
2-7	Test Parameters and Results for Sorbents.....	18
2-8	Test Parameters and Results for Simulated Sludge.....	19
2-9	Test Materials for Drum Collapse Tests.....	45
3-1	Drum Collapse Test Summary.....	51
3-2	Compaction Curves.....	61
4-1	TRU Waste Inventory Analysis.....	66

1.0 INTRODUCTION

A fundamental issue in evaluating performance of the Waste Isolation Pilot Plant (WIPP) facility near Carlsbad, NM, is the migration of fluids through the storage areas and the potential for dispersing radioactive materials in the event of human intrusion. The radioactive wastes to be stored in the WIPP consist of a variety of materials, including metals, combustibles (plastics and fibers), and "sludge." Unprocessed waste will be contained in 55-gallon drums (DOT-17C) or other containers such as standard waste boxes.

Most of the waste materials will initially have high porosities (or void volumes) and hence will be highly permeable if the waste remains unprocessed. However, over time the drums may be expected to collapse due to the closure of the rooms and the consequent loading of the containers. Under these conditions the contained materials will compact and cause a reduction in porosity and permeability (Butcher, 1989). These changes need to be defined as a function of time to evaluate the performance of the repository. For example, estimation of the change in density of the waste with time is required to predict what the final density of the waste will be and how soon states approaching this condition will occur. Information about the compaction characteristics of the waste must be obtained to make these predictions.

This report summarizes the results of a series of experiments and analyses performed to investigate the compaction of the waste materials and the collapse of waste filled drums.¹ Two phases of testing have been performed:

- Part I: Determined the stress-density consolidation curves of various mixtures of solid materials to provide a preliminary characterization of this behavior and to select a suitable description for the waste.
- Part II: Determined the collapse behavior of actual drums filled with a variety of materials.

1. These tests were performed by Science Applications International Corporation (SAIC) in their Las Vegas Rock Mechanics Laboratory under Sandia National Laboratories Contract 05-7501.

2.0 MATERIAL COMPACTION STUDIES

2.1 Objectives

The objective of the material compaction tests was to obtain initial information on the compaction properties of a variety of materials simulating the major components of the waste to be stored at the WIPP. A secondary objective of the study was to determine how the initial shape of a generic material, such as polyethylene, might influence its compacted state at low void fractions.¹ For example, we suspected that the difference between the compacted state of polyethylene in pellet form and the compacted state of polyethylene bottles with rigid caps under the same conditions would be small, a hypothesis that was confirmed by experiment. This observation will be used to demonstrate that the exact geometric shape of some waste was of secondary importance in regard to its compactibility, and that such materials could be represented by a single compaction curve.

Another objective of the study was to determine the decrease in density, or rebound, that the various materials would undergo as they were unloaded from the maximum compaction stress. A final part of the investigation was suggested by some of the preliminary results: some of the materials continued to increase in density, or creep, when the maximum loads were reached and were held constant for short periods of time. Although a correction has been applied to the results for continued time-dependent deformation at constant maximum load, particularly those involving tests on mixtures of plastics, cellulosics, and metals + salt, it is likely that greater densities than the measured values can be expected.

The materials selected for testing were based on analysis by Butcher (1989) of an earlier study of contact handled transuranic (CH TRU) waste drums from the Idaho National Engineering Laboratory (INEL) by Clements and Kudera (1985). Five dominant major waste components were identified:

Plastics
Fibers (Cellulosics: Paper, Cloth, Wood, etc.)
Sorbents
Metals and metal components
Sludge

-
1. The average void fraction in the room, although equivalent in value to average room porosity, is used as a variable in this plot to emphasize that it represents the assumption that void volume is distributed uniformly throughout the room.

These waste components were used as a basis for selecting various mixtures of simulation materials for the compaction tests. The various mixtures are described in Table 2-1. One additional combination of materials was metal waste in contact with crushed WIPP salt, with or without a sheet metal separator between the layers. These configurations were selected to evaluate the condition of metallic waste as it consolidated at the edge of a container wall.

Two compaction tests were run on each of the materials specified in Table 2-1 to a maximum axial stress of 13.8 MPa (2000 psi). This stress level approximates the lithostatic pressure that the waste would eventually have to withstand at the horizon of the repository.

2.2 Apparatus

This section briefly describes the test apparatus and procedures and presents and discusses the results.

The compaction apparatus consisted of a 10.2 cm (4") ID oedometer mounted in a 5.34 MN (1,200,000 lb) capacity test frame. The details of the oedometer are shown in Figure 2-1. A minimum gap between the piston and the oedometer bore assured that none of the sample material extruded out of the cavity during compression: this was verified by inspections after the tests. Holes were also provided to allow air to escape during compaction. The oedometer was fitted with two linear variable displacement transformers (LVDTs) to monitor axial deformation during the tests.

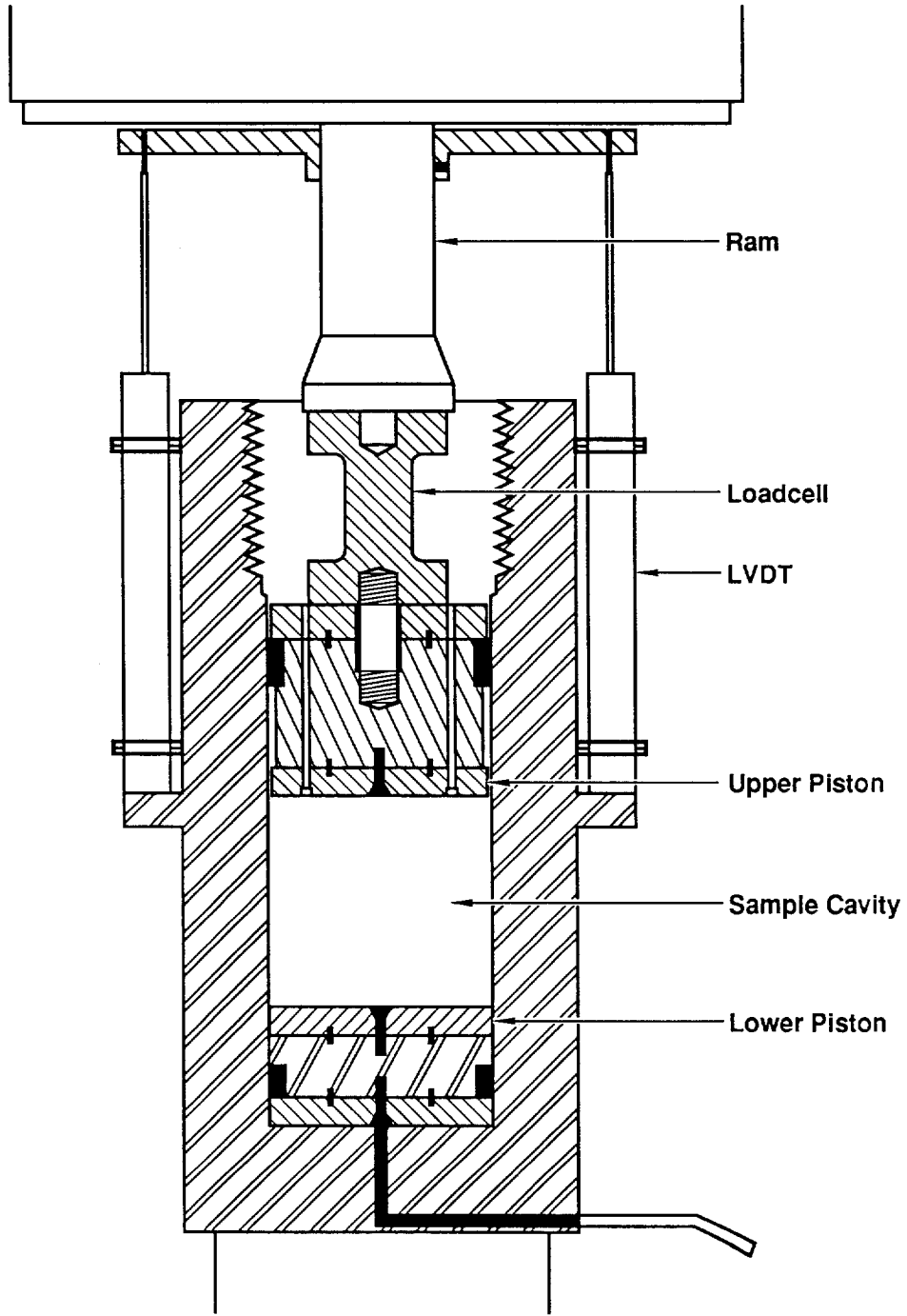
In addition to normal instrument calibration (load cell and LVDTs) and checks, two special system calibrations were performed prior to the testing. These special calibrations were an empty oedometer compaction test and a lead slug compaction test. The empty oedometer tests were performed to correct for system deformation during testing. The results showed that total displacements of about 0.38 mm (0.015 in) (equivalent to an oedometer cavity volume change of about 3 cc) occurred at 17.2 MPa (2500 psi). The results of tests performed before and after the materials tests compared favorably. A third order polynomial fit has been used to correct for this deformation in the data reported here.

A lead slug test was used to assure that the sample heights determined from the LVDT readings and from the end test measurements were correct. This test determined that the results from these external measurements agreed with the measured thickness of the slug after testing to within 1% of 12.7 mm (0.500 in) (the minimum compacted height).

TABLE 2-1. SIMULATED WASTE MATERIALS

Mixture #	Sample & Test #	Description
(1)	5,6	Pine sawdust
(2)	10,24	Pine wood cubes, approximately 1" in dimension
(3)	11,30	A mixture of 60% by weight pine wood cubes; 40% by weight cut-up rags
(4)	15,22	A mixture of intact (small) and cut-up (large) polyethylene bottles
(5)	7,8	Polyethylene pellets (Phillips Petroleum Marlex bottle blowing grade or equivalent)
(6)	12,26	A mixture of 40% by weight intact (small) and cut-up (large) polyethylene bottles with caps; 40% by weight PVC conduit of various diameters with fittings (loose); 20% by weight surgical gloves
(7)	23,27	A mixture of 50% by weight polyethylene pellets and 50% by weight PVC conduit of various diameters with fittings (loose)
(8)	13,21	Oil Dri ("SORB-ALL") [®]
(9)	9,20	Vermiculite
(10)	16,25	Portland cement
(11)	14,28	1" dimension cut-up steel, copper, lead, and aluminum scrap (thin-walled conduit, curtain rods, light hardware, small pipe fittings, other metal junk)
(12)	17,29	Up to 3" dimension cut-up steel, copper, lead, and aluminum scrap (thin-walled conduit, curtain rods, light hardware, small pipe fittings, other metal junk)
(13)	18,32*	A layered mixture of moist sand and dry cement. Several layers of each in a sample with the thickness of the sand layers at least equal to or as much as 2 times the thickness of the cement layers (simulated inorganic sludge)
(14)	19,31	The bottom of the sample was a layer of crushed salt with the rest of the sample metal waste

*Test #18 was allowed to set overnight (10 hours) before testing, test #32 was tested immediately.
(All materials were dry unless specified otherwise.)



TRI-6345-16-0

Figure 2-1. Oedometer set up for compaction testing.

Samples were prepared from specified materials in the "as purchased" condition. After weighing, logging, and photographing, they were introduced into the oedometer chamber in a "random" fashion, with no attention being paid to packing. The exception to this rule was for metal samples, where checks were made prior to testing to ensure that pieces of metal were not aligned in such a way as to act as columns and support more than the usual load during the early part of the test.

After the samples had been emplaced, the top piston was placed in the oedometer so as to lightly contact the sample. The original sample height was determined using a depth gauge on the top of the piston: the oedometer height and piston length were known from earlier measurements. Original density was then determined from this height, the known oedometer diameter, and the weight of the sample.

Load was applied at a constant strain rate for tests 5-19 and at constant stress rate for tests 20-32. The change to stress rate control was made to simplify the switch to constant stress on reaching peak stress when continued deformation with time occurred. In the early tests, stress was maintained constant for about 2-5 minutes to examine the development of creep deformation. Having established that creep of several materials did occur, a constant stress period of about 30 minutes was used in the later tests.

Upon unloading, the final height of the sample was determined using a depth gauge on the top of the piston, and the sample was extruded into a sample catching tube. In the earlier tests many of the samples were found to be poorly compacted after extrusion. In later tests certain of the samples were epoxy impregnated to allow later inspection of the form of the compacted materials. Post-test samples were photographed.

This work was done under a Quality Assurance Project Plan (QAPP) which required the use of Sandia National Laboratories approved Technical Procedures (TP's) and instrument calibrations traceable to the National Bureau of Standards. The TP's used during Phase I of this project covered operation of the test apparatus and the data acquisition system, material calibration, and sample handling.

2.3 Methods of Analysis

2.3.1 ANALYTIC REPRESENTATION OF COMPACTION CURVES

The results from a typical compaction test were usually stress vs density data, or, if the load was being held constant, density vs time data. The density data were usually converted to porosities because stress-porosity data was easier to fit with analytic relationships and are useful for

normalizing variations in theoretical solid densities. Values of the theoretical solid density of each mixture were estimated for the porosity calculations using the procedure described in a following paragraph. Analytic expressions were then constructed from linear, semilog, or log-log scale plots in order to make the data more manageable. The results of these constructions are described in Section 2.4.

2.3.2 ESTIMATION OF SOLID DENSITIES

Estimates of theoretical solid densities are required in order to determine how porous the waste is at a given time. Solid densities were computed as follows: Let w_1, w_2, w_i (for $i = 1$ to n), be the weight fractions of the n waste components. The volume fraction of each component, for a unit weight of the mixture is its weight fraction divided by its density in the solid state, ρ_{si} :

$$V_{si} = w_i / \rho_{si}.$$

The total solid volume of all the components per unit weight of the mixture is:

$$V_s = \sum_{i=1}^n V_{si} = \sum_{i=1}^n w_i / \rho_{si},$$

and the average solid density of the mixture is $\rho_s = 1/V_s$. Variations in solid densities with changes in pressure have not been included in computation of porosities because they are small relative to the changes in volume during compaction. Values assumed for solid densities of the individual components are given in Table 2-2.

2.3.3 CORRECTION FOR TIME-DEPENDENT COMPACTION

Two mathematical relationships were used to extrapolate the observed changes in bulk density with time of the simulated waste materials under constant stress to estimates of greatest possible densities, i.e., the limiting values of density after long times. These functions have been used in past investigations to describe the time-dependent deformation of materials; both have been applied in the past to the creep-consolidation of pure crushed salt.

TABLE 2-2. WASTE SOLID DENSITIES

Material	Density - kg/m ³	Reference
steel	7860	(1)
copper	8920	(1)
aluminum	2700	(1)
lead	11,300	(1)
tantalum	16,600	(1)
salt	2140	(3)
water	1000	(1)
sand (quartz)	2650	(2)
glass	2600	(2)
Portland cement	3000	(4)
wood (pine)	940	(5)
cloth (cotton)	1490	(2)

- (1) Handbook of Chemistry and Physics, 69th edition, (CRC Press, Inc, Boca Raton, Florida, 1989).
- (2) Mark's Standard Handbook for Engineers, 8th edition, McGraw-Hill Book Company, New York), pp 6-7 to 6-9.
- (3) Holcomb, D. J., and M. Shields, "Hydrostatic Creep Consolidation of Crushed Salt with Added Water." Sandia National Laboratories, Report SAND87-1990. October 1987.
- (4) Lea, F. M., The Chemistry of Cement and Concrete, Third Edition, (Edward Arnold, Ltd., United Kingdom, 1970), p. 361.
- (5) LASL Shock Hugoniot Data, Stanley P. March, Editor, University of California Press, Berkeley, 1980.

The first function is a power law relationship between the rate of change of density and time:

$$\frac{d\rho}{dt} = \alpha t^{-\beta} \quad (\beta > 0) \quad (2.3.3.1)$$

The integrated form of this equation is:

$$\rho = \frac{\alpha}{(1 - \beta)} \cdot t^{(1 - \beta)} + k_1, \quad (2.3.3.2)$$

where k_1 is a constant of integration. For $\beta > 1$, or $(1 - \beta) < 0$, the value of k_1 can be interpreted as the limiting value of the density after long times and is therefore a convenient estimate of the final state of the waste. This power law relationship is similar to the type used by Holcomb and Shields (1987) to describe results from tests measuring the consolidation of WIPP crushed salt, and like their relationship is not defined at $t = 0$.

Therefore, constants α and β were determined from values of $d\rho/dt$ and t , $t > 0$, at two points on curves defining the variation of $d\rho/dt$ with respect to t , and k_1 was found using the known value of ρ corresponding to one of the times. The two points defining the constants were usually at the beginning and end of the data curves. An example of the application of the power law relationship, Equation 2.3.3.1, to data representing the change in density with time of a mixture of polyvinyl chloride (PVC), polyethylene parts, and surgical gloves, under a constant axial stress of 13.8 MPa, is shown in Figure 2-2.² Computed density value limits for the various types of waste using the power law relationship are given in Table 2-3.

The second mathematical relationship relates the rate of change of density with time to the density:

$$\frac{d\rho}{dt} = a \exp(b\rho) - \exp(-(\rho - \rho^*)/c^*). \quad (2.3.3.3)$$

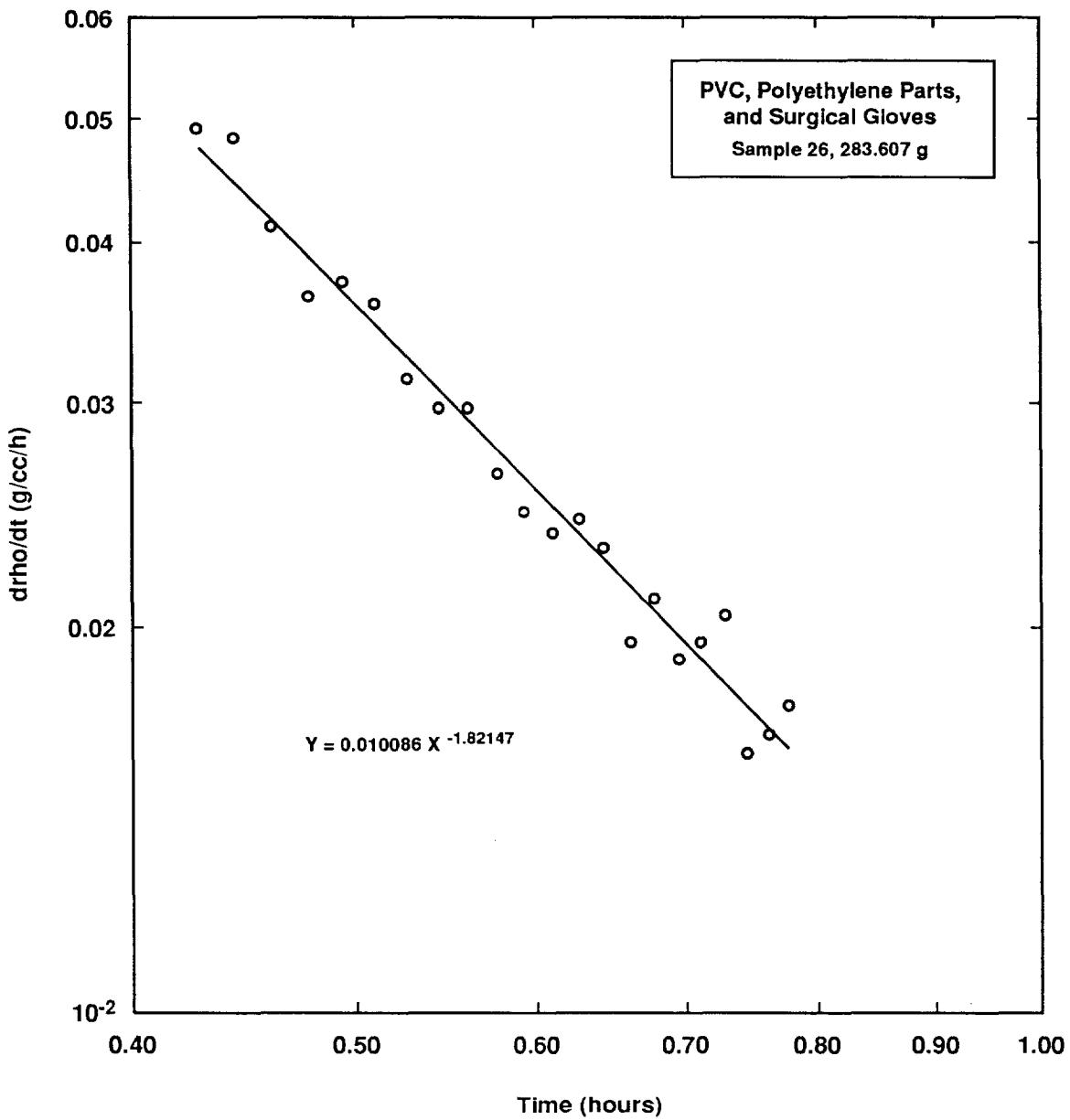
The integrated form of this equation is

$$(t - t_0) = -c^* \exp(-(\rho - \rho^*)/c^*) + k, \quad (2.3.3.4)$$

where t_0 is the time of initiation of the constant stress portion of the test, and a , b , ρ^* , and c^* are constants. The constant k is a constant of integration, which is small, relative to the long times under consideration, and under most circumstances can be set equal to zero. The constants for the exponential relationship were evaluated in the same manner as for the power law relationship, from two data points usually at the beginning and ends of the data curves. This functional form has been used by Sjaardema and Krieg (1987) to describe the consolidation of WIPP crushed salt. An example of the application of the exponential law relationship, Equation 2.3.3.3, to data representing the change in density with time of a mixture of PVC, polyethylene parts, and surgical gloves, under a constant axial stress of 13.8 MPa, is shown in Figure 2-3.

Two times appear appropriate for estimation of representative densities with the latter equation. The first time is three months, based on the practical duration of most laboratory creep tests. The second time is 200 years, the estimated maximum time for waste within the disposal rooms to consolidate to an equilibrium state. Computed density value limits for the various types of waste using the exponential relationship are given in Table 2-3.

2. The graphics software program GRAPHERTM was used to make the plots and to find mathematical equations for the curves.



TRI-6345-17-0

Figure 2-2. An example of the application of the power law relationship for sample consolidation with time, Equation 2.3.3.1, to data representing the change in density with time of a mixture of PVC, polyethylene parts, and surgical gloves under a constant axial stress of 13.8 MPa.

TABLE 2-3. WASTE DENSIFICATION WITH TIME

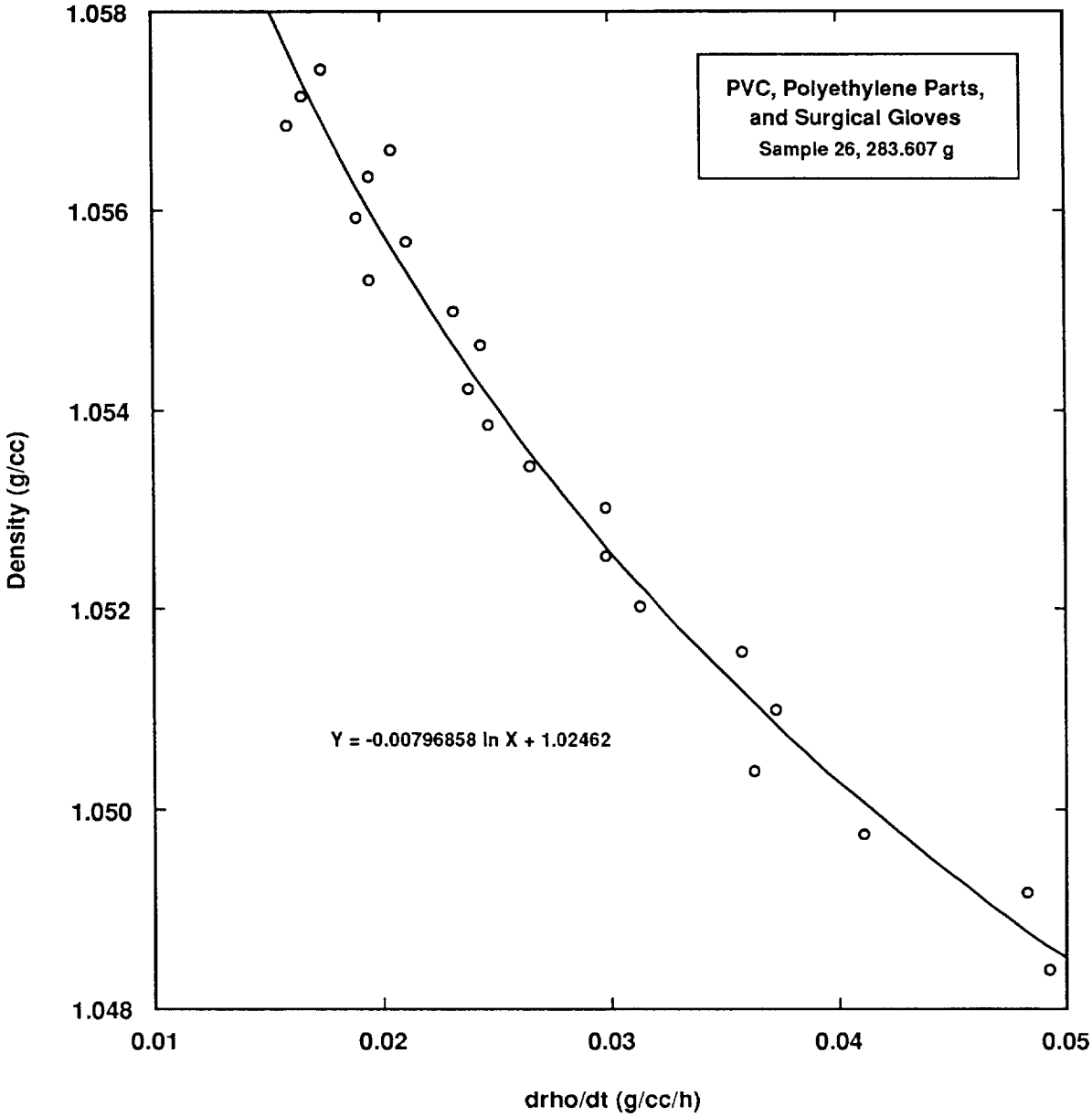
Waste Type (density)**	Power Law Relationship	Exponential Relationship	
	$k_1/(\text{density change})^*$ kg/m ³	3 months	200 years
Wood & Rags Material #3 (0.879)	918.0 (39.0)	1012.3 (133.3)	1099.0 (220.0)
Plastic Mix Material #6 (1.0485)	1072.6 (24.1)	1124.3 (75.8)	1177.6 (129.1)
Vermiculite Material #9 (2.3836)	2428 (44.4)	2480 (96.4)	2541 (158.0)
1" Metal Parts Material #11 (2.4220)	2500 (32.0)	2545 (74.5)	2588 (117.8)
3" Metal Parts Material #12 (2.0776)	2097 (19.2)	2131 (53.0)	2168 (90.9)

* The density value represents the extrapolated state of the material at the condition indicated. The difference in density is the difference between the extrapolated density and the density at the beginning of the constant stress part (13.8 MPa or 2000 psi) of the test.

** The density at the beginning of the constant stress part (13.8 MPa or 2000 psi) of the test, in kg/m³.

2.3.4 COMPOSITE CURVES

Composite compaction curves for different waste categories can be constructed from the compaction curves of their individual waste components. The state of waste compaction at a given stress is obtained by computing the total volumes and void volumes of the individual waste components and adding them together. Assume that w_1, w_2, w_i ($i = 1$ to n) are the weight fractions of the n waste components in a given waste category, and ρ_1, ρ_2, ρ_i ($i = 1$ to n) are the respective bulk densities of the waste at the assumed stress. The



TRI-6345-18-0

Figure 2-3. An example of the application of the exponential relationship for sample consolidation with time, Equation 2.3.3.3, to data representing the change in density of a mixture of PVC, polyethylene parts, and surgical gloves under a constant axial stress of 13.8 MPa.

volume (including voids) of each component, per unit weight of the mixture, is its weight fraction divided by its bulk density, ρ_i :

$$V_i = w_i/\rho_i,$$

the total volume of all the components and voids, per unit weight of the mixture, is:

$$V = \sum_{i=1}^n V_i = \sum_{i=1}^n w_i/\rho_i, \quad (2.3.4.1)$$

and the average bulk density of the mixture is $\rho = 1/V$. The porosity of the mixture is $(1-\rho_s/\rho)$, where ρ_s , the theoretical solid density, is defined in Section 2.3.2. Porosities are useful for normalizing variations in theoretical solid densities. These equations were used to estimate the average compaction curve for each category of waste and then applied to estimate an average compaction curve for the entire repository.

2.4 Results

The results for the various tests are presented in Tables 2-4 to 2-8 and Figures 2-4 to 2-22. Data are presented in terms of densities and porosities for various assumed values of solid density. Initial densities were determined from the weights of the samples and their initial volumes (computed from the known cross-sectional area of the oedometer and the initial height of the sample). Densities at later times during the test were computed from initial weights, and the volumes for these density values were calculated from the initial volumes and the changes in height recorded by the axial LVDTs. Except as noted, porosities have been calculated using the solid densities for the materials listed in Table 2-2. Composite curves for combustible and metallic waste forms have been constructed and are given in Figures 2-23 and 2-24, respectively.

2.4.1 CELLULOSICS (WOOD AND CLOTH)

Samples #11 and #30 were a mixture of 60% by weight pine wood cubes; 40% by weight cut-up rags (Mixture #3: 1100 kg/m³ solid density). Solid densities were computed as indicated in Section 2.3.2 using the material solid densities given in Table 2.2. Stress-density curves including unloading are shown in Figure 2-4. The data, plotted in Figure 2-5, show that compaction is to final porosities of about 0.16 (920 kg/m³ density) at 13.8 MPa (2000 psi).

TABLE 2-4. TEST PARAMETERS AND RESULTS FOR COMBUSTIBLES

	TEST NUMBER					
	05	06	10	24	11	30
<u>COMPOSITION</u>						
Material	5	5	6	6	7	7
Sample Weight (gm)	80.000	80.005	139.314	92.633	153.243	121.682
Sawdust	100.0%	100.0%				
Pine Cubes			100.0%	100.0%	60.0%	60.0%
Rags					40.0%	40.0%
<u>DENSITY DATA</u> (Densities in kg/m ³)						
Initial Bulk Density	94	96	172	113	189	144
Bulk Density at 2000 psi	1096	1147	703	704	764	821
Time of Creep (mins)	5.8	5.6	4.0	32.0	4.7	35.3
Bulk Density at end of Creep	1133	1229	742	761	822	947
Bulk Density after Unload	963	1036	538	668	705	564
Rebound Time (mins)	0	0	0	0	3.2	0
Bulk Density after Rebound	963	1036	538	668	447	564

TABLE 2.5. TEST PARAMETERS AND RESULTS FOR PLASTICS

	TEST NUMBER							
	15	22	07	08	12	26	23	27
COMPOSITION								
Material	1	1	2	2	3	3	4	4
Sample Weight (gm)	78.700	85.184	80.004	72.006	138.494	283.553	366.864	202.186
Polyethylene Bottles	100.0%	100.0%			39.5%	39.7%		
Marlex Beads			100.0%	100.0%			50.0%	50.0%
PVC Conduit and Fittings					39.7%	39.8%	50.0%	50.0%
Surgical Gloves					20.8%	20.5%		
BULK DENSITY DATA (Densities in kg/m ³)								
Initial Density	94	105	101	87	170	355	449	251
Density at 13.8 MPa	945	948	1031	1028	1066	996	966	1016
Time of Creep (min)	5.8	35.5	5.3	5.8	6.7	35.4	31.4	4.7
Density after Creep	998	1000	1077	1089	1143	1057	1011	1042
Density after Unload	793	842	898	877	913	951	931	958
Rebound Time (min)	0.2	0.2	1.3	0.2	0.2	0	0.2	0
Density after Rebound	686	468	417	831	858	753	931	908

TABLE 2-6. TEST PARAMETERS AND RESULTS FOR METALS

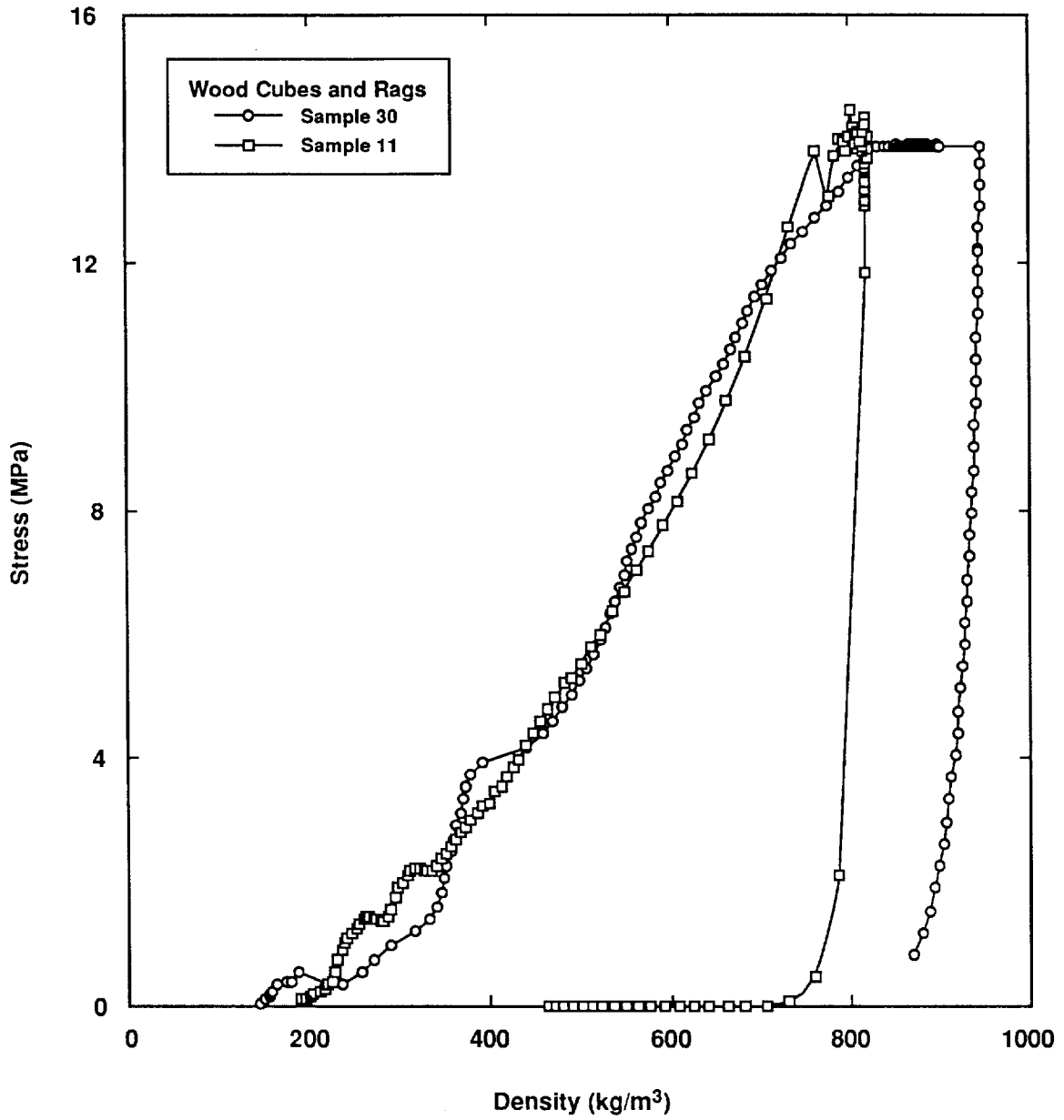
	TEST NUMBER					
	14	28	17	29	19	31
COMPOSITION						
Material	11	11	12	12	14	14
Sample Weight (gm)	536.40	449.33	801.016	711.58	867.282	795.239
Copper/Brass	14.5%	24.2%	21.5%	38.1%		
Steel/Iron	35.6%	37.0%	46.0%	28.7%		
Aluminum	16.8%	20.0%	16.0%	21.5%		
Lead	33.1%	18.8%	16.5%	11.6%		
Salt			52.6%	47.7%		
DENSITY DATA (Densities In kg/m ³)						
Initial Bulk Density	667	575	968	862	1039	957
Bulk Density at 2000 psi	3095	2439	2965	2026	2050	2251
Time of Creep (mins)	5.8	34.7	5.8	41.0	7.0	31.6
Bulk Density at end of Creep	3236	2494	3107	2087	2076	2287
Bulk Density after Unload	3042	2376		2014	2023	2231
Rebound Time (mins)	0.7	0.2		0.2	0.2	0.2
Bulk Density after Rebound	2574	1892		1620	1855	2069

TABLE 2-7. TEST PARAMETERS AND RESULTS FOR SORBENTS

	TEST NUMBER					
	13	21	09	20	16	25
<u>COMPOSITION</u>						
Material	8	8	9	9	10	10
Sample Weight (gm)	331.33	356.39	183.496	207.837	698.11	489.39
Oil Dri	100.0%	100.0%				
Vermiculite			100.0%	100.0%		
Cement					100.0%	100.0%
<u>DENSITY DATA</u> (Densities in kg/m ³)						
Initial Bulk Density	409	429	2276	2587	829	585
Bulk Density at 2000 psi	1182	1160	2667	2345	2032	2048
Time of Creep (mins)	7.7	32.7	4.0	31.8	8.0	41.2
Bulk Density at end of Creep	1194	1173	2731	2404	2036	2055
Bulk Density after Unload	1132	1132	1441	1885	1982	1997
Rebound Time (mins)	0.2	0.2	1.8	0	0	0
Bulk Density after Rebound	1107	1087	302	1885	1982	1997

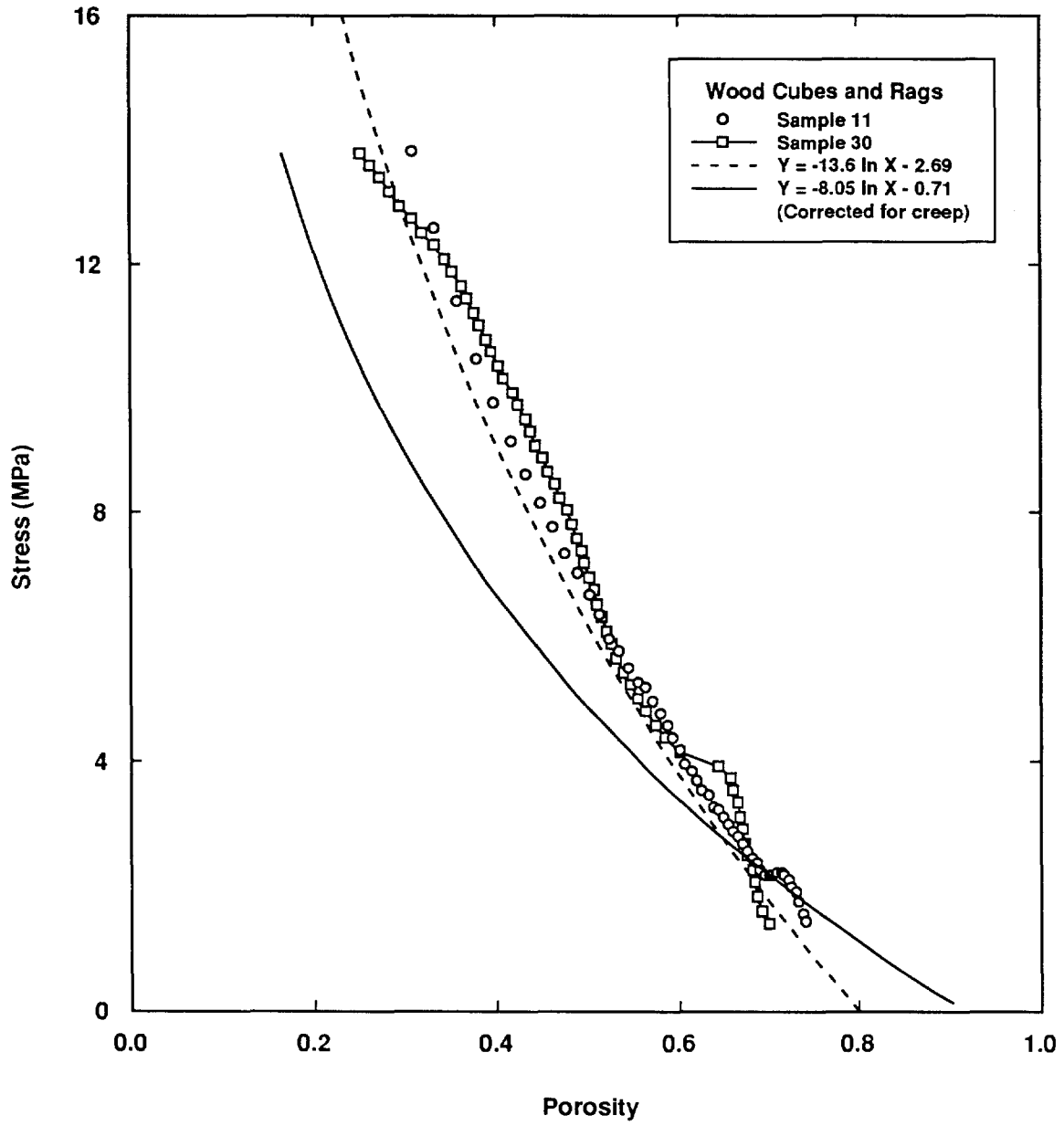
TABLE 2-8. TEST PARAMETERS AND RESULTS FOR SIMULATED SLUDGE

	TEST NUMBER	
	18	32
<u>COMPOSITION</u>		
Material	13	13
Sample Weight (gm)	709.622	737.187
Cement (% of Solids)	32.8%	35.7%
Sand (% of Solids)	67.2%	64.3%
Water (% of Wet Weight)	14.2%	13.6%
<u>DENSITY DATA</u> (Densities in kg/m ³)		
Initial Bulk Density	850	888
Bulk Density at 2000 psi	1960	2313
Time of Creep (mins)	7.2	33.1
Bulk Density at end of Creep	1981	2341
Bulk Density after Unload	1891	2163



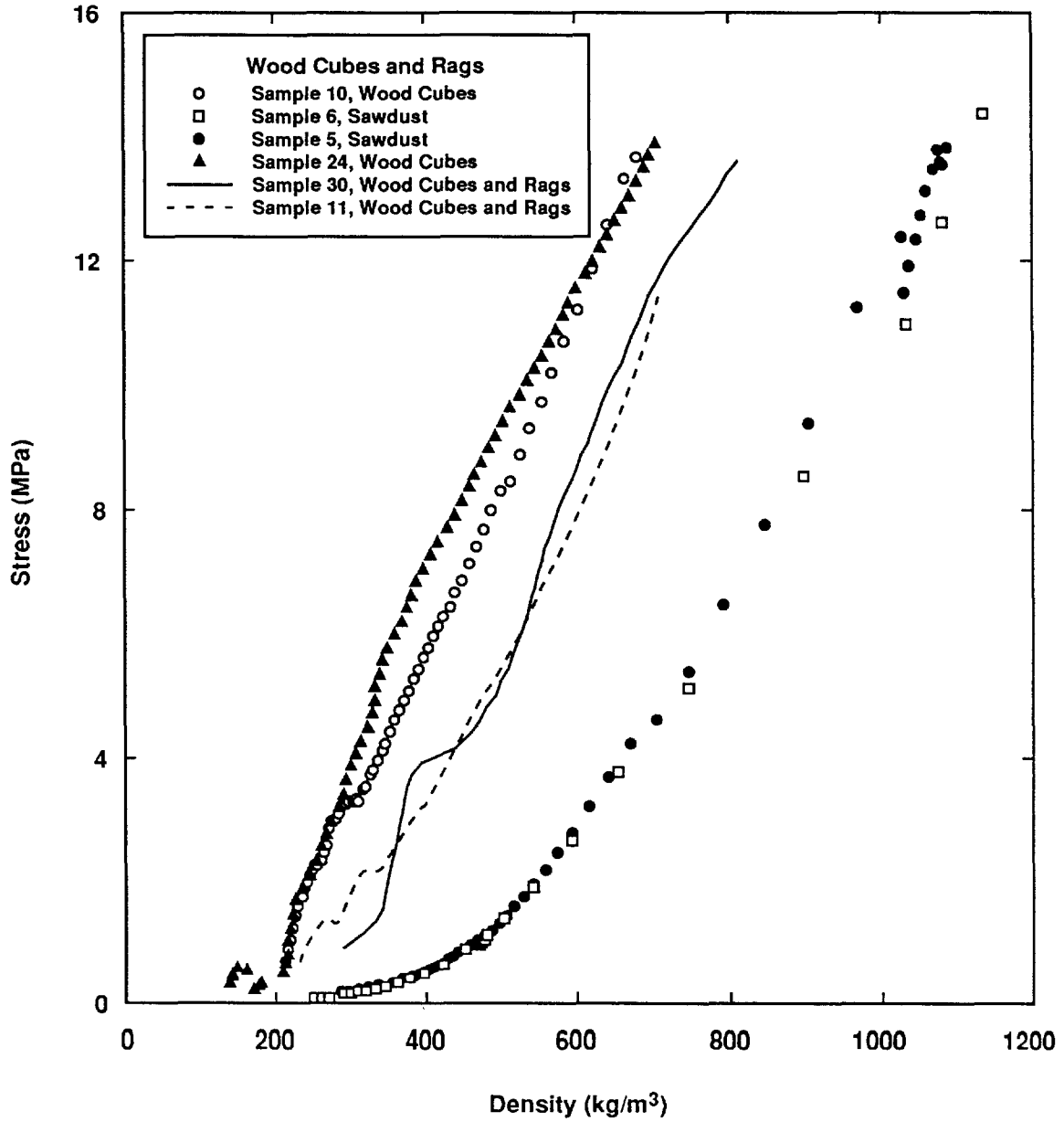
TRI-6345-19-0

Figure 2-4. Wood cubes and rags stress versus density curves.



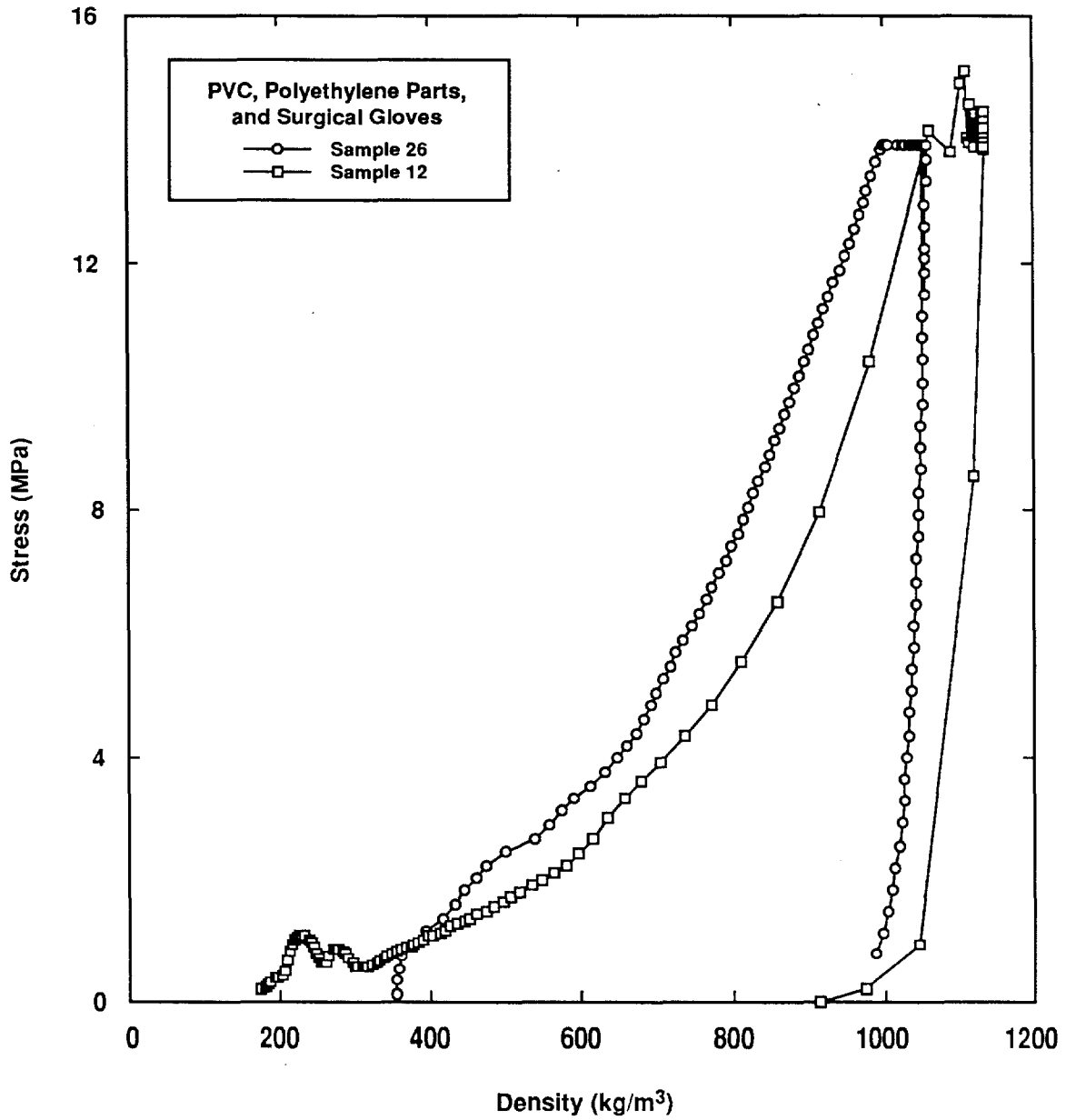
TRI-6345-20-0

Figure 2-5. Wood cubes and rags stress versus porosity curves.



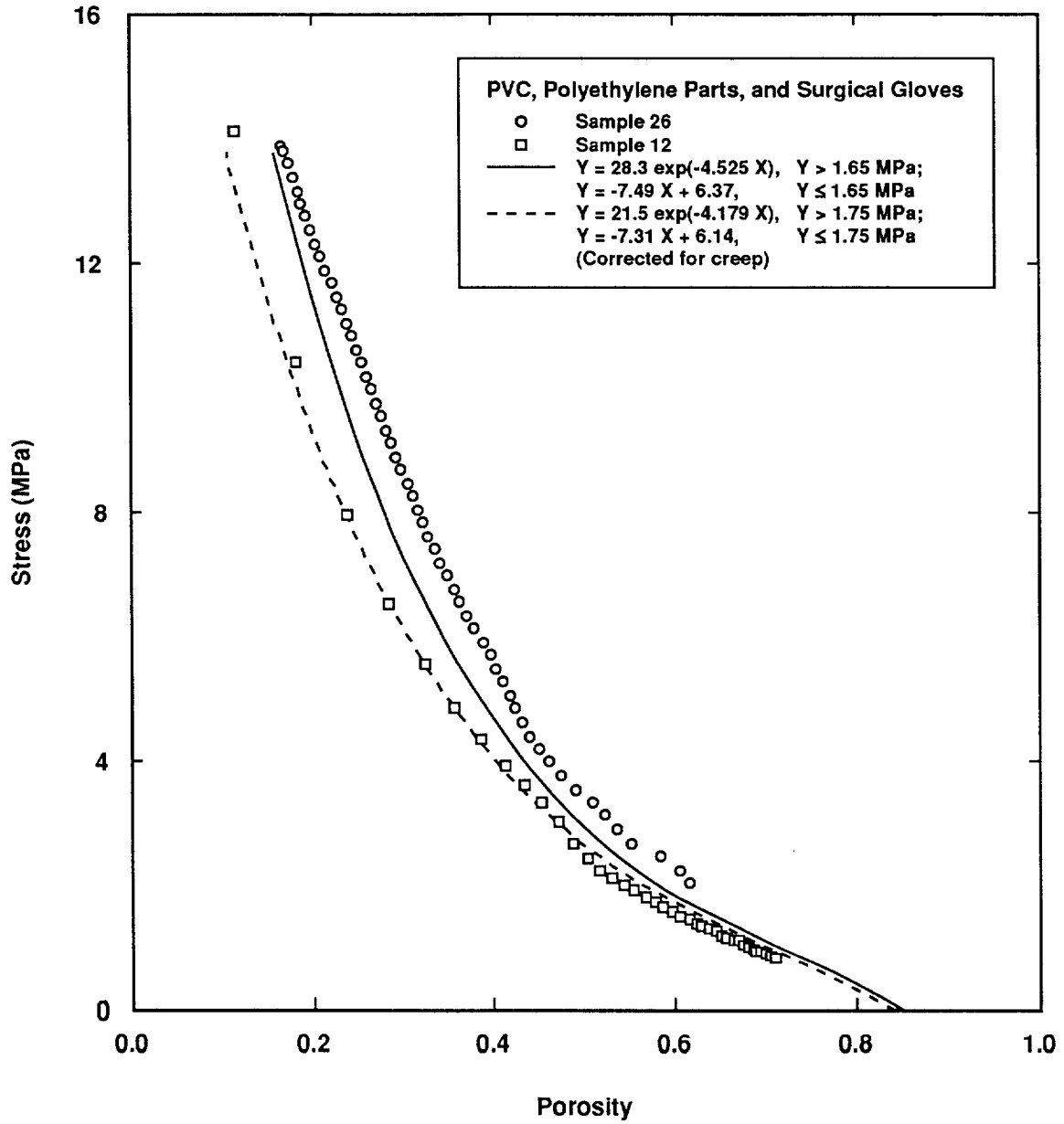
TRI-6345-21-0

Figure 2-6. Cellulosic compaction curve variability.



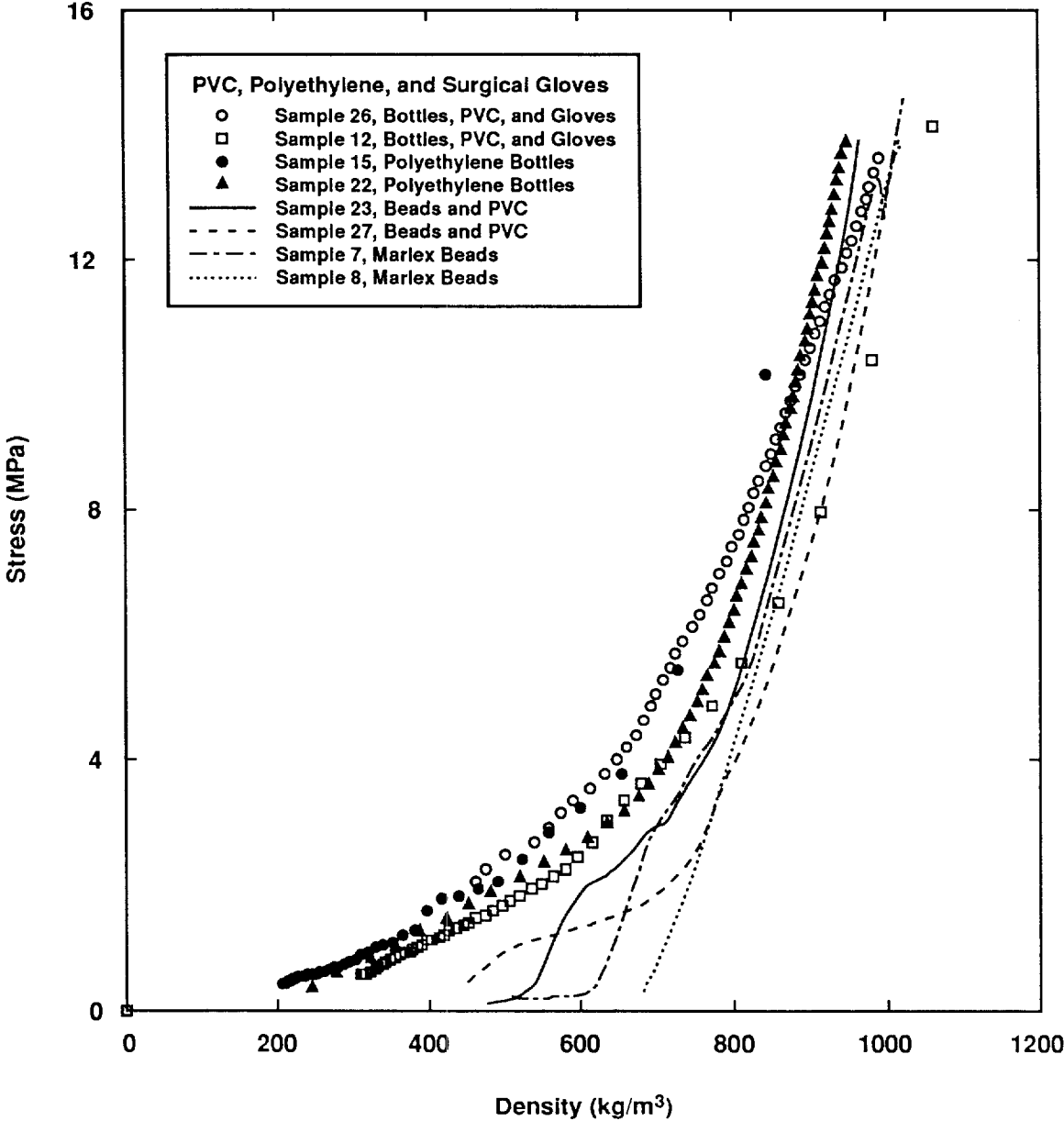
TRI-6345-22-0

Figure 2-7. PVC, polyethylene parts, and surgical gloves stress versus density curves.



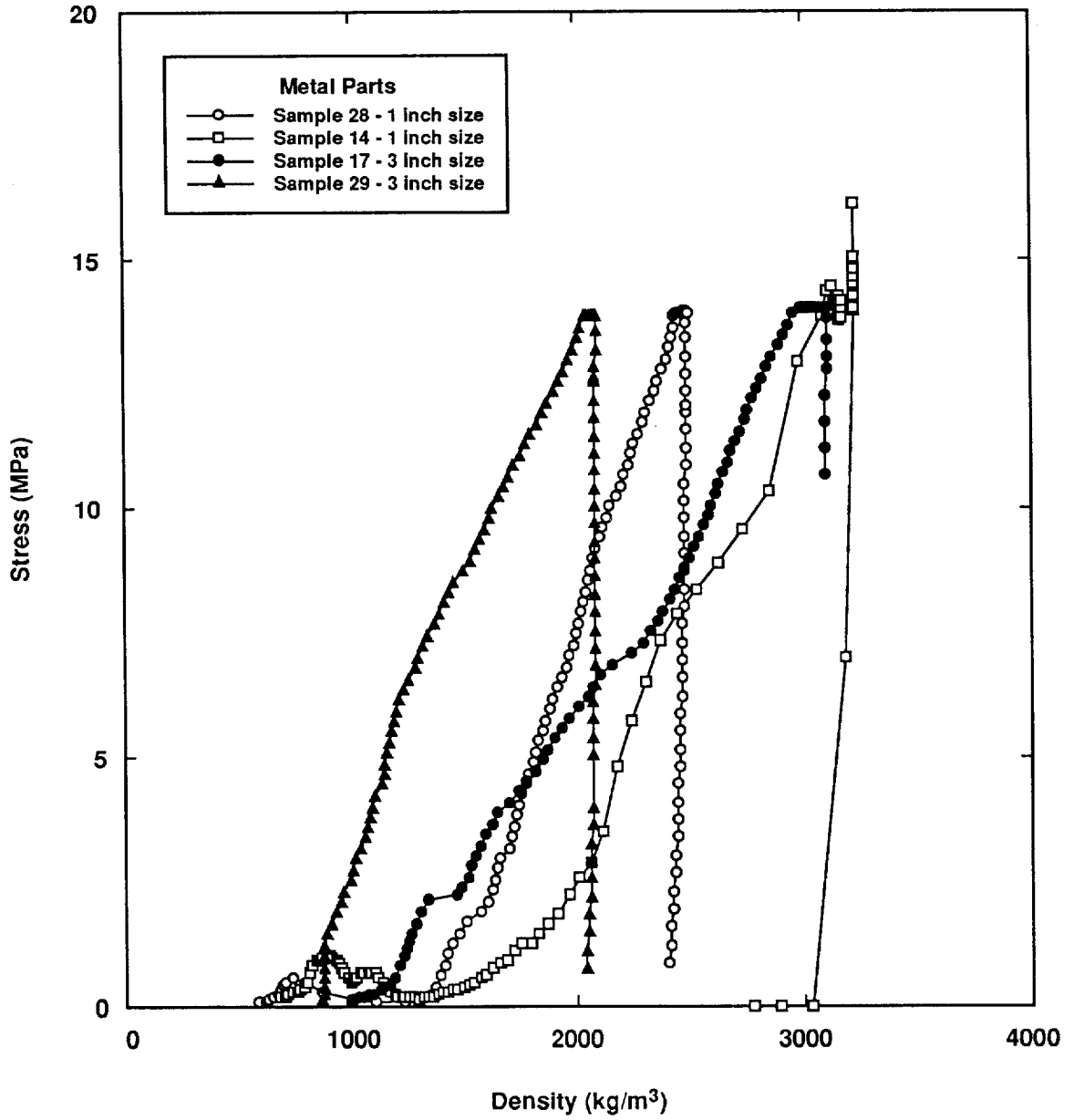
TRI-6345-23-0

Figure 2-8. PVC, polyethylene parts, and surgical gloves stress versus porosity curves.



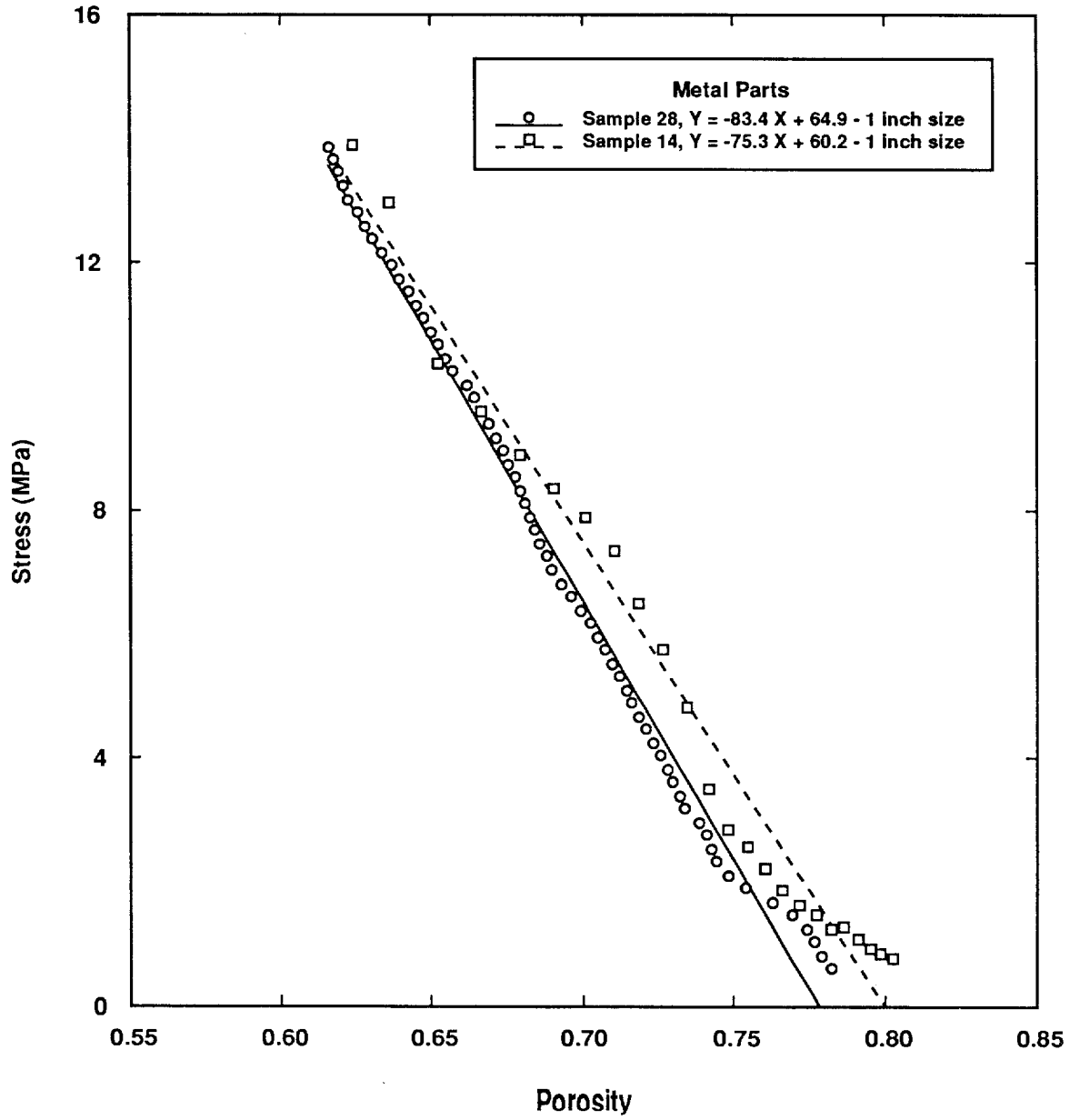
TRI-6345-24-0

Figure 2-9. Plastics compaction curve variability.



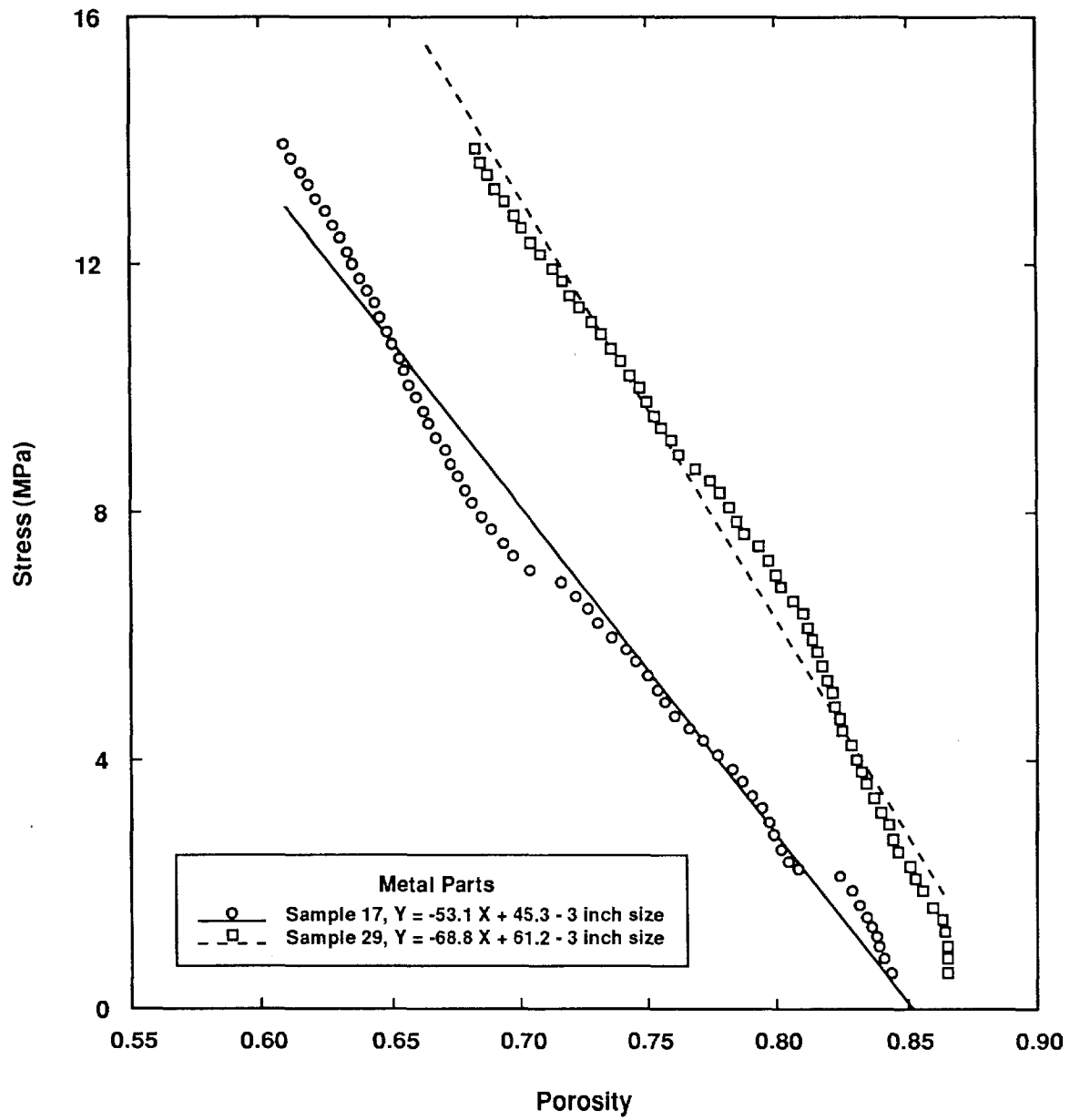
TRI-6345-25-0

Figure 2-10. Metal parts stress versus density curves.



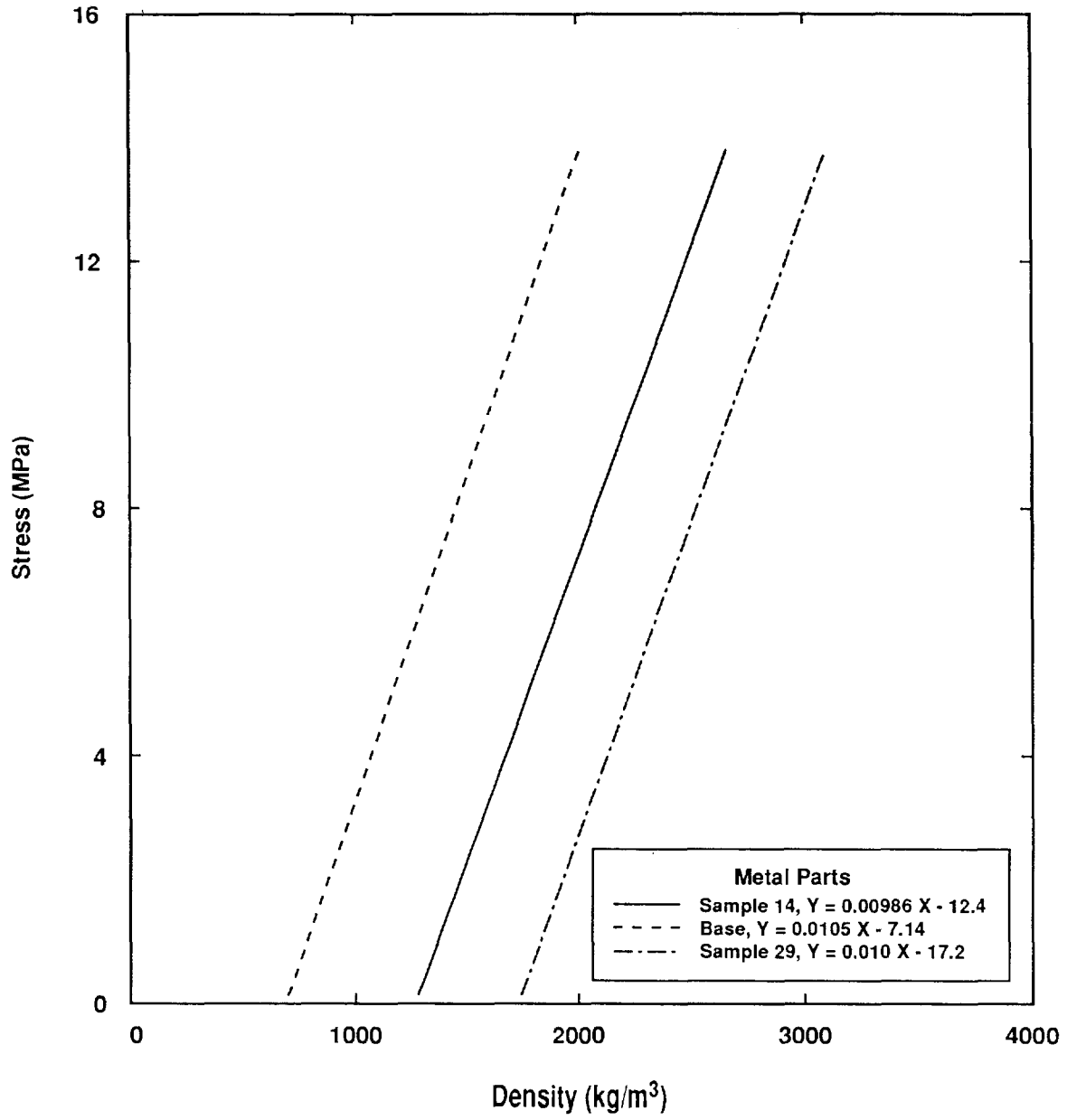
TRI-6345-26-0

Figure 2-11. 2.5 cm (1 inch) metal-parts stress versus porosity curves.



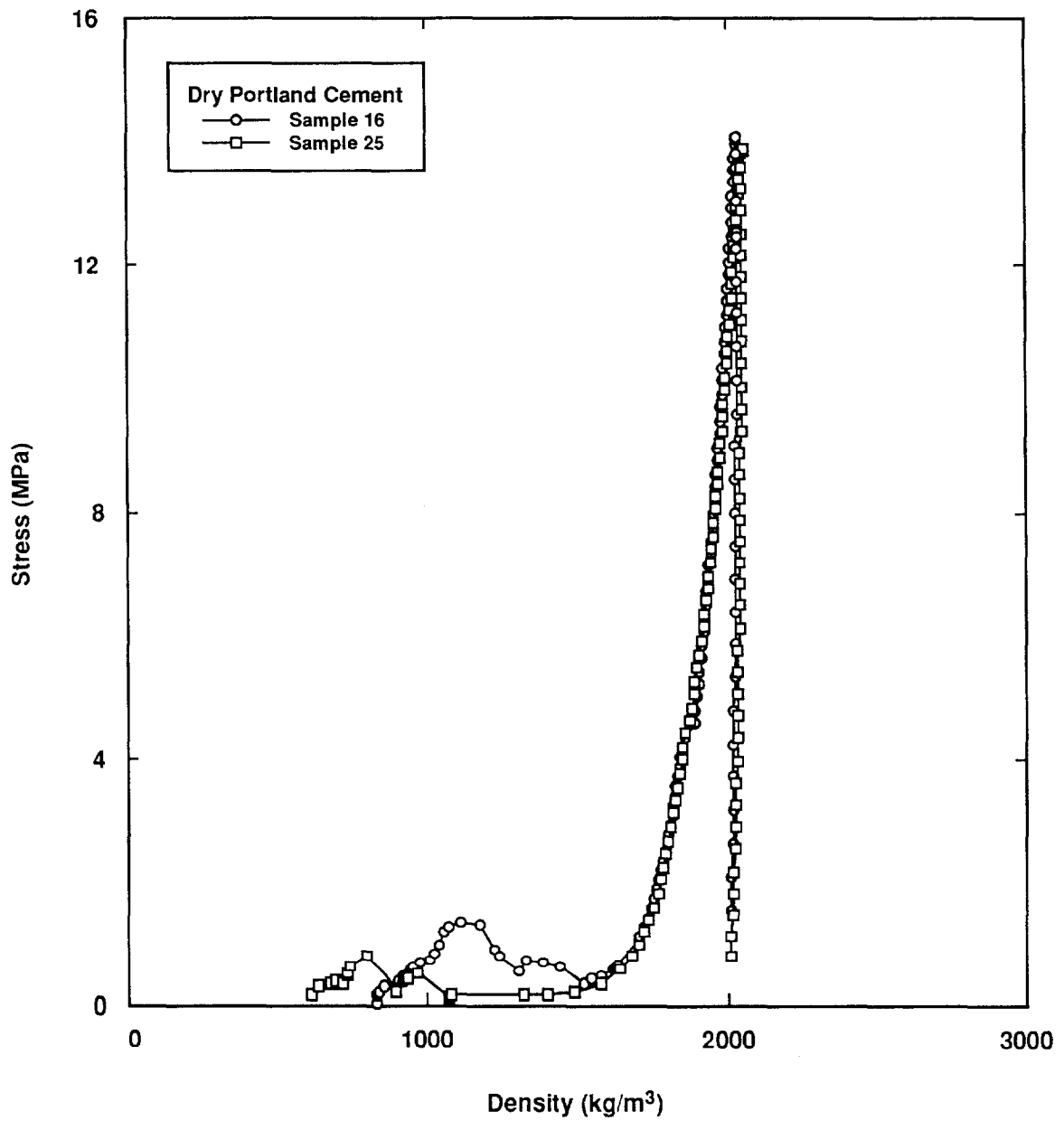
TRI-6345-27-0

Figure 2-12. 7.6 cm (3 inch) metal-parts stress versus porosity curves.



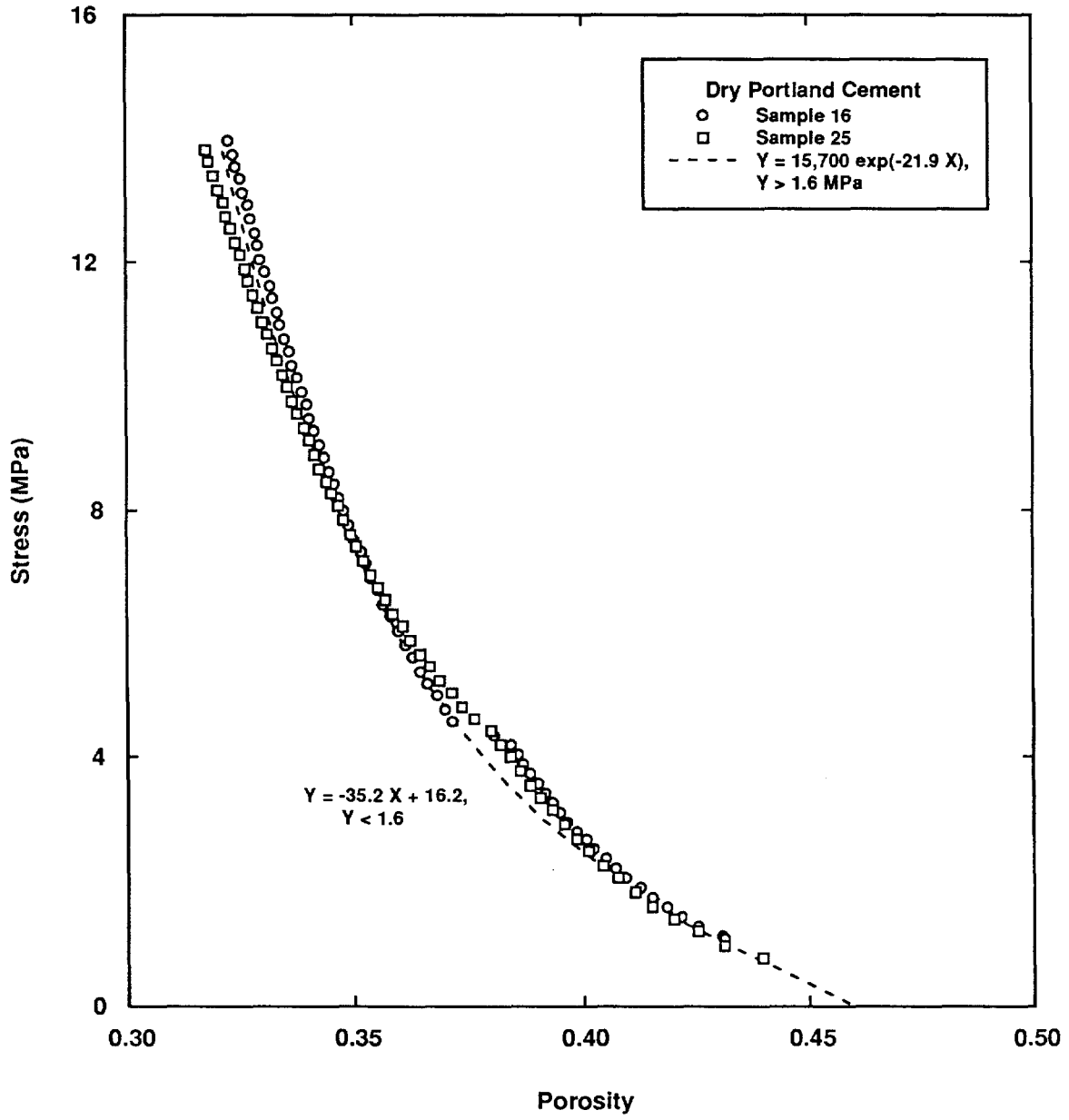
TRI-6345-28-0

Figure 2-13. Metal parts compaction curves.



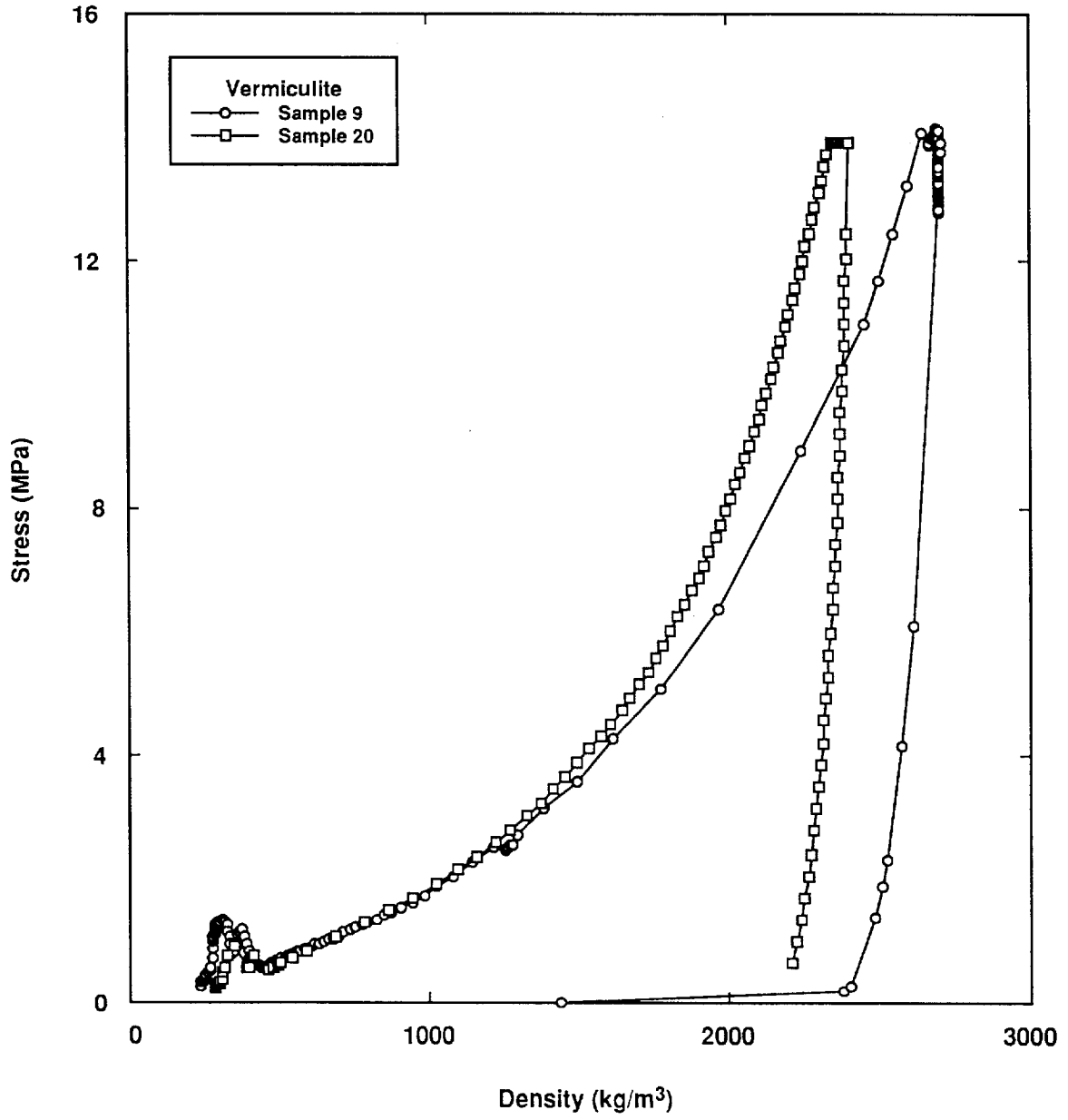
TRI-6345-29-0

Figure 2-14. Dry Portland cement stress versus density curves.



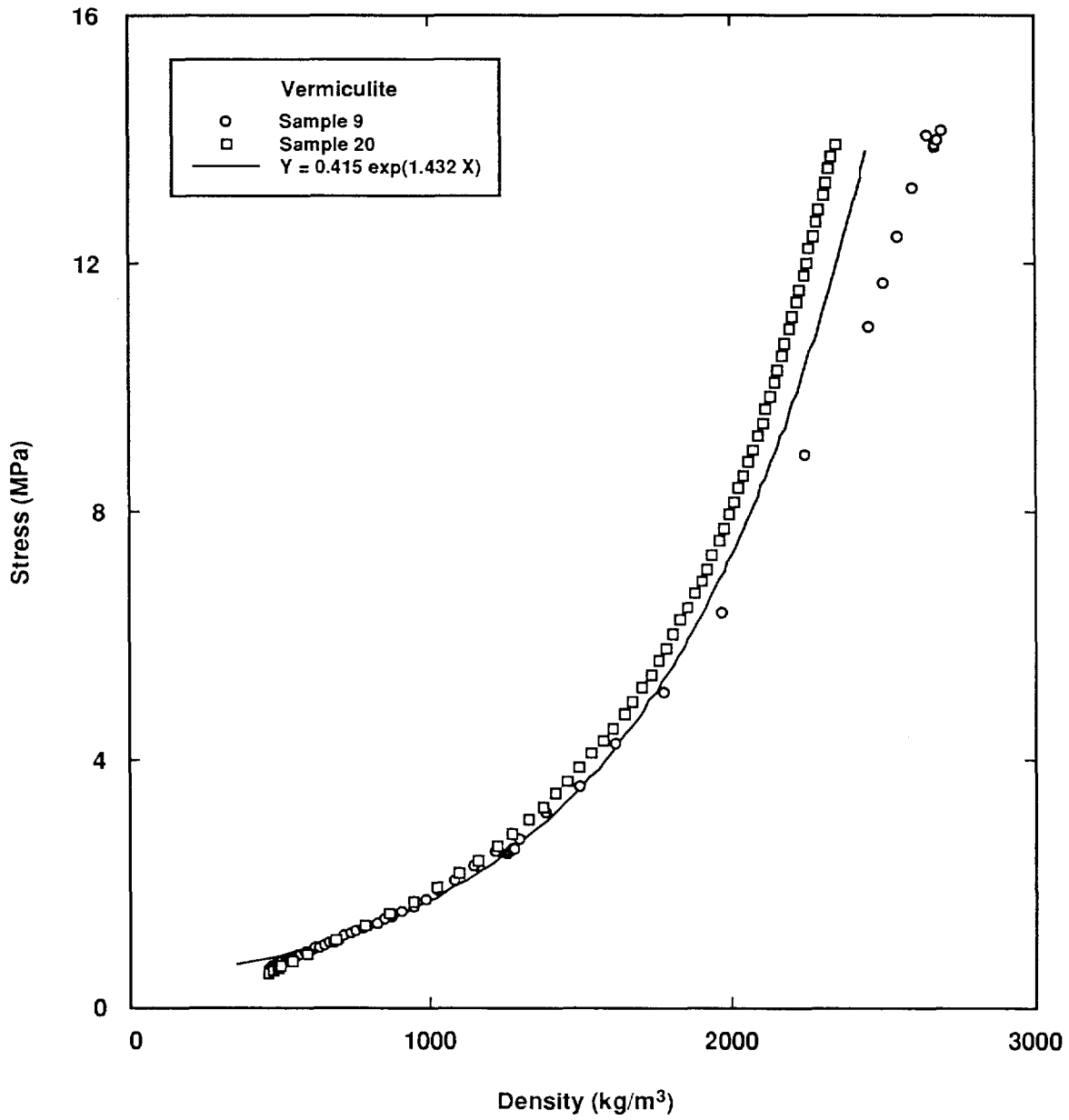
TRI-6345-30-0

Figure 2-15. Dry Portland cement stress vs porosity curves.



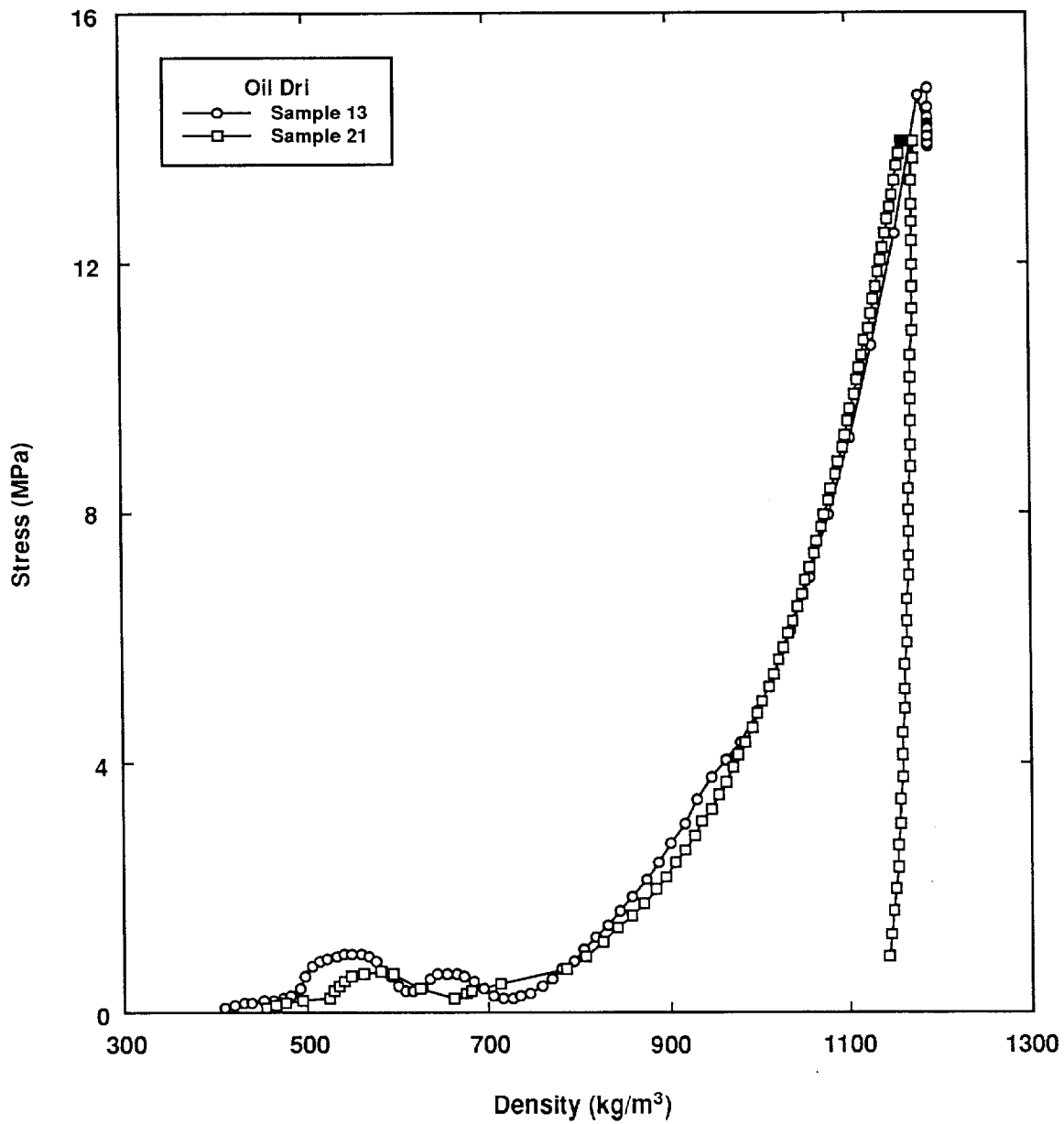
TRI-6345-31-0

Figure 2-16. Vermiculite stress versus density curves.



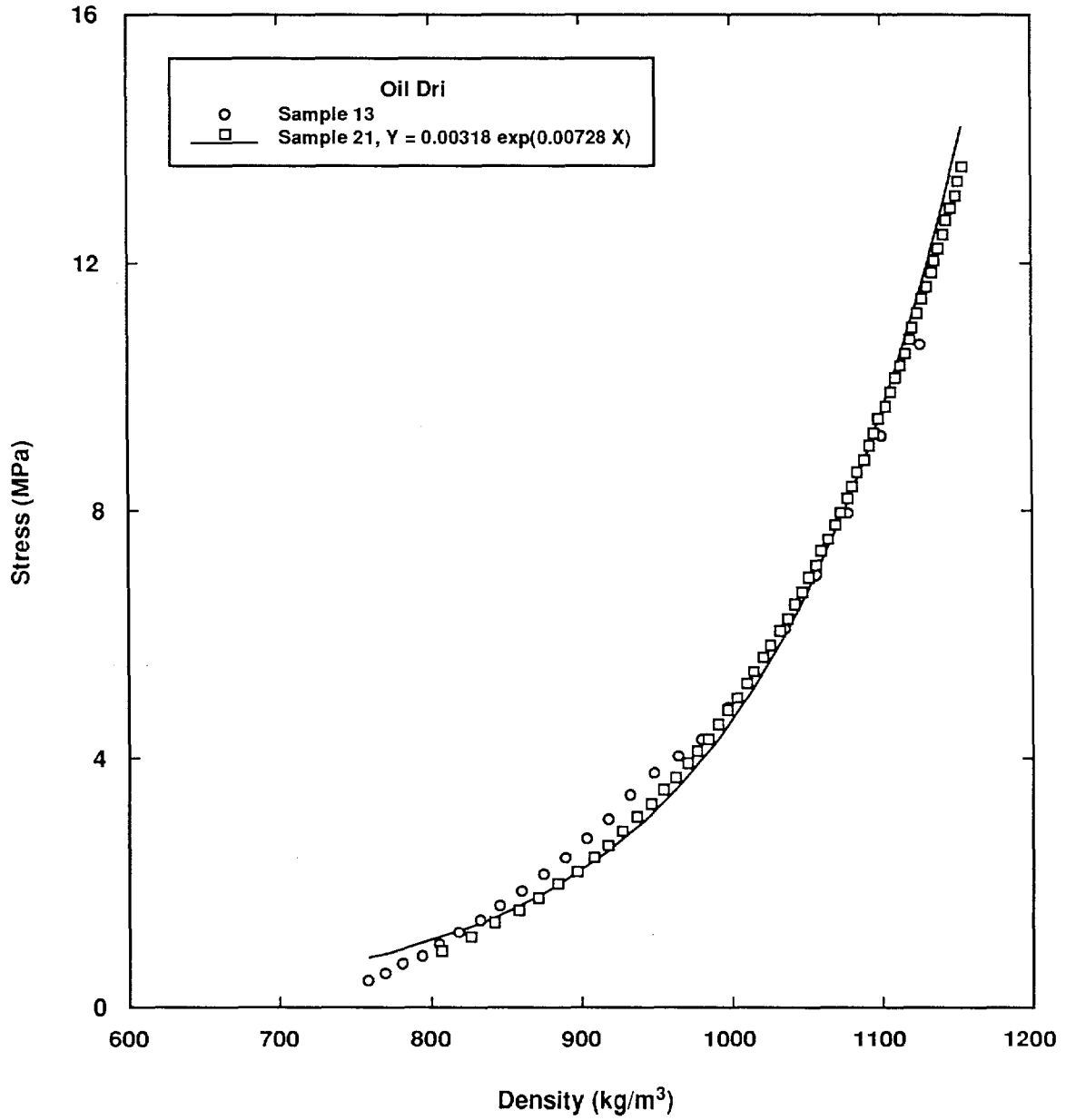
TRI-6345-32-0

Figure 2-17. Modified vermiculite stress versus density curves.



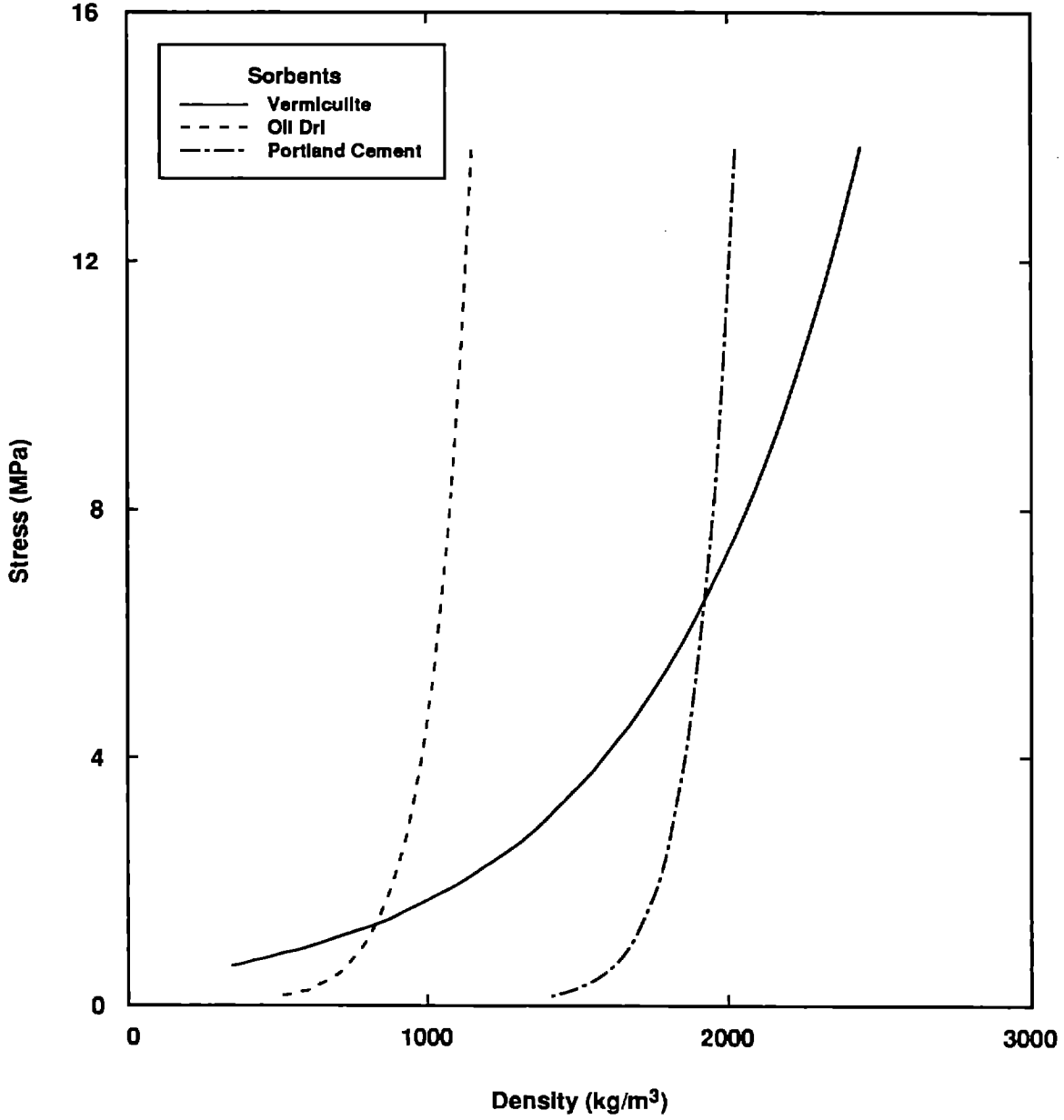
TRI-6345-33-0

Figure 2-18. Oil Dri[®] stress versus density curves.



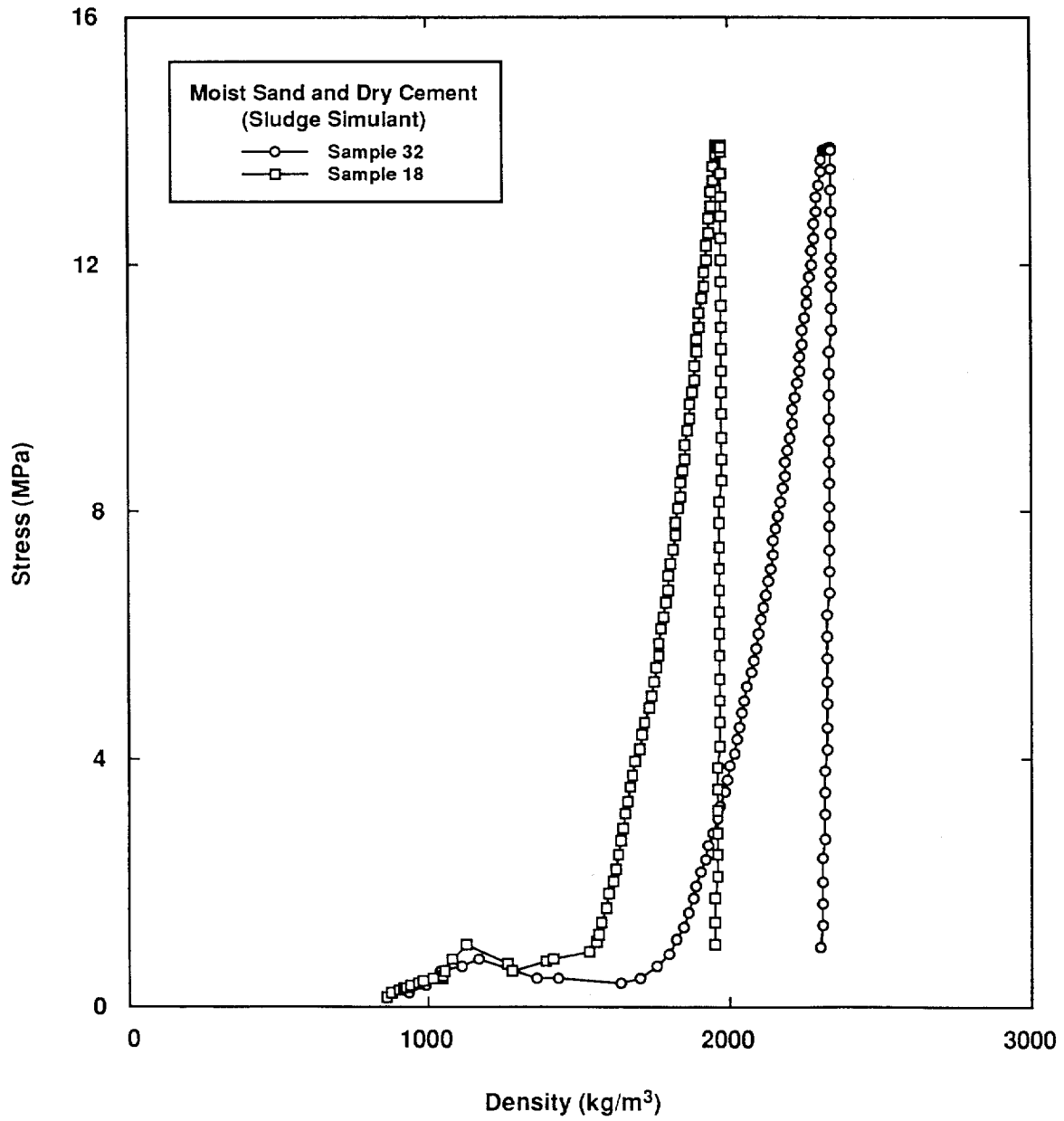
TRI-6345-34-0

Figure 2-19. Modified Oil Dri[®] stress versus density curves.



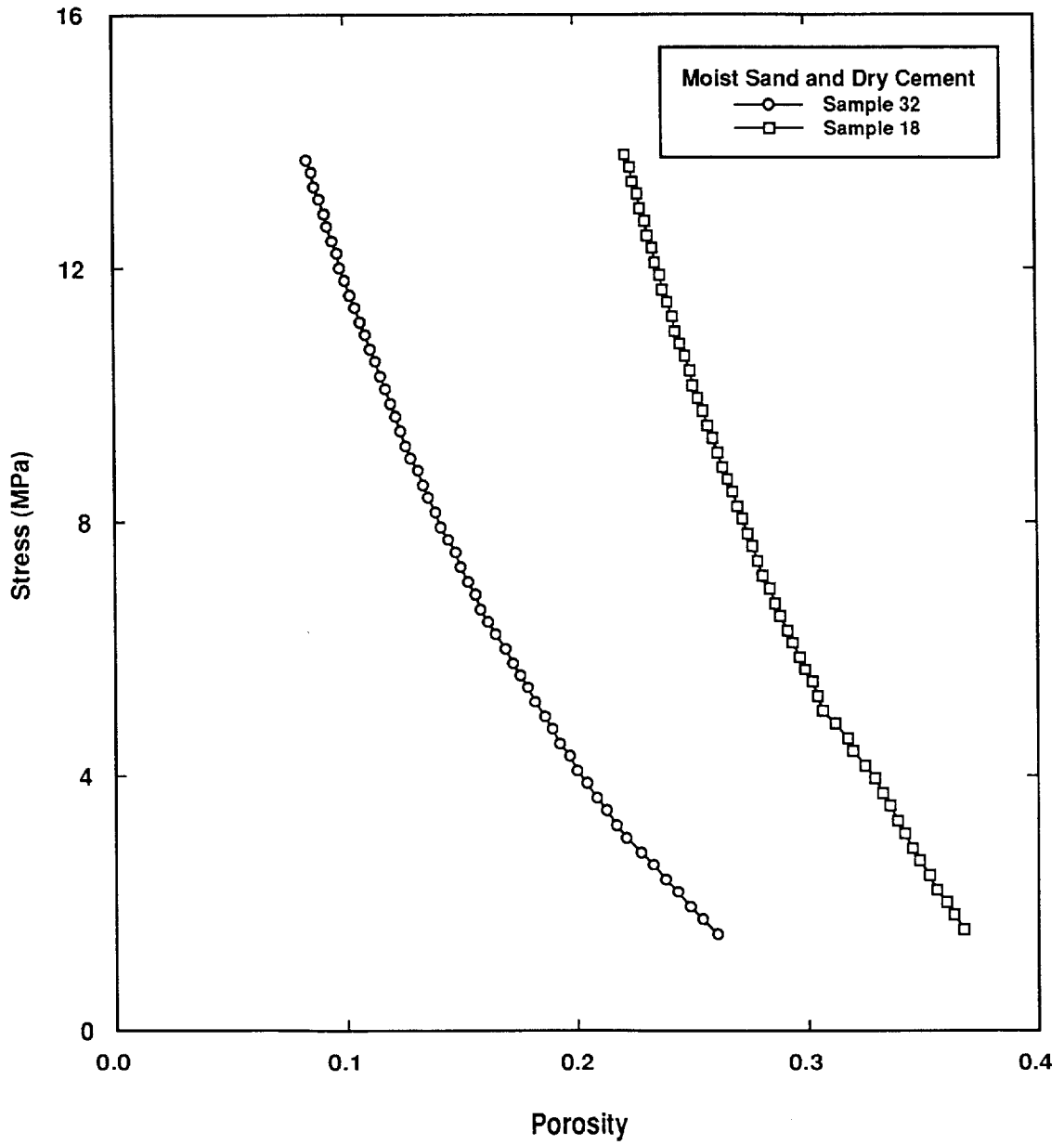
TRI-6345-35-0

Figure 2-20. Compaction curves for sorbents.



TRI-6345-36-0

Figure 2-21. Moist sand and dry cement (sludge simulant) stress versus density curves.



TRI-6345-37-0

Figure 2-22. Modified moist sand and dry cement (sludge simulant) stress versus porosity curves.

Compaction strains in the wood and cloth samples are more time-dependent than the other samples, as illustrated by the plateau of the curve for sample #30 in Figure 2-4. Therefore, the porosity of these samples is predicted to continue to decrease to less than 0.16 with time at constant stress, using the power law relationship, a correction that has been incorporated into the recommended compaction relationship (Figure 2-5). Estimated densities corresponding to three months and 200 years at constant stress are 1010 kg/m³ and 1100 kg/m³, respectively, based on the power law creep model. While the latter value is equal to the value assumed for the theoretical solid density of the mixture, the undefined uncertainties in both values and the variability of the results are more than sufficient to make questionable any implication that the mixture is compacted to theoretical solid density in 200 years.

An indication of the variation in compactibility of wood and cloth waste is shown in Figure 2-6. This figure shows that wood in the form of sawdust showed the greatest compaction, and 1" wood cubes were the least compactible. The curve for wood cubes and cloth lies between these two bounds, probably because cloth is pliant and fills up void space between pieces of wood. This mixture was considered more typical of cellulosic waste than cloth and sawdust or just wood cubes and was selected for further analysis.

Representation of the results from compaction tests on the wood and cloth component of waste by a mathematical equation is useful for additional analysis. The original curve, without correction for time-dependent deformation, is:

$$\sigma = -13.6 \ln n - 2.69,$$

where n is the porosity and σ is in psi. When a correction for creep (based on the power law model) is added, the equation becomes:

$$\sigma = -8.05 \ln n - 0.71.$$

For a given stress and estimated solid density for the mixture, density values (including correction for creep) are:

$$\rho = \rho_s(1 - \exp(-(\sigma + 0.71)/8.05))$$

The value of the density of cellulose at $\sigma = 13.8$ MPa (2000 psi) is 920 kg/m³.

2.4.2 PLASTICS

Samples #12 and #26 were described as a mixture of 40% by weight intact (small) and cut up (large) polyethylene bottles with caps; 40% by weight PVC conduit of various diameters with fittings (loose); 20% by weight surgical gloves (Mixture #6: 1200 kg/m³ solid density). Stress-density curves for these samples are shown in Figure 2-7. The data, plotted in Figure 2-8, show that compaction is to final porosities of about 0.16 at 13.8 MPa (2000 psi). The porosity is predicted to continue to decrease to less than 0.11 when correction is made for the change in density at constant stress, using the power law model. This correction has been incorporated into the recommended compaction relationship shown in Figure 2-7. Estimated porosities using the exponential law, corresponding to three months and 200 years at constant stress, are 0.063 and 0.019, respectively.

Figure 2-9 shows that the variations in compactibility for various forms of plastic are small. Aside from fluctuations from sample to sample, which appear normal, all curves show about the same compressibility near 13.8 MPa (2000 psi). Some minor differences exist at low stress levels, but these do not appear to influence later compaction.

An equation for the experimental results of compaction tests on the plastics component of waste has also been defined. The original curves, without correction for time-dependent deformation, are:

$$\sigma = 28.3 \exp(-4.525 n), \quad \sigma > 1.65 \text{ MPa},$$

$$\sigma = -7.49 n + 6.37, \quad \sigma < 1.65 \text{ MPa},$$

where n is the porosity and σ is in MPa. The linear relationship for $\sigma < 1.65$ MPa was added because subsequent analysis showed that the exponential relation gave an unrealistic stress when n approached 1 in value. When a correction for creep (using the power law model) is added, the equations become:

$$\sigma = 21.5 \exp(-4.179 n), \quad \sigma > 1.75 \text{ MPa},$$

$$\sigma = -7.31 n + 6.14, \quad \sigma < 1.75 \text{ MPa}.$$

For a given stress and estimated solid density for the mixture, density values (with creep) can be estimated from:

$$\rho = \rho_s(1 + \ln(\sigma/21.5)/4.179), \quad \sigma > 1.75 \text{ MPa},$$

$$\rho = \rho_s(1 + (6.14 - \sigma)/7.31), \quad \sigma < 1.75 \text{ MPa}.$$

The value of the density of plastics at $\sigma = 13.8 \text{ MPa}$ (2000 psi) is 1030 kg/m^3 .

2.4.3 METALS

Samples #14 & #28 were described as 2.5 cm (1") dimension cut-up steel, copper, lead, and aluminum scrap (thin-walled conduit, curtain rods, light hardware (avoiding perfectly flat pieces), some nuts, small pipe fittings, nails). The differences in the stress-density curves for these samples (Figure 2-10) is directly attributable to their differences in estimated solid densities (6350 kg/m^3 vs 8200 kg/m^3). Sample #28 had more lead in it.

An interesting feature of the metals compaction results was that the best mathematical fit to the data was a linear relationship between stress and density. This observation is interpreted as evidence that compaction was to a large extent controlled by bending and buckling of the various components. While plastic deformation occurs at the hinge points, a large portion of the metal parts remains elastic. Post-test examination of the samples also indicates considerable spring back of the material upon removal of the load. Although the density curves for the samples appear quite different (Figure 2-10), the data are more consistent when the density data are converted to porosity (Figure 2-11). This conversion shows that when differences in solid density are normalized, the results of the two tests are similar.

Metallic samples #17 & #29 were similar to Samples #14 & #28, with the exception that they contained metal up to 7.6 cm (3") dimension. Estimated solid densities were 7600 kg/m^3 and 6420 kg/m^3 . The compaction curves for these samples were also linear (Figure 2-12), but more variable because bridging of load occurred between the more massive pieces of scrap. Waviness in the curves is attributed to buckling of a dominant piece of scrap, followed by a period of easy collapse until another stiff spot is encountered and repetition of the cycle. The stress-porosity curves (Figure 2-12) also were more consistent than the density curves and provide a better representation of the compaction response of the samples.

The experimental results from compaction tests on the metals component of waste can be represented by the equation:

$$\sigma = -70.3n + 57.9,$$

where n is the porosity and σ is in MPa. The constants in this equation are a simple average of the constants of the linear relationships for the individual samples, based on an average value of 7110 kg/m^3 for the solid density. For a given stress and estimated solid density for the metal mixture, ρ_s , densities can be estimated using the relationship:

$$\rho = \frac{\rho_s}{70.3} (\sigma + 12.4).$$

Any correction for the change in density at constant stress during the tests, according to the power law model, has been neglected in these equations because it would change the porosity at 13.8 MPa (2000 psi) by less than 1%. Such an adjustment would be much less than the variations from test to test. Corrections using the estimated changes for three months and 200 years are no more than 3% and are likewise considered insignificant. The value for the porosity of metals at $\sigma = 13.8 \text{ MPa}$ (2000 psi) is 0.61.

Figure 2-13 illustrates the extent of variability of the metal waste compaction results. Sample #14 showed the greatest compaction and sample #29 showed the least. The recommended or base curve shown in the figure was calculated using the estimated solid density of 7140 kg/m^3 , which was the average solid density for the four samples. The different curves shown in Figure 2-13 reiterate that unlike plastic waste, the compactibility of metal waste is very sensitive to its initial geometric form.

2.4.4 SORBENTS

2.4.4.1 Dry Portland Cement

Samples #16 and #25 were dry Portland cement. Stress-density curves are shown in Figure 2-14. Porosity data plotted in Figure 2-15 (3000 kg/m^3 solid density) show that compaction is to final porosities of about 0.32 (2000 kg/m^3 density) at 13.8 MPa (2000 psi). Compaction was virtually time-independent.

The experimental results from compaction tests on dry Portland cement are represented by the equations:

$$\sigma = 15700 \exp(-21.9 n), \quad \sigma > 1.6 \text{ MPa},$$

$$\sigma = -35.2 n + 16.2, \quad \sigma < 1.6 \text{ MPa},$$

where n is the porosity and σ is in MPa. For a given stress and solid density, ρ_S , in kg/m^3 , density values in kg/m^3 can be estimated from:

$$\rho = \rho_S(1 + \ln(\sigma/15700)/21.9), \quad \sigma > 1.6 \text{ MPa},$$

$$\rho = \rho_S(\sigma + 19.0)/35.2, \quad \sigma < 1.6 \text{ MPa}.$$

The value of the density of Portland cement at $\sigma = 13.8$ MPa (2000 psi) is about 2040 kg/m^3 .

2.4.4.2 Vermiculite

Samples #9 and #20 were vermiculite. Stress-density curves are shown in Figures 2-16 and 17. Changes in density with time at constant stress, according to the power law model, were too small to consider. Porosity curves were not computed because a suitable value for the theoretical solid density of vermiculite was not available.

The experimental results from compaction tests on vermiculite can be represented by the equation:

$$\sigma = 0.415 \exp(0.001432 \rho),$$

where σ is in MPa and ρ is in kg/m^3 . For a given stress, density values in kg/m^3 can be estimated from:

$$\rho = \ln(\sigma/0.415)/0.001432.$$

The value of the density of vermiculite at $\sigma = 13.8$ MPa (2000 psi) is 2450 kg/m^3 .

2.4.4.3 Oil Dri

Samples #13 and #21 were Oil Dri[®] a commercial oil sorbent. Stress-density curves for these samples, in Figures 2-18 and 19, were very similar to those for Portland cement, although the final densities were much less. Compaction strains were also observed to be virtually time-independent.

The experimental results from compaction tests on Oil Dri are represented by the equation:

$$\sigma = 0.00318 \exp(0.00728 \rho),$$

where σ is in MPa. Density values in kg/m^3 can be estimated from:

$$\rho = \ln(\sigma/0.00318)/0.00728.$$

The value of the density of Oil Dri at $\sigma = 13.8$ MPa (2000 psi) is 1150 kg/m^3 . A comparison between Portland cement, vermiculite, and Oil Dri in Figure 2-20 shows that these three most widely used sorbents have quite different compaction responses.

2.5 Moist Sand and Dry Cement

Samples #18 and #32 were layered mixtures of moist sand and dry cement, simulating inorganic sludge. Several layers of each component were present in each sample, with the thickness of the sand layers at least equal to or as much as 2 times the thickness of the cement layers. Stress-density curves for these samples are shown in Figures 2-21 and 22. The results differ because sample #32 was tested almost immediately after preparation, whereas sample #18 was tested more than a day later. It is likely that some of the water in sample #18 migrated to the cement, setting it, and making compaction more difficult; therefore, additional testing may be warranted before confidence in a compaction curve can be established. However, sludges represent a smaller portion of TRU waste by volume and therefore may not require as precise a definition of their compaction response as is required for combustible and metallic waste.

2.6 Composite Curves for Metallic and Combustible Waste

Composite compaction curves for different waste categories were constructed from the compaction curves of the individual waste components, using the methods outlined earlier. For combustible waste, the average weight of the contents of a 55-gallon drum is estimated to be about 40 kg (88.1 lbs), and has the contents described in Table 2-9. Approximately 9% of the waste is metallic with a solid density, according to Section 2.4.3, of 7110 kg/m^3 .³ The state of compaction of the waste at a given stress level was estimated by adding the total volumes and void volumes of the individual waste components. The composite compaction curve for combustible waste, estimated in this manner, is shown in Figure 2-23. The average value for the solid density of combustible waste is 1330 kg/m^3 (Section 2.3.2).

3. According to Clements et al. (1985), the actual inventory by weight was 4% tantalum, 64% steel, 7% lead, and 25% other metals such as aluminum and copper. The solid density for this mixture is 6600 kg/m^3 .

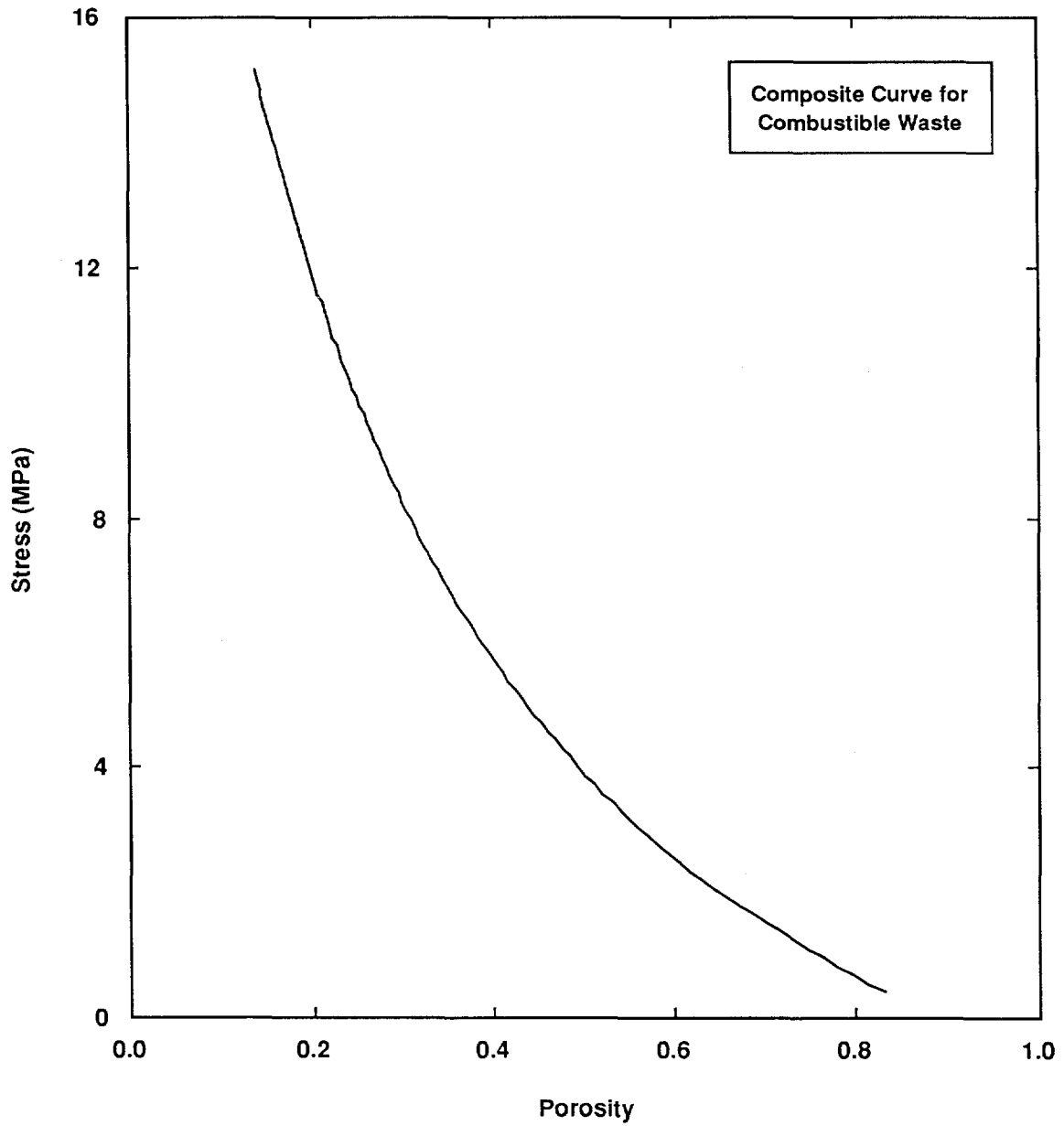
TABLE 2-9. TEST MATERIALS FOR DRUM COLLAPSE TESTS

Material No.	Material Type	Material Description	
1	Combustible Wastes	Metal	9%
		Fiber	37%
		Plastics	45%
		Sorbents	9%
2	Metallic Wastes	Metal	83%
		Fiber	2%
		Plastics	10%
		Sorbents	5%
3	Sludge Wastes	Sludge	91%
		Plastics	1%
		Sorbents	8%

Notes: Individual materials were as follows:

- Metal: Up to 12" dimension cut-up steel, copper, lead, and aluminum scrap (conduit, fittings, junk). Approximately 60% of the metal for each drum was steel.
- Fiber: A mixture of 60% by weight pine wood cubes or pieces (maximum dimension 12" long x 3" wide x 1" thick: 50% of the pieces full size, the remainder equal to or less than 6" long): 40% by weight rags.
- Plastics: A mixture of 50% by weight polyethylene bottles with caps and other pieces of polyethylene: 40% by weight PVC conduit and fittings: 10% by weight surgical gloves.
- Sorbents: 50% by weight Oil Dri[®] (baked clay pellets): 50% Portland cement. The materials were not mixed.
- Sludge: A layered mixture of moist sand and dry cement, with the thickness of the sand layers equal to, up to twice, the thickness of the cement layers.

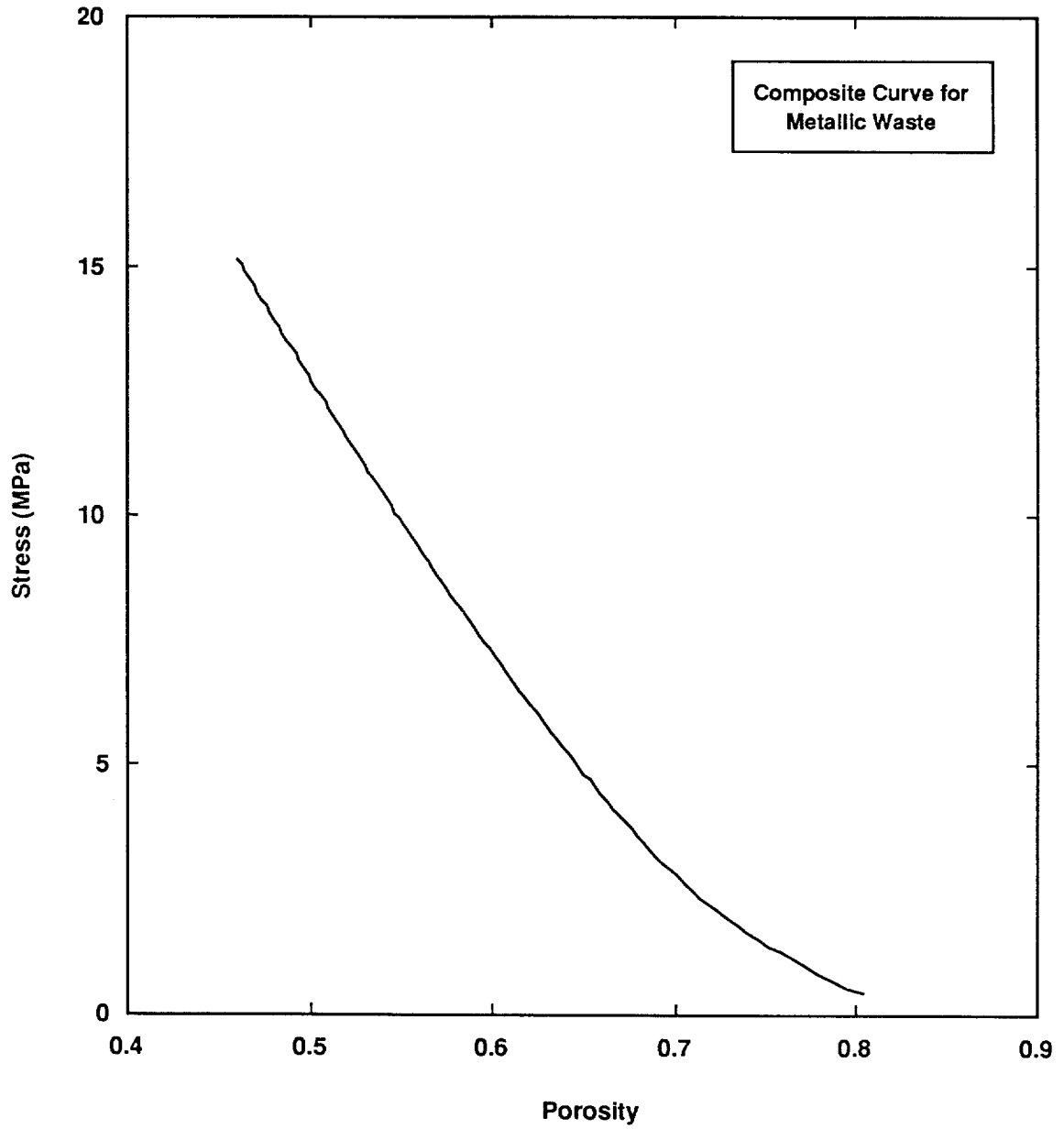
All commercial grade materials were obtained from local retailers or standard manufacturing or laboratory suppliers.



TRI-6345-38-0

Figure 2-23. Composite compaction curve for combustible waste.

For metal waste, the average weight of the contents of a 55-gallon drum is estimated to be about 64.5 kg (142 lbs) and has the contents described in Table 2-9. About 83% by weight of this waste is composed of metals. The composite compaction curve for metallic waste, estimated in this manner, is shown in Figure 2-24. The average value for the solid density of metallic waste is 4270 kg/m³.



TRI-6345-39-0

Figure 2-24. Composite compaction curve for metallic waste.

3.0 DRUM COMPACTION MEASUREMENTS

3.1 Objectives

The objective of the second part of the testing program was to acquire collapse data for drums filled with different materials. These full-scale loading tests were conducted on single drums of waste by crushing them along their axis of symmetry with no restriction on lateral expansion. Loading continued until an axial stress of 13.8 MPa was exceeded. DOT-17C 55-gallon drums with standard 90 mil polyethylene liners were used in all tests.

An empty drum was tested first for baseline information and to check out the mechanical systems and quality-assurance procedures. Next, a total of 10 waste-filled drums representing of combustible, metallic, and sludge waste were compacted. No lateral restraint was placed on the drums during the tests. Data acquired during compaction usually consisted of the force exerted on the top of the drum and its height.

A special feature of the tests incorporated both photographic and VCR coverage at prescribed time intervals to determine approximate drum volumes. Collapse was expected to be nonuniform, but only the sludge drums showed evidence of extensive bulging. Both the combustible and metallic waste drums were observed to compact uniformly with little indication of lateral deformation. Bulging was probably slight because tensile hoop stresses within the walls of the drums were sufficient to restrict any lateral movement of the waste.

3.2 Materials

As noted in Section 2.0, the materials tested in Part I of the program are present in various combinations in the waste. Typical waste combinations were classified as follows:

- | | |
|--------------------|--|
| Combustible Waste: | Fiber and plastic, with smaller quantities of metals and sorbents |
| Metallic Waste: | Metals, with smaller quantities of fiber, plastics and sorbents |
| Sludge Waste: | Inorganic or organic sludge with smaller quantities of plastics and sorbents |

These mixtures formed the basis for the simulated waste used in this phase of the test program (summarized in Table 2-9). The drum tests are summarized in Table 3-1.

All materials were tested in their "as purchased" condition; thus, paint was not removed from the surfaces of metal objects, such as curtain rods, before they were cut up for sample material. Most of the materials were purchased new from commercial sources. The metal wastes were made up of a mixture of new and used items, the latter being sorted to find appropriate items in terms of composition, size, and shape. Materials were weighed and logged on the appropriate sample sheets, and all materials were photographed before testing. Sample materials were placed into the 90 mil rigid plastic liners in a random manner and pressed down until the lid could be attached. The liners were placed inside the steel drums, and the threaded bung hole on the lid was left open to allow air to escape as the drum was crushed.

The drums were placed in the test machine and loaded to a stress of 13.8 MPa (2000 psi) in a series of 7.6 to 10.2 cm (3 to 4") strokes, 7.6 cm (3") spacers being inserted under the load cell after each stroke to increase the displacement range of the testing machine. All tests were run at a constant axial deformation rate of 0.9 mm (0.035") per second. During the tests axial load and drum height were monitored on the computer based data acquisition system.

"Spring-back" was a problem that developed as waste filled drum testing proceeded. Some of the drums, after being crushed down 10.2 cm (4") during the loading, would spring back as much as 5.1 cm (2") during unloading, making it impossible to insert the next 7.6 cm (3") thick spacer into the stack. Two extendable rods attached to the top platen of the test frame were eventually used to hold the platen in place on the drum during the spacer insertion cycle, thus preventing spring-back. The drums also tended to shift position on the lower frame platen during the tests. This shifting, or operator repositioning of the drums (and sometimes the apparent "repacking" of the waste during the unloading and reloading) caused jumps in the data curves. Since these jumps were test-machine related, they were manually removed (to the extent possible) during data reduction.

3.3 Description of Analysis

3.3.1. METHOD OF INTERPRETATION OF RESULTS

The approach for analyzing the drum collapse results estimated drum collapse as a function of load from the individual compaction results for each material present in drum. Collapse predictions were then compared with

TABLE 3-1. DRUM COLLAPSE TEST SUMMARY

TEST NO.	MATERIAL NO.	WASTE WEIGHT (lb.)	MATERIAL DESCRIPTION	MATERIAL TYPE
01	1	97.9	Metals 9%, Plastics 45%, Fibers 37%, Sorbents 9%	Combustibles
02	2	151.88	Metals 83%, Plastics 10%, Fibers 2%, Sorbents 5%	Metals
03	2	152.0	Metals 83%, Plastics 10%, Fibers 2%, Sorbents 5%	Metals
04	2	151.99	Metals 83%, Plastics 10%, Fibers 2%, Sorbents 5%	Metals
05	2	151.98	Metals 83%, Plastics 10%, Fibers 2%, Sorbents 5%	Metals
06	3	392.99	Sludge 90%, Plastics 3%, Sorbents 7%	Sludge ¹
07	3	392.99	Sludge 90%, Plastics 3%, Sorbents 7%	Sludge ²
08	1	97.91	Metals 9%, Plastics 45%, Fibers 37%, Sorbents 9%	Combustibles
09	1	97.9	Metals 9%, Plastics 45%, Fibers 37%, Sorbents 9%	Combustibles
10	1	97.9	Metals 9%, Plastics 45%, Fibers 37%, Sorbents 9%	Combustibles

1. Cement layered with wet sand, allowed to set overnight (10 hrs)

2. Cement layered with wet sand, tested immediately

actual test results to determine the accuracy of the predictive method. The amounts of the different materials in each category of waste, i.e., how much fiber, plastics, metals, and sorbents will actually be in a typical type of waste, are expected to change as more information about the waste becomes available. If the response of the drums can be predicted from the properties of their contents, then adjustment of the drum-collapse characteristics for future changes in waste content will become more credible.

Four types of information were needed in order to predict the behavior of the full-scale drum-crush tests from the results of the material compaction tests. First, compaction equations for each waste component were required. These were defined (Section 2.0) in terms of densities corresponding to a given stress. The no-creep equations were used because the duration of the drum-crushing tests was too short to allow any significant time-dependent consolidation of the waste. Second, the weights of each component of the drum contents had to be defined in order to determine how much is present. If the initial volumes of each component are given, initial densities also need to be specified in order to compute weight fractions and the total weight of each type of drum. Third, theoretical solid densities were needed, in order to estimate solid volumes. The fourth type of information is defined in Section 3.3.2.

3.3.2 RING FORMATION IN THE DRUMS DURING COLLAPSE

The last information needed for drum collapse predictions was the way that the drums collapse during the tests. Cross-sections of the drums showed that they collapsed uniformly and independently of the drum contents, at least during the early parts of the tests, and formed crushed rings around the waste.¹ Because the drum appeared to crush straight down, without significant change in diameter, the assumption was made for data reduction purposes that a constant cross-section could be assumed in calculating drum densities.

To test this assumption, two tests were performed by filling the voids in the filled waste drum with water before compaction. During the crush down, the water was allowed to move through tubing to another drum where the volume was measured to define the height versus volume of the waste relationship. These tests indicated that throughout most (about 2/3) of the crush down, the constant cross-section assumption was reasonable. For about the first half of the crush down, the cross-section was less than original, suggesting that the drum folded inward. Later, the volume reduction was less than assumed, showing that the drum was starting to bulge outward as compaction continued. The tendency of the curve of water-out versus drum

-
1. Buckling patterns appearing along "rolls" (strengthening hoops) in the drum were sinusoidal in shape, with five full sine waves at each roll. The sine wave pattern stayed stationary but grew in amplitude as the drum collapsed. After the pattern "matured," at a first ridge (generally the center of the drum), a second sinusoidal pattern would start at a second location on the drum (usually the bottom of the drum). The sine wave would contain five full waves as before, and the wave pattern would be a simple vertical translation from the wave pattern developed before. The third wave pattern would form like the second, at still another location on the drum.

height to reach a limit suggested that water would have eventually stopped coming out of the drum. This point was never reached in our tests; leaks either in the seal or the lid of the drum required an end to the water-collection portion of the test.

In contrast to the tests on simulated combustible and metallic waste, ring formation was not obvious during collapse of the sludge drums because both their total amount of collapse and the compressibility of the material was less. Compaction of the waste caused the drums to bulge outward slightly at the center, stretching the steel drums circumferentially and eventually causing them to break open at the seam, at which point some of the material near the seam would extrude from the drum and the tops of the drums would tilt downward towards the seam opening. However, the assumption was made, in reducing the sludge drum collapse data, that the drum crushed straight down without change in diameter. Therefore, the reduced data is truly representative of the early portions of the tests when bulging was minimal. The stress required to cause additional collapse rose so rapidly during the latter part of the test, however, that the constant cross-section assumption was probably adequate as a first approximation during the later portions of the tests.

3.3.3 DRUM COMPACTION CURVES

The compaction curve for a full-size drum will be defined by computing the degree of drum collapse in terms of the fraction of its original height, h , assuming no significant lateral deformation of the waste-filled drum during collapse. Collapse may be estimated in three different ways. The first method is to assume that the steel-drum material is no different than metal in the waste. This assumption makes the drum compaction response the same as the compaction response of metallic materials within the drum. Estimates of drum collapse using this assumption do not produce very good agreement with experimental observations.

The second computation method is suggested by observations of the final states of the drum by sectioning them post-test. These sections showed that practically no waste intruded into the drum rings during collapse. For the ring model suggested by these observations, an inner cylinder of waste would be assumed to support part of the total load on a drum, and a ring of drum material supports the remainder. Analysis of this configuration was possible because the plates loading the drum were essentially rigid, thus causing both the ring and the waste to have the same compacted height at any given time during the test. The collapse for the ring was assumed to be the same as the load-deformation curve for collapse of an empty drum.

Estimates of the load required to collapse a drum to a given fraction of its original height, h , assuming no significant lateral deformation of the waste-filled drum during collapse, were made in the following manner. The width of the ring, w , was assumed to be 6.35 cm (2.5") from post-test examination of the crushed drums. Since, the drum is approximately 0.61 m (24") in diameter, with a cross-sectional area of 0.292 m^2 (452 in^2), the cross-sectional area of the waste is 0.183 m^2 (284 in^2). This information is applied as follows: (1) for a given value of h , the density of the waste mixture, ρ_w , can be computed, and the corresponding stress to achieve this state of compaction, σ_w , determined from its compaction curve; (2) using the same value of h , the load, L_d , required to collapse an empty drum to h can also be defined from its collapse curve; (3) therefore, the average stress acting on the drum is:

$$\sigma = (L_d + 0.292 \sigma_w)/0.183,$$

and the average density is:

$$\rho = (W_w + W_d)/(0.21 h),$$

where W_w is the weight of the waste in kilograms, W_d is the weight of the drum in kilograms, and 0.21 m^3 is the approximate initial volume of the drum.

A third method, completely different from the ring model, is to neglect the presence of the drums entirely. Actually, this alternative is the other bound of the second method. In the second method, $w = 6.35 \text{ cm}$, an upper bound, in the third method, $w = 0$, the lowest bound of w . For this assumption, the average stress on the drum is:

$$\sigma = \sigma_w,$$

and the average density is:

$$\rho = W_w/(0.21 h).$$

Although this assumption makes the least sense from a physical viewpoint, comparison of predictions with the test results show that it produces the best agreement.

3.4 Definition of Waste Material for the Drum Tests

After review of the results of the material compaction studies, Mixture 3 (Table 2-1) was selected as the most appropriate simulated cellulosic waste for use in the drum tests. The plastics component was Mixture 6. Mixture 12 was modified for the metallic component by increasing the size of cut-up steel, copper, lead, and aluminum scrap (conduit, pipe fittings, junk) from 7.6 cm (3") to 30 cm (12") and assuring that over 60% of the scrap was steel.

Although drums in the actual inventory contain either Portland cement, vermiculite, or Oil Dri as sorbents, as a simplification all sorbents were modeled using the properties of Portland cement. The sludge was a layered mixture of moist sand and dry cement, as specified by Mixture 13.

These mixtures were placed in layers in the drums, inside the plastic drum liners (Table 2-10). The average actual weight of the contents of combustible waste drums was 44.5 kg (98 lbs), and the contents consisted of 0.09 weight fraction metals, 0.45 weight fraction plastics, 0.37 weight fraction cellulose, and 0.09 weight fraction sorbent, which was assumed to be Portland cement.² When the weight of the drum liner (7.0 kg or 15.4 lb measured weight) was added to the plastics component of the combustible waste, the composition of the contents changed to 0.08 weight fraction metals, 0.52 weight fraction plastics, 0.32 weight fraction cellulose, and 0.08 weight fraction sorbents. A solid density of 7110 kg/m³ was assumed for the metals in this waste. When the weight of the drum was added to the waste contents (27.9 kg or 61.4 lb measured weight empty), the composition changed to 0.40 weight fraction metals, 0.34 weight fraction plastics, 0.21 weight fraction cellulose, and 0.05 weight fraction sorbent. For this option, the solid density of the metallic components was the combination of 13% by weight (the waste) at 7110 kg/m³ and 87% by weight (the drum) at 7860 kg/m³, or 7750

2. This weight is slightly larger than the average drum weight of 40 kg (88.1 lbs) for combustibles suggested by Butcher (1989), but is considered acceptable because the weight fractions of the waste components are the same. Similarly, the metallic waste drum contents are 69 kg (152 lbs) as opposed to 64.5 kg (142 lbs). Drums in the actual inventory contain either Portland cement, vermiculite, or Oil Dri as sorbents. However, no attempt was made to make the sorbent curve representative of the actual portions of each material in the inventory.

kg/m³. With these changes, and the average solid density for the entire drum was 1920 kg/m³ (Section 2.3.2).³

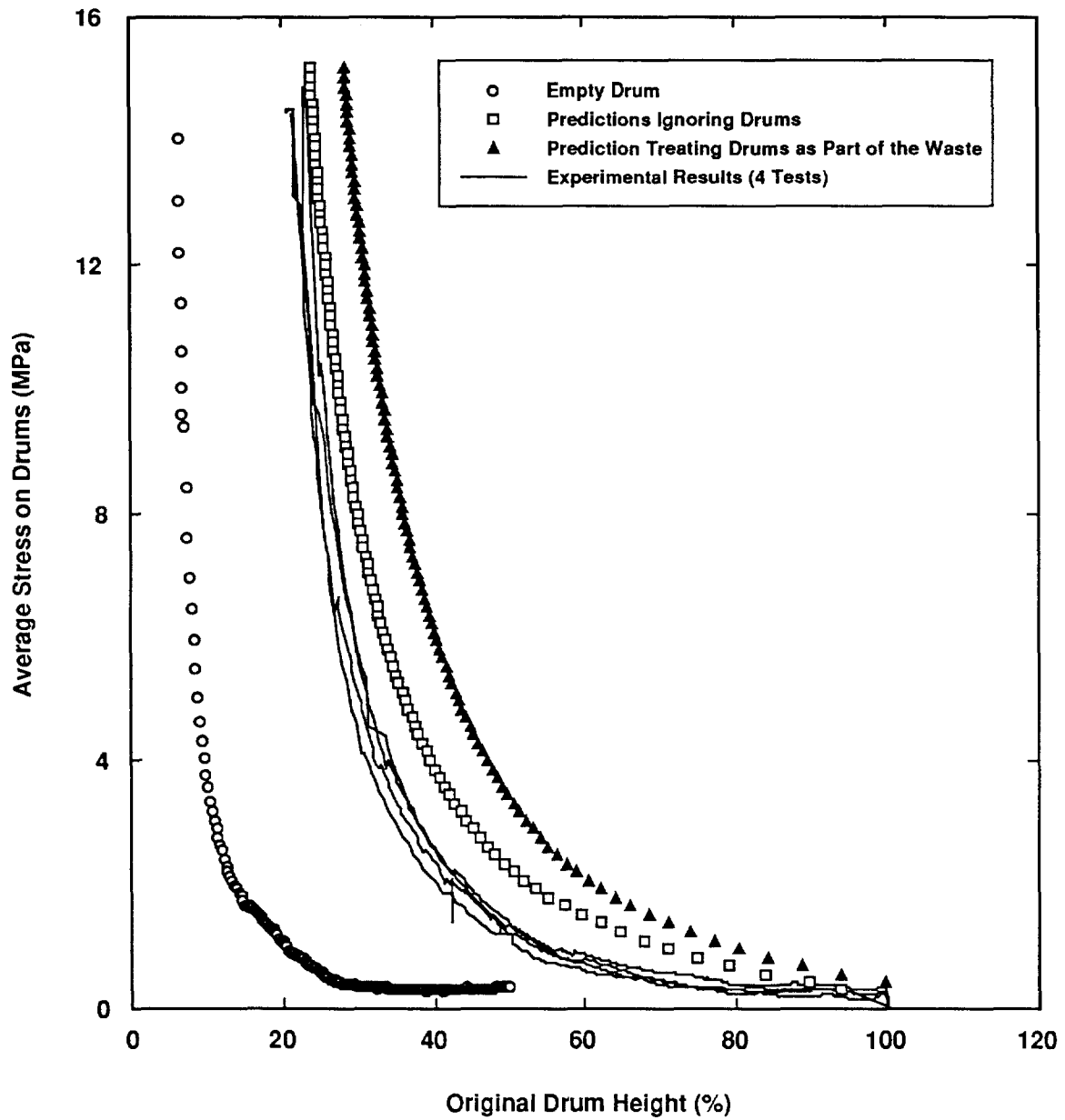
The contents of metallic waste drums had an actual weight of 69 kg (152 lbs) and were composed of 0.83 weight fraction metals, 0.10 weight fraction plastics, 0.02 weight fraction cellulose, and 0.05 weight fraction sorbent, which was assumed to be Portland cement. When weight of the drum liner was added to the plastics component of the metallic waste, the composition changed to 0.75 weight fraction metals, 0.18 weight fraction plastics, 0.02 weight fraction cellulose, and 0.05 weight fraction sorbents. When the weight of the drum was added to the metallic waste, the composition changed to 0.82 weight fraction metals, 0.14 weight fraction plastics, 0.01 weight fraction cellulose, and 0.03 weight fraction sorbents. The solid density of the metallic components was weighted between 67% by weight (the waste) at 7110 kg/m³ and 33% by weight at 7860 kg/m³ (the drum) to give an average of 7340 kg/m³, and the average solid density for the entire drum became 4040 kg/m³.

Since ring formation was not apparent during sludge drum collapse, the drum and drum liner weights were combined with the weights of the respective waste components. When the contents of sludge waste drums, assumed to have an actual weight of 179 kg (393 lb) by Butcher (1989) were combined with the 8.7 kg (19.3 lb) weight of the liner and the 29.3 kg (64.5 lb) weight of the drum, they totaled 217 kg. The drum composition was 0.76 weight fraction sludge, 0.13 weight fraction metals, 0.04 weight fraction plastics, 0.0 weight fraction cellulose, and 0.07 weight fraction sorbent, which was assumed to be Portland cement. The average solid density for the entire drum was 2370 g/m³.

3.5 Results

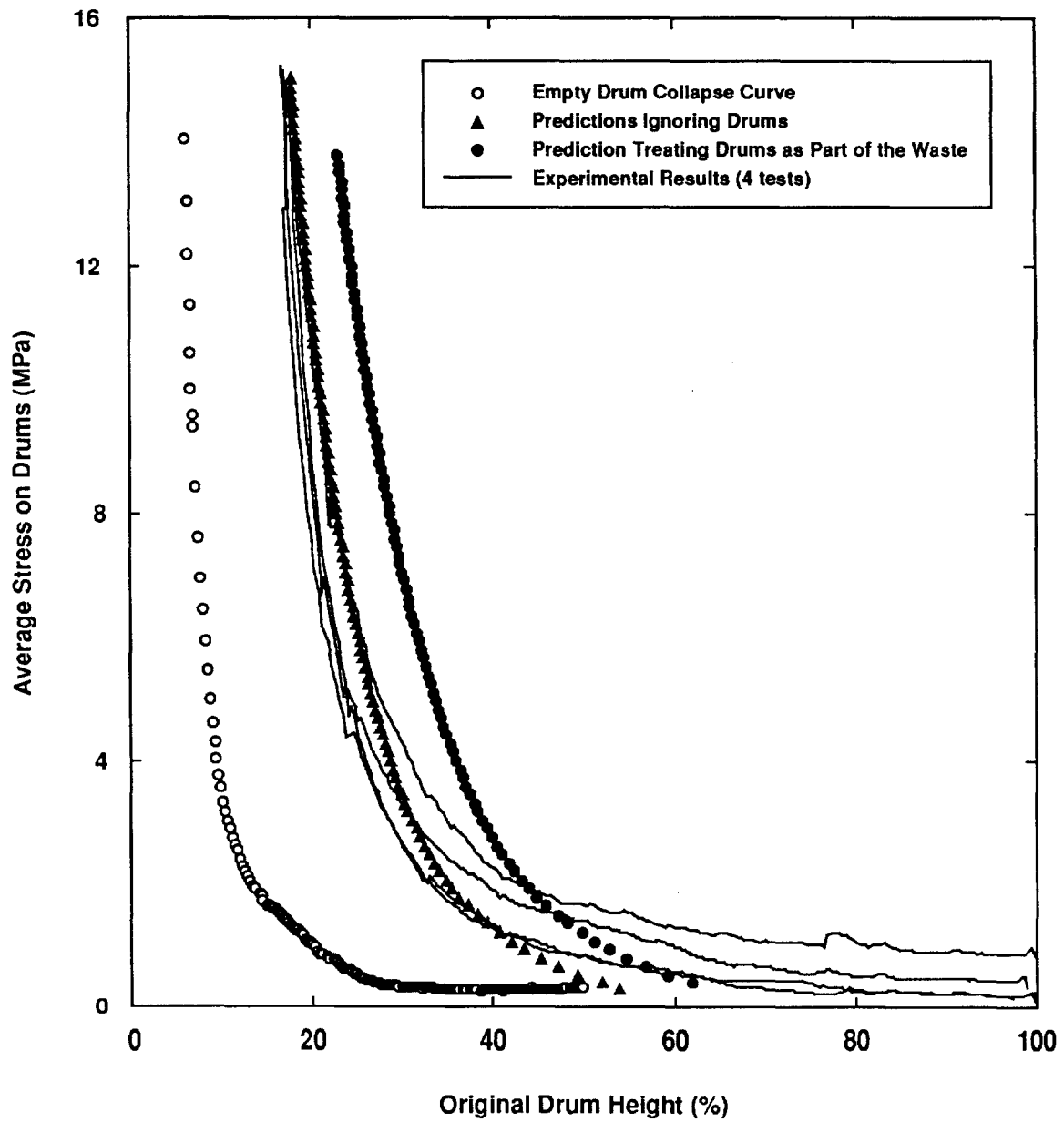
The easiest comparison of drum collapse results with predictions is in terms of the fraction of original height of the drum at a given average stress. The experimental results for simulated combustible and metallic waste are shown in Figures 3-1 and 3-2. For combustible waste the computation method based upon ring formation ($w = 6.35$ cm) gives the worst prediction, followed by the method that included the drum material as part of the waste. The best agreement is obtained from the predictive method that

3. The computed value for this waste was actually 1850 kg/m³. However, this value gave a slightly negative porosity at 13.8 MPa. Therefore, the solid density was slightly increased, to remove the physical inconsistency, a procedure that is considered reasonable in view of the uncertainties in the solid densities of the respective components of the waste.



TRI-6345-40-0

Figure 3-1. A comparison between experimental results showing the relationship between applied load and state of collapse of simulated combustible waste drums (4 tests) and predictions either assuming that the drum material is part of the waste or ignoring the drum completely.



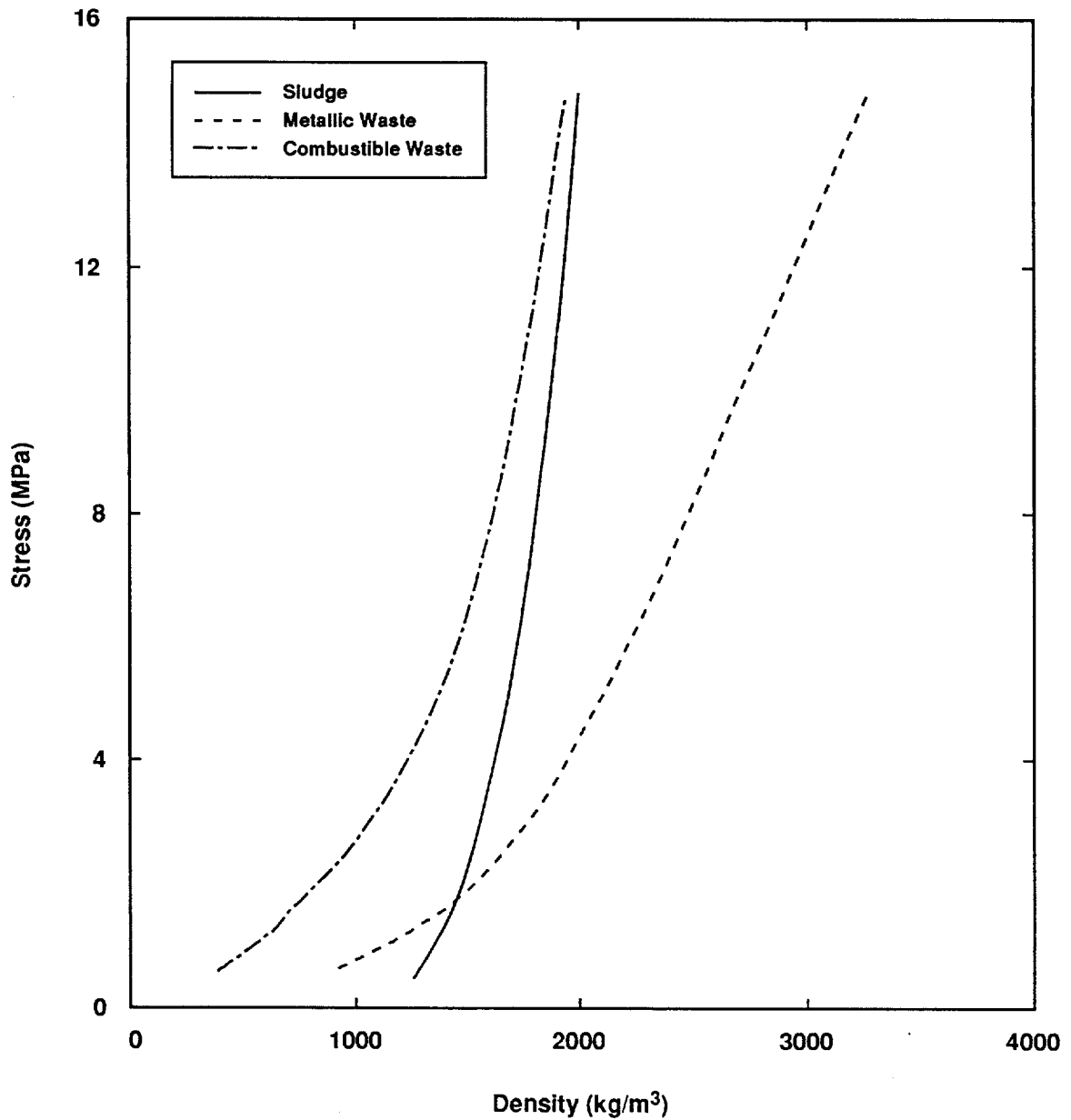
TRI-6345-41-0

Figure 3-2. A comparison between experimental results showing the relationship between applied load and state of collapse of simulated metallic waste drums (4 tests) and predictions either assuming that the drum material is part of the waste or ignoring the drum completely.

ignores the presence of the drum ($w = \emptyset$), although this assumption makes the least sense from a physical viewpoint. Similar observations apply to the metallic waste results (Figure 3-2). The curve for $w = 6.35$ cm is not present in this figure because it added little to the comparison: the curve for $w = \emptyset$, although not exact, was still the best representation of the data.

The reader is reminded that the no-creep equations were used for these predictions because the duration of the drum-crushing tests were too short to allow any significant time-dependent waste consolidation. To translate the results back into general compaction curves for combustible and metallic waste, which can be used for estimation of room and repository closure, the $w = \emptyset$ calculations were repeated using density rather than drum height for the independent variable and equations corrected for time-dependent deformation. These standard curves, shown in Figure 3-3, and the data they were obtained from, tabulated in Table 3-2, are recommended for use in calculations defining the final waste consolidation states for assessment analysis. Data values in Table 3-2 were obtained using Equation 2.3.4.1; the continuous curves in Figure 3-3 were obtained by connecting the data points with either solid or dashed lines. Curve fitting of the data with simple mathematical relationships is not reported because the available functions did not provide an accurate correlation to permit this simplification.

Interpretation of the collapse of sludge-containing drums assumed that simulated sludge was represented by Sample #18, which was moist sand and dry Portland cement (Figure 2-22), with any ring formation by the drum ignored. Another difficulty in interpreting the sludge-drum-collapse results was caused by the fact that drums started to burst during the test. Bursting was expected because dense sludge materials can exert substantial internal pressure on the drums during compaction, as indicated by discontinuities in the collapse curves between 1000 and 1500 psi (Figure 3-4). Nevertheless, intuition indicates that had breaching of the drums not occurred, the compressibility of the drums would have continued to rise steeply, as later portions of the tests indicate. Figure 3-4 also shows, however, that the estimated curve for simulated sludge drums is in approximate agreement with the experimental results and with earlier results reported by Huerta et al. (1983). The standard curve for sludge is shown in Figure 3-3, and the data for this curve is tabulated in Table 3-2. Attempts to curve fit the sludge data with simple functions did not provide an accurate enough correlation to permit such simplification.



TRI-6345-42-0

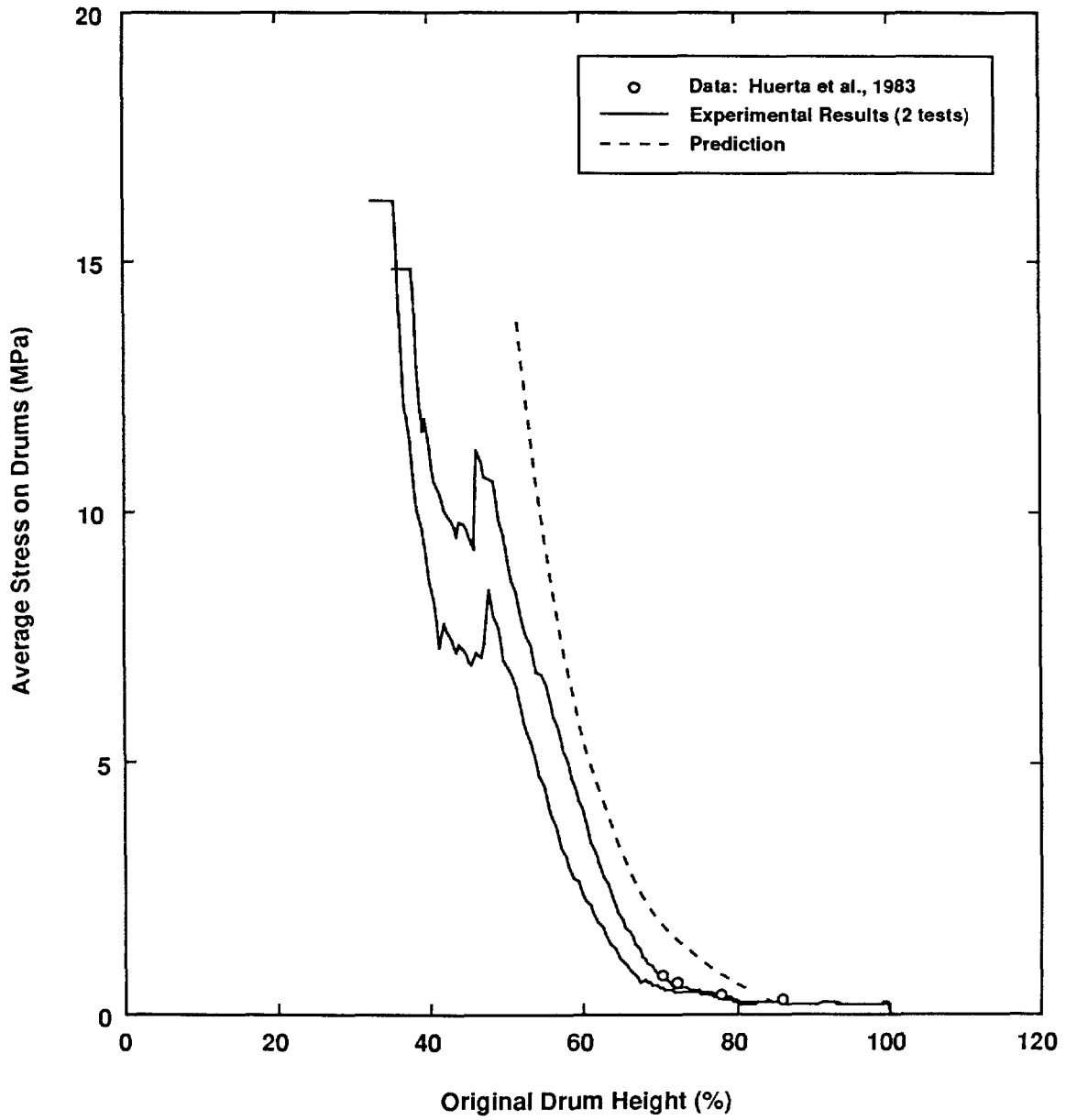
Figure 3-3. Recommended drum collapse curves for combustible, metallic, and simulated sludge wastes.

TABLE 3-2. COMPACTION CURVES

Stress MPa	Average Repository Porosity	Metallic Waste Porosity	Combustible Waste Porosity	Sludge Waste Porosity
0.4	0.765	0.805	0.830	0.549
0.6	0.722	0.783	0.801	0.410
0.8	0.696	0.768	0.776	0.394
1.0	0.672	0.755	0.752	0.377
1.2	0.649	0.741	0.729	0.363
1.4	0.628	0.729	0.706	0.350
1.6	0.607	0.717	0.683	0.338
1.8	0.588	0.706	0.661	0.328
2.0	0.570	0.696	0.640	0.318
2.2	0.553	0.687	0.620	0.310
2.4	0.538	0.678	0.602	0.302
2.6	0.525	0.670	0.584	0.296
2.8	0.512	0.662	0.567	0.289
3.0	0.499	0.655	0.552	0.284
3.2	0.488	0.649	0.536	0.278
3.4	0.477	0.642	0.522	0.273
3.6	0.467	0.636	0.508	0.268
3.8	0.457	0.630	0.494	0.263
4.0	0.447	0.624	0.482	0.258
4.2	0.438	0.618	0.469	0.253
4.4	0.429	0.612	0.457	0.247
4.6	0.421	0.607	0.446	0.243
4.8	0.412	0.602	0.435	0.237
5.0	0.404	0.596	0.424	0.231
5.2	0.397	0.591	0.414	0.228
5.4	0.390	0.586	0.404	0.224
5.6	0.383	0.581	0.394	0.221
5.8	0.376	0.576	0.385	0.217
6.0	0.370	0.572	0.376	0.214
6.2	0.363	0.567	0.367	0.211
6.4	0.357	0.562	0.358	0.208
6.6	0.351	0.558	0.350	0.204
6.8	0.345	0.553	0.342	0.201
7.0	0.339	0.549	0.334	0.198
7.2	0.334	0.544	0.326	0.195
7.4	0.328	0.540	0.319	0.192
7.6	0.323	0.535	0.312	0.190
7.8	0.318	0.531	0.305	0.187
8.0	0.313	0.527	0.298	0.184
8.2	0.308	0.523	0.291	0.181
8.4	0.303	0.518	0.285	0.179
8.6	0.298	0.514	0.278	0.176
8.8	0.293	0.510	0.272	0.174

TABLE 3-2. COMPACTION CURVES (CONCLUDED)

Stress MPa	Average Repository Porosity	Metallic Waste Porosity	Combustible Waste Porosity	Sludge Waste Porosity
9.0	0.289	0.506	0.266	0.171
9.2	0.284	0.502	0.260	0.169
9.4	0.280	0.498	0.254	0.167
9.6	0.276	0.494	0.249	0.164
9.8	0.272	0.490	0.243	0.162
10.0	0.267	0.486	0.238	0.160
10.2	0.263	0.482	0.232	0.157
10.4	0.259	0.478	0.227	0.155
10.6	0.255	0.475	0.222	0.153
10.8	0.252	0.471	0.217	0.151
11.0	0.248	0.467	0.212	0.149
11.2	0.244	0.463	0.208	0.147
11.4	0.241	0.459	0.203	0.145
11.6	0.237	0.456	0.198	0.143
11.8	0.233	0.452	0.194	0.141
12.0	0.230	0.448	0.190	0.139
12.2	0.226	0.445	0.185	0.137
12.4	0.223	0.441	0.181	0.135
12.6	0.220	0.438	0.177	0.133
12.8	0.216	0.434	0.173	0.131
13.0	0.213	0.430	0.169	0.129
13.2	0.210	0.427	0.165	0.128
13.4	0.207	0.423	0.162	0.126
13.6	0.204	0.420	0.158	0.124
13.8	0.201	0.417	0.154	0.122
14.0	0.198	0.413	0.151	0.120
14.2	0.195	0.410	0.147	0.118
14.4	0.192	0.406	0.144	0.117
14.6	0.189	0.403	0.140	0.115
14.8	0.186	0.399	0.137	0.113



TRI-6345-43-0

Figure 3-4. Simulated sludge drum collapse curves.

4.0 REPOSITORY COMPACTIBILITY

4.1 Method of Analysis

A composite compaction curve for the entire repository will be defined in this section. This calculation proceeds in the same manner as for the composite compaction curves (Section 2.3.4), but what should be a simple procedure becomes more uncertain when the data for the inventory of CH-TRU waste from the most current references are examined. The basic problem is that the inventory data from DOE/RW-0006, Rev 4, (1988), and Drez and James-Lipponer (1989), summarized in Table 4-1, are difficult to correlate. The first source reports only volume data, whereas the second source quotes only weight data and is incomplete.

4.2 Repository Inventory

4.2.1 METALS INVENTORY

Definition of how much waste will eventually be stored in the repository (Table 4-1) started with metal waste. Metal and glass waste, according to Drez and James-Lipponer (1989), is composed of 2% by weight tantalum, 68% iron and steel, 17% lead (an upper bound), 4% Copper, and 9% aluminum. Using the theoretical solid densities listed in Table 2-2, and assuming that: (1) the weight assigned to leaded gloves in Drez's inventory was assumed to be entirely due to the lead, and (2) waste in the form of paint cans was added to the total weight of iron and steel waste, although the paint cans probably are filled with stabilized sludge, this mixture is estimated to have a theoretical solid density of 7110 kg/m³.

The total amount of steel waste reported by Drez also requires some adjustment because sometimes the weights of the containers were included in the totals for metallic waste given by INEL and the Los Alamos National Laboratory (LANL), and sometimes they were not separated out. Although Drez did not attempt to adjust his summary of results for this inconsistency, it was required for estimation of repository-wide averages, and was accomplished by estimating the volumes of INEL and LANL waste, finding the number of equivalent 55-gallon drums the volumes represented, and using this information to estimate the total weight of the containers. This procedure is a poor substitute for actual information, but it represents the best estimate that is possible at present. Thus, the estimates in this report that depend upon the separation of the total weight of the metal containers from the total weights of the waste categories must be redone as soon as more definitive information becomes available.

TABLE 4-1. TRU WASTE INVENTORY ANALYSIS

	Weight kg	Volume m ³	Volume Fraction ¹	Weight of			Total Weight kg	Weight Fraction
				Container steel, kg	Plastic liners & bags, kg	Wood contain- ers		
Metals	7,330,000							
Glass	1,120,000							
Metal/Glass	8,450,000	54,000	.40	4,400,000	744,000	596,000	14,190,000	.28
Combustibles	8,590,000	55,400	.41	4,510,000	763,000	611,000	14,480,000	.28
Sludge	20,300,000 ²	25,400	.19	2,090,000	353,000	283,000	23,030,000	.44
Steel Containers	11,000,000							
Polyethylene Liners	1,550,000							
PVC liners, bags	310,000							
Wood/Fiberboard	1,490,000							
	51,700,000	134,800	1.00	11,000,000	1,860,000	1,490,000	51,700,000	1.00

1. Values of the volume fraction were computed assuming the volume of the "other" category of waste to be proportionally distributed among the three major categories of waste.

2. Estimated value.

In the absence of any better information, the total weight of the INEL and LANL containers was estimated to be 7,350,000 kg, reducing the total weight of steel waste from the value of 9,170,000 kg quoted by Drez to 1,820,000 kg. The weight of iron in the Drez inventory remained unchanged at 2,620,000 kg. The total weight of metals in the inventory was 7,330,000 kg, and the weight of glass was estimated to be 1,120,000 kg.

A comparison of the new metallic waste inventory values by Drez with previous estimates by Clements and Kudera (1985) is also of interest. Clements and Kudera's study determined that the metals inventory was 4% tantalum, 64% steel, 7% lead, and 25% other metals such as aluminum and copper, by weight, with an average solid density of 6650 kg/m³. The principal difference between the two compilations is that there is a greater amount of lead, and less aluminum and copper in the Drez inventory.

4.2.2 COMBUSTIBLES INVENTORY

For combustible waste, Drez reported that the total weight of cellulose was 4,350,000 kg, the weight of plastics was 4,180,000 kg, and other combustibles were present in the amount of 60,500 kg. In the absence of additional information, we will assume that the cellulose is composed of about 60% wood and paper and 40% cloth (Butcher, 1989), with a solid density of 1100 kg/m³ estimated from the densities quoted in Table 2-2. The category of "other" combustibles" was assumed to be 50% cellulose and 50% plastics, and a solid density of 1200 kg/m³ was assumed for plastics.

4.2.3 SLUDGE INVENTORY

The total weight of the sludges in the waste was not available at the time this report was prepared, nor was information available for estimating its solid density. Therefore, the weights of the sludge drum contents, estimated by Butcher (1989), from Clements and Kudera's (1985) data, were used to define the total weight of the sludge. These values were 170 kg for uncemented inorganic sludge, with an estimated solid density of 1330 kg/m³ and 188 kg with an estimated solid density of 1480 kg/m³ for uncemented organic sludge. For comparison, the mixture of water, quartz sand, and Portland cement for the tests used to simulate sludge in this investigation was estimated to have a no-void density of 2200 kg/m³. The sand-cement mixture was relatively unsaturated, however, and addition of water could have easily reduced its no-void density to the order of the densities computed for the Clements and Kudera results.

For an estimate of the total weight of sludges, the assumption was made that an average drum of sludge weighs approximately 180 kg. To obtain the number of equivalent drums of sludge-like material, the volumes of adsorbed liquids and sludges, concreted or cemented sludges, and dirt, gravel or asphalt categories, listed in Table 4-1, were added together. This sum, 23,700 m³ was divided by 0.21 m³, the volume of an average 55-gallon drum, and the result multiplied by 180 kg to arrive at 20,300,000 kg for the total weight of sludge.

4.2.4 CONTAINER MATERIALS

The total weights of the steel in the containers, the plastic liners, and the wood/plywood boxes were determined by Drez to be 11,000,000 kg of steel containers, 1,550,000 kg of polyethylene rigid liners, 1,490,000 kg of fiberboard liners or wood/plywood boxes, and 310,000 kg of PVC liners and bags.

4.2.5 INVENTORY DISCREPANCIES

Discrepancies in the inventory data are best illustrated by using the weights and volumes given in Table 4-1 (257,000 equivalent drums assumed), and assuming a drum volume of 0.21 m^3 , to determine that the weight of an average drum of metal and glass combustible waste is 55.2 kg. Of this amount, the drum itself weighs about 29 kg, with the remaining 26 kg, or approximately 60 lb the weight of the contents. The computed value of 26 kg appears far too low, when compared with the average weight of the contents of INEL metallic waste drums of 64.5 kg (142 lb), estimated by Butcher (1989), even when the additional weight of a liner (approximately 8 kg) is added to the weight of the waste. The computed value for the contents of combustible waste drums, using the data in Table 4-1, would also be 26 kg, versus 40 kg from the INEL survey. There is also no information from Drez's study for determining the average weight of sludge in a typical 55-gallon drum.

The differences in the weights of single drums of metallic waste obtained, computed from the results in Table 4-1 suggest that either the estimated volumes are too large by a factor of 2 or the weights are too small by a factor of 2 in Table 4-1. Attempts to reconcile such inconsistency are likely to be even more difficult in the future as waste volumes are constantly being revised downward because of greater utilization of pre- or supercompaction without being specific about how the weight of the waste will change.

Other methods of estimating the inventory of nonradioactive materials in the waste have been explored (Appendix A), because the inventory data is not consistent. The conclusion of this study is that the best current estimate is that 0.28 by weight of the inventory will be metallic waste, that the weight fraction of combustible waste will be 0.28, and the weight fraction of sludges will be 0.44. The initial porosity of the waste in the repository will be 0.79, its average theoretical solid density will be 2000 kg/m^3 , and the average initial density will be 426 kg/m^3 .

4.3 Repository Curves for Axial Drum Compaction

For axial compaction, the average compaction curve for the repository is estimated using the predicted compaction curves for the three major types of waste. These curves differ slightly from the experimental drum collapse curves and include the corrections for creep. The method of estimation was as follows: (1) For a given value of the compaction stress, the density of each category of waste was obtained; (2) the assumption was made that the weight fraction of combustible waste was 0.28, the weight fraction of

metallic waste was 0.28, and the weight fraction of sludge was 0.44 (c.f. Table 4-1 and Appendix A). Using the simple mixture rule (Sections 2.3.2 and 2.3.4), the average compacted density and the average solid density of the waste in the repository were then estimated in a similar manner, assuming average solid densities of 3440 kg/m³ for metallic waste,¹ 1310 kg/m³ for combustibles, and 2370 kg/m³ for sludges (cf. Appendix I). (3) The porosity was then computed from quantity $(1 - \rho/\rho_S)$, where ρ is the compacted density at the given stress, and ρ_S is the solid density. Results are given in Figure 4-1. The initial density of the waste, derived in Appendix A, is 426 kg/m³, corresponding to a porosity of 0.787.²

The following extrapolations of the density curves for combustible and metallic waste were used to extend the respective curves in Figure 4-1 beyond lithostatic pressure (14.8 MPa):

$$\text{Combustibles: } \sigma = 0.392 \exp(0.001876 \rho), \quad \sigma > 13.8 \text{ MPa.}$$

$$\text{Metallic: } \sigma = 0.00867 \rho - 13.55, \quad \sigma > 13.8 \text{ MPa.}$$

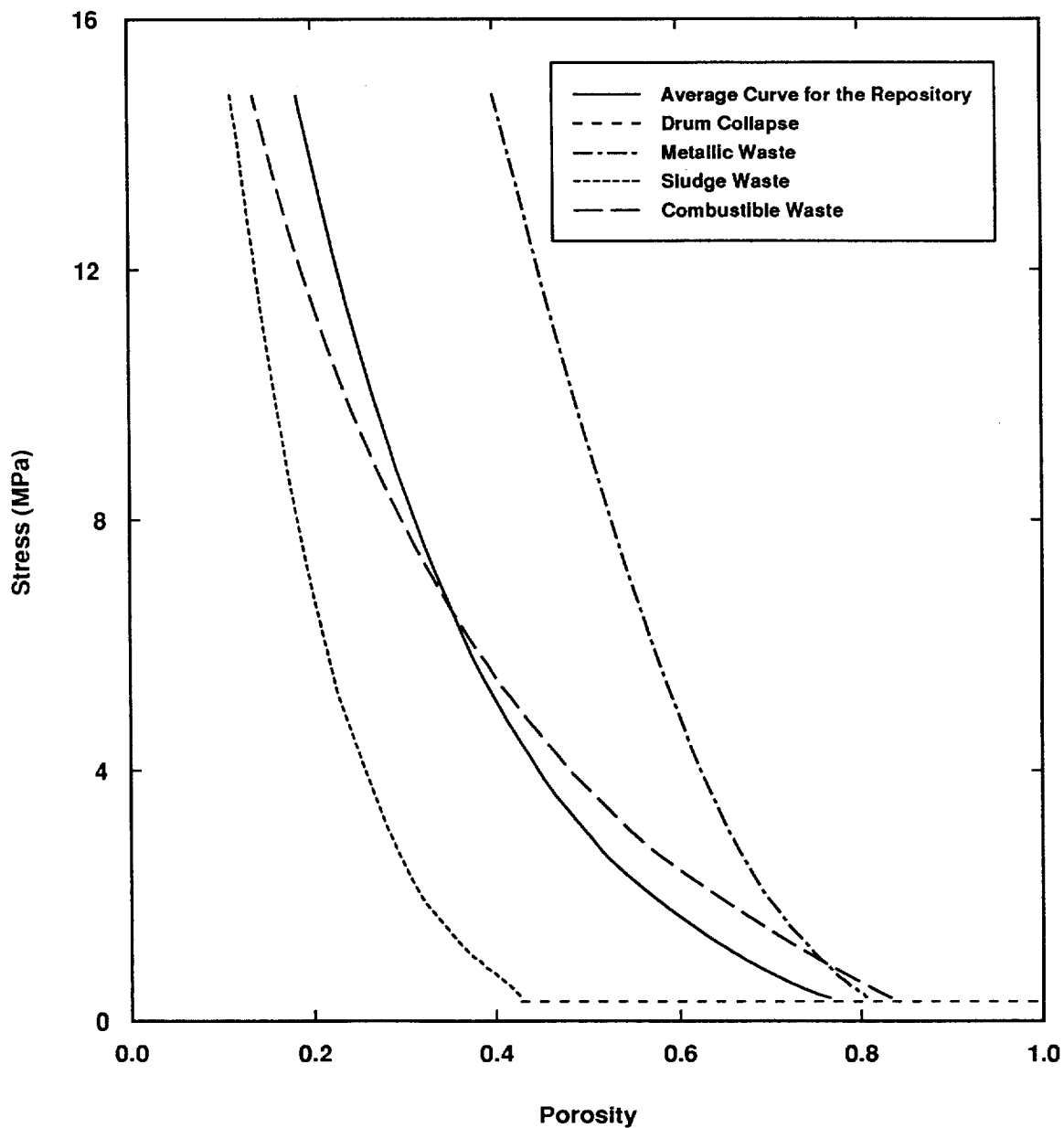
$$\text{Sludge: } \sigma = 0.0379 \rho - 61.0, \quad \sigma > 13.8 \text{ MPa.}$$

While curve fitting of the data below these stress limits with simple functions did not provide a sufficient correlation to warrant their use for the individual components of waste, the average curve for the repository is approximately represented by:

$$\sigma = 31.6772 - 118.511\eta + 161.808\eta^2 - 79.227\eta^3, \quad \sigma < 13.8 \text{ MPa,}$$

where σ is the stress in MPa and η is the porosity. The results, shown in Figure 4-1 and Table 3-2, indicate that the average drum would collapse to a minimum porosity of about 0.186.

-
1. For combustible waste, we assume 0.08 weight fraction metal with a solid density of 7110 kg/m³, 0.52 plastics with a solid density of 1200 kg/m³, 0.32 cellulose with a solid density of 1100 kg/m³, and 0.08 sorbents with a grain density of 3000 kg/m³. For metal waste, we assume a composition (waste + drums) of 0.75 weight fraction metal, 0.18 weight fraction plastics, 0.02 weight fraction cellulose, and 0.05 weight fraction sorbents (Portland cement). For sludge, we assume 0.134 weight fraction metals, 0.048 plastics, 0.058 sorbents, and 0.76 sludges. The sludge is assumed to have a solid density of 2200 kg/m³.
 2. Although the quality of the data does not warrant it, three significant figures are retained here to assure compatibility with an empirical fit of the repository consolidation curve defined below.



TRI-6345-44-0

Figure 4-1. A comparison between the predicted compaction curve for all the waste in the WIPP repository and the recommended compaction curves for combustible, metallic, and simulated sludge wastes.

Finally, it is useful to compare the results for axial compaction of combustible and metallic waste in Table 3-2 with the assumptions for the final mechanical state of a typical disposal room made for analyses supporting the Draft Supplemental Environmental Impact Statement (DSEIS) (Lappin et al., 1989). The DSEIS assumptions were made prior to the availability of any test data. In the DSEIS analyses, the assumption was made that combustible waste would compact to a porosity of 0.1 or less. The results of this investigation predict a final porosity of 0.137 at 14.8 MPa (Table 3-2):

For metallic waste, a porosity of 0.4 was assumed for the DSEIS analyses. The results of this investigation suggest that metallic waste will compact to the DSEIS porosity estimate of 0.4. For sludge, a porosity of 0.1 was assumed for the DSEIS, and the results of this investigation suggest that sludge waste will compact to 0.113 porosity. However, the assumptions of this last porosity were similar to the DSEIS assumptions; therefore, little difference should be expected between the two values.

4.4 Repository Curves for Lateral Compaction of the Waste

4.4.1 THE INFLUENCE OF SHEAR STRESS ON COMPACTION

All of the information up to this point in the report has been concerned with the axial stress that must be applied to achieve a given state of compaction. The axial stress is defined as the stress along the axis of symmetry of a drum. The axial representations were necessary because the simulated wastes were too heterogeneous to permit direct measurement of lateral stresses during testing and because of the impossibility of making such measurements during drum collapse. Limiting results to a one-dimensional description, was justified, therefore, because either the waste was contained in a rigid die and could not expand, or that little lateral expansion of the drums occurred during collapse. Shear stresses within the waste during drum collapse were believed to be small, because otherwise the outward lateral stresses exerted by the wastes against the walls of the drums would have exceeded the yield stress of the drums, expanding them outward during the tests. The exception was that the shear stresses in the simulated sludge material were sufficient to burst the drums.

Nevertheless, although the assumption that shear stresses could be ignored was convenient for data representation, the magnitude of shear stress that when exceeded will produce plastic deformation is one of the parameters that must be specified for a general mechanical description of the waste. Further, since measurement of shear stresses did not appear feasible, the

alternative that was selected was to use computational means to determine how sensitive the results of closure analysis would be to various assumptions about the deviatoric (shear) behavior of the waste.

To illustrate the approach further, assume that a cylinder of waste with a yield stress Y is loaded axisymmetrically, under stresses σ_z , $\sigma_r = \sigma_\theta$, with $\sigma_z > \sigma_r$ the axial stress, and that it is plastically deforming. For this state of stress, the mean stress, p , that is considered to have the same magnitude as the hydrostatic pressure, is:

$$p = (\sigma_z + 2\sigma_r)/3,$$

and the yield point is the difference between the axial and lateral stress:

$$\text{Yield point } Y = \sigma_z - \sigma_r.$$

Therefore:

$$\sigma_z = p + 2/3*Y,$$

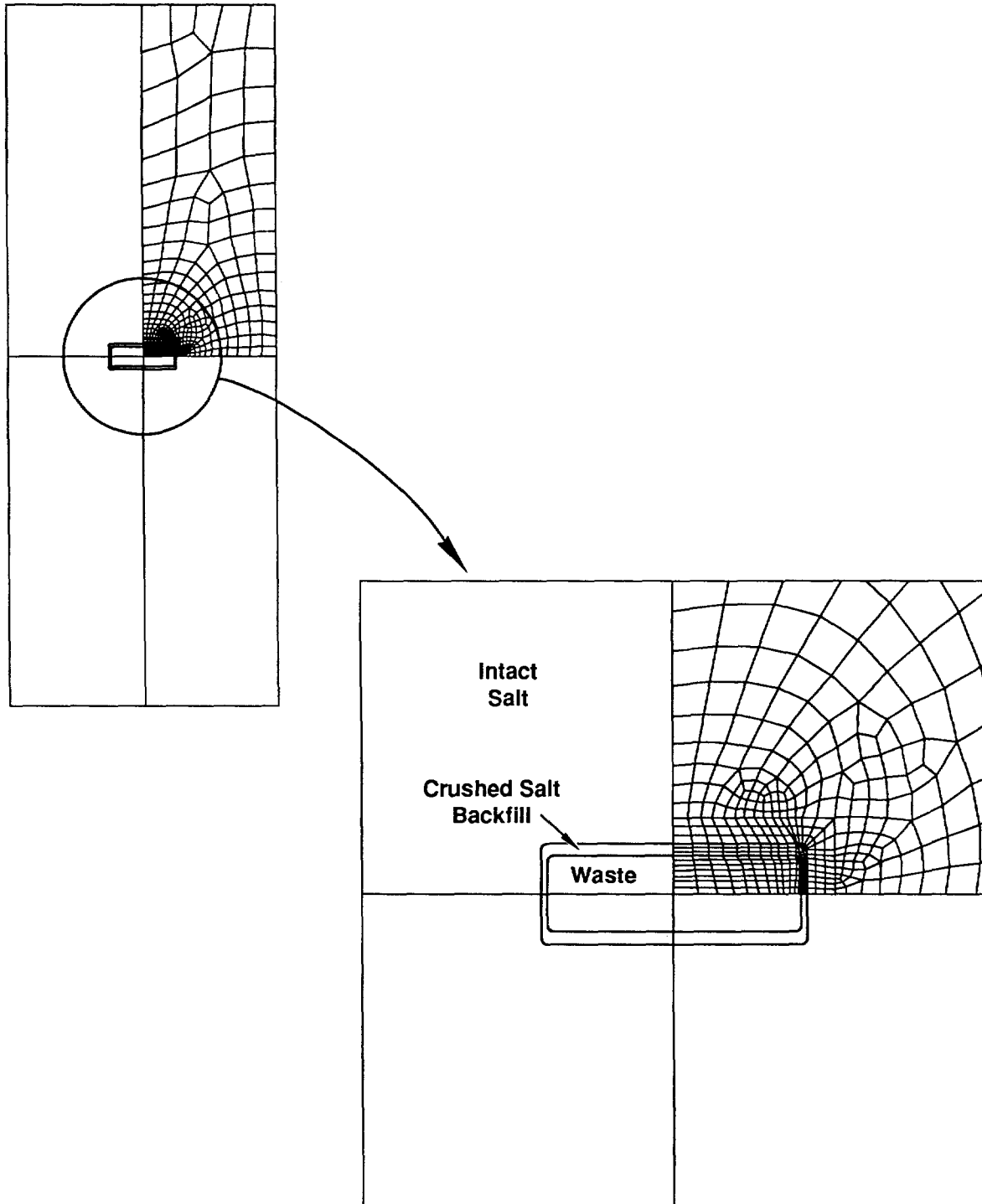
$$\sigma_r = p - Y/3,$$

and the extremes of possible experimental drum response are:

- 1) If $\sigma_r = 0$; then $p = Y/3 = \sigma_z/3$; $Y = \sigma_z$,
- 2) If $\sigma_r = \sigma_z$; then $p = \sigma_z$; $Y = 0$.

4.4.2 CLOSURE OF A ROOM ENTIRELY FILLED WITH WASTE AND SALT/BENTONITE BACKFILL

This reasoning must now be implemented in a full-fledged numerical closure calculation. The room configuration selected for the calculations was approximately the same as the design configuration of a typical disposal room with the exceptions that a 0.61 m (2 ft) air gap at the top of the room was omitted, since its presence occasionally caused numerical stability problems. This omission is not likely to influence the results greatly because it simply implies that contact of the waste with the surrounding salt begins immediately, rather than after the short time predicted for closure of the 0.61 m (2 ft) gap. Gap closure is estimated to occur within less than ten years. Another major assumption was that the room was symmetric with regard to both its vertical center line and its horizontal center line (Figure 4-2). The calculation has the vertical symmetry plane common to these problems, but use of a horizontal symmetry plane differs from past investigations. The assumption of horizontal symmetry greatly reduces



TRI-6346-114-2

Figure 4-2. Plane strain-finite element model of a TRU storage room.

computer run time, and it is a close enough approximation of the actual configuration to justify its use.

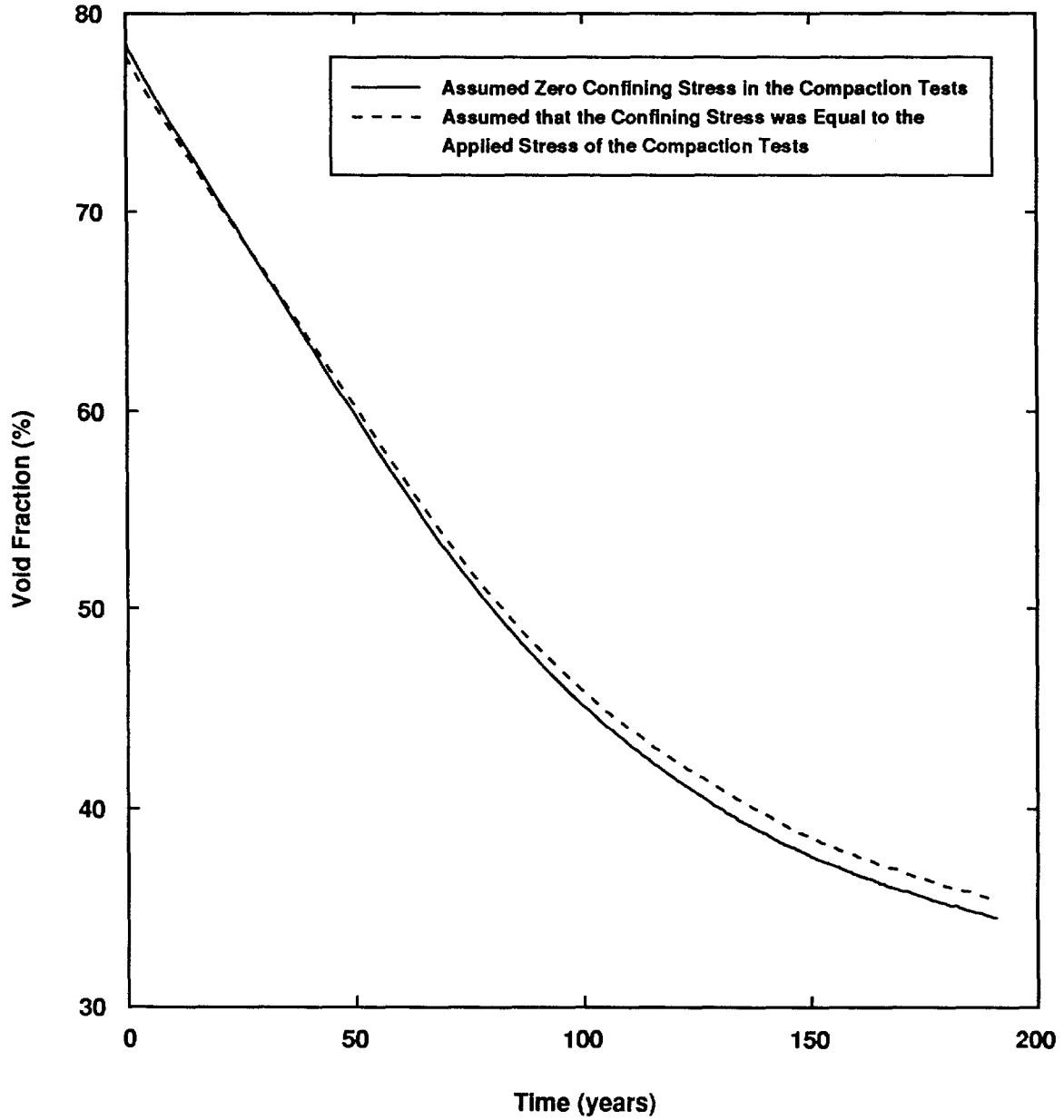
The calculations were estimates of the closure of a room filled with TRU waste and salt/bentonite backfill, using the finite-element, finite strain code SANCHO (Stone et al., 1985). Salt/bentonite backfill was selected because closure times predicted for its consolidation are longer than those for pure crushed salt backfill; therefore, variations caused by different assumptions about the shear stress in the waste would be more apparent.

Two compaction models were considered: (1) a model based on the assumption that the confining stress during laboratory compaction tests on the various waste types was zero ($\sigma_r = 0$), and (2) a model based on the assumption that the confining stress in the compaction tests was equal to the applied stress ($\sigma_r = \sigma_z$). These assumptions represent the bounds of waste response as reflected by the magnitudes of the shear stresses that might be generated during consolidation. Assumption (1) represents a material that can support large shearing stresses, and assumption (2) represents a more fluid-like response, with essential no shear stresses developing during consolidation.

The results of the calculations, in Figure 4-3, show little difference between the closure history computed using a maximum possible value for the shear stress in the waste and the history for fluid-like response (the shear stress in this calculation was simply made very small) (Weatherby, personal communication 1991). Void fraction is plotted in this figure because, being equivalent to porosity (as discussed further in Footnote 2) it is the parameter most closely related to the permeability of the room contents. The conclusion from these results is that the closure histories are not very sensitive to the exact value of shear stress selected for the waste; therefore, a precise definition of this parameter is not needed. This observation also supports the original hypothesis of this investigation that a one-dimensional description would prove beneficial in describing waste compaction.

4.4.3 LATERAL COMPACTION OF DRUMS

In reality, lateral compaction curves for the waste are expected to lie somewhere between the limits of $Y = \sigma_z$, and $Y = 0$, defined in Section 4.4.1. Further, in the sense that (1) axial drum compaction also does not appear to be sensitive to the details of how the drums collapse; and (2) lateral drum collapse is expected to exhibit even less buckling than axial collapse, the exact way that the drums collapse laterally is expected to have little effect on compaction of the waste. Some secondary effects will exist at the ends of the drums because of buckling of the lids, but the creation of collapse



TRI-6345-45-0

Figure 4-3. Predicted average void fraction-time history for waste in a room filled with TRU waste and 70% salt/30% bentonite backfill.

rings, such as those observed in the axial drum collapse tests, are considered unlikely. In the absence of information about the magnitude of the shear stresses within the waste, but with the likelihood that they will be small, the recommendation is made that shear stresses be neglected.

The reader is cautioned, however, that predictions of how drums collapse laterally within the repository are not nearly as straight forward as for axial collapse. In the axial collapse mode, lateral expansion of the drums is minimal and little or no intrusion into spaces between drums occurs. On the other hand, lateral collapse of the drums is likely to involve considerable alteration of their shapes, depending upon where they are located within the room, and the extent of this shape change will depend upon the nature of the material between them. However, refinement of models to account for this type of detail during consolidation would cause changes in how the waste initially consolidates, but probably not have much effect on the final end point (at lithostatic pressure). Such analyses are presently beyond the capabilities of numerical closure analyses, and it is not clear whether such detail, even if it could be incorporated in the codes, would have much additional impact on performance assessment.

5.0 SUMMARY

The objective of this investigation was to construct a TRU waste compaction model for use in numerical calculations of how the disposal rooms close with time. This model is used to estimate backstress developed within the waste as it compacts so that their effect on closure rates and the final state of the waste can be estimated.

The first step in model construction was to determine compaction curves for various materials characteristic of the components of the combustible, metallic, and sludge TRU waste categories. Since most TRU waste categories contain more than one of these materials, a mixing rule based upon the weight fraction of each component was constructed for each of three waste categories. For example, combustible waste contains cellulose, plastics, and lesser amounts of metals and sorbents. The curves for each of these components were then used to construct a compaction curve for combustible, metallic, and sludge waste categories, as described in Section 2.

Tests that axially compacted full-sized 55-gallon drums of simulated combustible, metallic and sludge waste were the next step in the investigation. These test results served to provide: (1) data that can be directly applied to room consolidation, and (2) a check of the use of the properties of individual waste components in a given waste category (obtained in Section 2.0) to predict drum compaction curves. Prediction of axial drum compaction from individual material compaction curves considered the buckling response of the drums. Container buckling caused rings of steel to form around the waste that carried part of the load applied to the drums, but this mode of collapse appeared to have little influence on consolidation of the waste. Test results for axial drum collapse were described in Section 3. Lateral compaction of the drums was not feasible because of insufficient testing machine capacity.

Recommended compaction curves for combustible, metallic, and sludge wastes, and a curve that represents the averaged waste inventory of the entire repository was derived in Section 4. A critical part of this section was the examination reconciliation of contradictory data from various published projections of the amount of waste to be stored at the WIPP. Repository curves for axial and lateral drum compaction were recommended. The results for axial compaction of combustible and metallic waste were also found to be quite consistent with the assumptions for the final mechanical state of a typical disposal room, as initially assumed as supporting information for the DSEIS for the WIPP.

For the present, the most detailed model of drum collapse that can be applied to numerical closure analyses is a hydrostatic model of mechanical response. Estimation of closure histories of a room filled with waste and salt/bentonite backfill was used to imply that the hydrostatic description is an acceptable approximation, whether or not consolidation is occurring laterally or vertically. Actual directions of consolidation depend upon the location of the waste the disposal room. Refinements of the model to a more general form, that involves both hydrostatic and deviatoric (shear) stresses is necessary to confirm understanding of room closure, but they may not cause enough change in closure times to impact performance assessment.

6.0 REFERENCES

- Butcher, B.M. 1989. *Waste Isolation Pilot Plant Simulated Waste Compositions and Mechanical Properties*. SAND89-0372. Albuquerque, NM: Sandia National Laboratories.
- Clements, T.L. Jr. and D.E. Kudera. 1985. "TRU Waste Sampling Program: Volume 1 -- Waste Characterization." EGG report EGG-WM-6503-Vol.1.
- DOE/RW-0006, Rev 4. 1988. "Integrated Data Base for 1988: Spent Fuel and Radioactive Waste Inventories, Projections, and Characteristics." Oak Ridge, TN: Oak Ridge National Laboratory.
- Drez, P.E. and P. James-Lipponer. 1989. "Examination of Preliminary Nonradioactive Inventory for CH-TRU Waste." Albuquerque, NM: International Technology Corporation.
- Holcomb, D.J. and M. Shields. 1987. *Hydrostatic Creep Consolidation of Crushed Salt With Added Water*. SAND87-1990. Albuquerque NM: Sandia National Laboratories.
- Huerta, M., G.H. Lamoreaux, L.E. Romesberg, H.R. Yoshimura, B.J. Joseph, and R.A. May. 1983. *Analysis, Scale Modeling and Full-Scale Tests of Low-Level Nuclear Waste Drum Response to Accident Environments*. SAND80-2517. Albuquerque, NM: Sandia National Laboratories.
- Lappin, A.R. and R.L. Hunter, eds. 1989. *Systems Analysis, Long-Term Radionuclide Transport, and Dose Assessments, Waste Isolation Pilot Plant (WIPP), Southeastern New Mexico, March 1989*. SAND89-0462. Albuquerque, NM: Sandia National Laboratories.
- Sjaardema, G.D. and R.D. Krieg. 1987. *A Constitutive Model for the Consolidation of WIPP Crushed Salt and Its Use in Analyses of Backfilled Shaft and Drift Configurations*. SAND87-1977. Albuquerque, NM: Sandia National Laboratories.
- Stone, C.M., R.D. Krieg, and Z.E. Beisinger. 1985. *SANCHO, A Finite Element Computer Program for the Quasistatic, Large Deformation, Inelastic Response of Two-Dimensional Solids*. SAND84-2618. Albuquerque, NM: Sandia National Laboratories.

**APPENDIX A:
THE AVERAGE INITIAL DENSITY OF WASTE IN THE REPOSITORY**

Estimation of the initial density of waste in the repository is necessary for room closure calculations.

Method 1:

The initial density of the waste was computed from the information in Table 4-1. The total weight of the waste is 51,700,000 kg and its estimated volume is 134,800 m³, for an initial density of 384 kg/m³. The initial porosity of the waste was estimated using weight fractions 0.28 for metals and glass, 0.28 for combustibles, and 0.44 for sludges, and values of 3440 kg/m³, 1310 kg/m³ and 2150 kg/m³ for the average solid densities of the metallic, combustible, and sludge wastes. The average solid density was 2001 kg/m³ (Section 2.3.2) and the initial porosity is $(1 - 384/2001)$ or 0.81.

Method 1A:

Alternate method 1A uses the same information, but computes the initial porosity ignoring the containers, since better agreement of the drum test results with predicted drum collapse response was obtained when the containers were not included in the computations. The total weight of the waste is 40,700,000 kg and its estimated volume is 132,500 m³, for an initial density of 307 kg/m³. The average solid density was 2018 kg/m³, and the initial porosity is 0.85.

Method 2:

Alternate method 2 is based on the assumption that the volume estimates for the waste given in Table 4-1 are more accurate than estimates of the waste. Assume that each drum will contain 0.21 m³. The equivalent number of drums of metallic waste would be 257,000 drums; the drums of combustible waste would be 264,000 drums. The number of drums of sludge was already estimated in this manner (Section 4.2.3 of this report), their volume and weight remain unchanged at 25,400 m³ and 23,030,000 kg.

This information was then used to estimate the total weight of each waste component, assuming the results of Butcher's (1989) analysis of Clements and Kudera's (1985) waste inventory data for waste stored at Idaho National Engineering Laboratory and the Los Alamos National Laboratory was typical of other generator sites. This study showed that, on the average, the weight of metallic waste and container material, per drum, was 101 kg, or 26,000,000 kg for the repository, and the weight of combustible waste and container material, per drum, was 77 kg, or 20,300,000 kg for the repository. The initial density of this waste was computed to be 514 kg/m³, the average solid density was 2060 kg/m³, and the initial porosity is $(1 - 514/2060)$ or 0.75.

Method 2A:

This method is the same as method 2, but neglecting the container material. Without the container material, the weight of metallic waste per drum was 72 kg, or 18,500,000 kg for the repository, and the weight of combustible waste per drum, was 48 kg, or 12,700,000 kg for the repository. The initial density of this waste was computed to be 382 kg/m³, the average solid density was 2104 kg/m³, and the initial porosity is 0.82.

Method 3:

The inventory used for calculations in support of the Draft Supplemental Environmental Impact Study assumed a storage capacity of 556,000 equivalent drums in the repository (Lappin et al., 1989). An average drum of metallic waste was assumed to contain 14.6 kg of metallic waste, and the drum weighed approximately 29 kg. The estimate for cellulose in a drum was 8.02 kg (not including rubber); no estimate was made for plastics. The Drez and James-Lipponer (1989) estimate for "plastics and others," including rubber, in the repository was 4,240,000 kg, but may not have included liners, which would represent another 1,550,000 kg (Table 4-1). On this basis, using 0.21 m³ for the volume of an individual drum, total volume of waste in the repository would be 117,000 m³, and the weight of the individual waste components would be:

	Weight/drum	Total Weight kg	Weight Fraction
Metals and glass waste	14.6 kg/drum	8,120,000	
Drums	29.2 kg/drum	16,200,000	0.44
Combustible waste	15.6 kg/drum	8,670,000	
Liners	2.8 kg/m ³	1,550,000	0.19
Sludge waste		20,300,000	0.37
		54,840,000	

The initial density of this waste was computed to be 468 kg/m³, the average solid density was 2240 kg/m³, and the initial porosity is 0.79.

Method 3A:

If the container material is ignored, then the initial density of the waste was 330 kg/m³, the average solid density was 1976 kg/m³ and the initial porosity is 0.83.

A.1.2 Discussions and Recommendation:

The results of the calculations described in the previous paragraphs and summarized in Table A.1 will be used first to discuss the role of the container material when estimating an average consolidation curve for the entire repository. On one hand, estimates of compaction curves for simulated waste drums of metallic, combustible, and sludge waste, derived from the compaction characteristics of the various waste components, were in better agreement with experimental observations when the containers were ignored. In other words, no consideration of the effect of the drum material was made in specifying the consolidation characteristics of individual 55-gallon drums of metallic, combustible, or sludge waste. Perhaps another reason for being able to ignore the drums in estimates of average properties for the entire repository is that the containers themselves are not porous and take up practically no volume.

Large inconsistencies were also encountered in specifying the waste inventory for the entire repository. As a consequence, there were several different ways of estimating the weight fractions of metallic, combustible, and sludge waste, and no consistent trend or accurate argument to support the selection of any one set of weight fractions for the average contents of the repository. Selection is on the basis of the following arguments, therefore. First, in the absence of any guidance about how to proceed, the observation is made that averages of the weight fractions of metallic waste and combustible waste calculated by methods 1A, 2A, and 3A (three independent methods) are about equal (0.28 versus 0.25). The sludge waste fraction is somewhat greater (0.47) than the metallic and combustible waste weight fractions. Average values are considered to damp out unknown errors that may be present in the individual calculations. A second observation is that, in principle, methods 1 or 1A, should eventually become the most direct methods of estimating inventories, particularly as more information becomes available. However, method 1A currently requires so many assumptions about the containers that its utility becomes questionable.

Therefore, the results from Method 1 have been chosen to represent the repository, even though the weight of the containers was mixed in with the weights of the various waste components. The reasons for this selection are that (1) the weight fractions of combustible and metallic waste were about equal and consistent with the average of the results from methods 1A, 2A, and 3A, and (2) Method 1 represents the most consistent approach to estimation of the inventory. The weight fraction of metallic waste is therefore defined as 0.28, the weight fraction of combustible waste is 0.28, and the weight fraction of sludges is 0.44. Assuming values of 3440 kg/m^3 , 1310 kg/m^3 , and

TABLE A-1. THE RESULTS FROM VARIOUS METHODS OF ESTIMATING THE INVENTORY OF NONRADIOACTIVE MATERIALS IN THE REPOSITORY

Method	Initial Density kg/m ³	Estimated Solid Density kg/m ³	Porosity	Weight Fraction		
				Metallic	Combustible	Sludge
Calculated including the container material:						
#1	384 kg/m ³	2001 kg/m ³	0.81	.28	.28	.44
#2	514	2060	0.75	.38	.29	.33
#3	<u>468</u>	<u>2240</u>	<u>0.79</u>	<u>.44</u>	<u>.19</u>	<u>.37</u>
Average	455	2100	0.78	.37	.24	.38
Calculated ignoring the container material:						
#1A	307	2018	0.85	.245	.245	.51
#2A	382	2104	0.82	.37	.25	.38
#3A	<u>330</u>	<u>1976</u>	<u>0.83</u>	<u>.21</u>	<u>.26</u>	<u>.53</u>
Average	340	2033	0.83	.28	.25	.47

2150 kg/m³ for the average solid densities of the metallic, combustible, and sludge wastes, and the theoretical solid density of the waste in the repository becomes 2000 kg/m³.

Definition of the initial porosity of the waste in the repository requires some additional discussion. According to Table A.1, the average porosity for the waste in the repository estimated by different methods ranges from 0.85 to 0.75. For consistency, the porosity obtained by Method 1, or 0.81, should probably be used. However, use of the zero intercept, 0.787, of the analytic fit of the average compaction curve for the repository (Section 4.3 of this report) simplifies calculations considerably because a single smooth curve then represents waste consolidation (the elastic limit for drum collapse is ignored). The value of 0.787 is also close enough in magnitude to 0.81 to argue that the uncertainties are such that, in the absence of additional information, it would be impossible to distinguish which of the two values are more representative of the waste. A value of 0.79 is assumed, therefore, and since the solid density of the waste is 2000 kg/m³, an initial density 426 kg/m³ should be used.

Appendix A: The Average Initial Density of Waste in the Repository

DISTRIBUTION

FEDERAL AGENCIES

U. S. Department of Energy, (5)
Office of Civilian Radioactive Waste
Management

Attn: Deputy Director, RW-2
Associate Director, RW-10
Office of Program
Administration and
Resources Management
Associate Director, RW-20
Office of Facilities
Siting and Development
Associate Director, RW-30
Office of Systems
Integration and
Regulations
Associate Director, RW-40
Office of External
Relations and Policy

Forrestal Building
Washington, DC 20585

U. S. Department of Energy (3)
Albuquerque Operations Office
Attn: J. E. Bickel
R. Marquez, Director
Public Relations Division
P.O. Box 5400
Albuquerque, NM 87185-5400

U. S. Department of Energy
Attn: National Atomic Museum Library
Albuquerque Operations Office
P.O. Box 5400
Albuquerque, NM 87185

U. S. Department of Energy (4)
WIPP Project Office (Carlsbad)
Attn: Vernon Daub
J. E. Carr
D. C. Blackstone
R. Batra
J. A. Mewhinney

P.O. Box 3090
Carlsbad, NM 88221-3090

U. S. Department of Energy
Research & Waste Management Division
Attn: Director
P.O. Box E
Oak Ridge, TN 37831

U. S. Department of Energy
Waste Management Division
Attn: R. F. Guercia
P.O. Box 550
Richland, WA 99352

U. S. Department of Energy (1)
Attn: Edward Young
Room E-178
GAO/RCED/GTN
Washington, DC 20545

U. S. Department of Energy (6)
Office of Environmental Restoration
and Waste Management
Attn: Jill E. Lytle, EM-30
Mark Frei, EM-34(3)
Mark Duff, EM-34
Clyde Frank, EM-50
Washington, DC 20585

U.S. Department of Energy (3)
Office of Environment, Safety and
Health
Attn: Ray Pelletier, EH-231
Kathleen Taimi, EH-232
Carol Borgstrom, EH-25
Washington, DC 20585

U. S. Department of Energy (2)
Idaho Operations Office
Fuel Processing and Waste
Management Division
785 DOE Place
Idaho Falls, ID 83402

U.S. Department of Energy
Savannah River Operations Office
Defense Waste Processing
Facility Project Office
Attn: W. D. Pearson
P.O. Box A
Aiken, SC 29802

U.S. Environmental Protection
Agency (2)
Attn: Ray Clark
Office of Radiation Protection
Programs (ANR-460)
Washington, D.C. 20460

U.S. Geological Survey
Branch of Regional Geology
Attn: R. Snyder
MS913, Box 25046
Denver Federal Center
Denver, CO 80225

U.S. Geological Survey
Conservation Division
Attn: W. Melton
P.O. Box 1857
Roswell, NM 88201

U.S. Geological Survey (2)
Water Resources Division
Attn: Kathy Peter
Suite 200
4501 Indian School, NE
Albuquerque, NM 87110

U. S. Nuclear Regulatory Commission
(4)
Attn: Joseph Bunting, HLEN 4H3 OWFN
Ron Ballard, HLGP 4H3 OWFN
Jacob Philip
NRC Library
Mail Stop 623SS
Washington, DC 20555

BOARDS

Defense Nuclear Facilities Safety
Board
Attn: Dermot Winters
600 E. Street NW
Suite 675
Washington, DC 20004

U.S. Department of Energy
Advisory Committee on Nuclear
Facility Safety
Attn: Merritt E. Langston, AC21
Washington, DC 20585

Nuclear Waste Technical Review Board
(2)
Attn: Don Deere
Dr. Sidney J. S. Parry
Suite 910
1100 Wilson Blvd.
Arlington, VA 22209-2297

Nuclear Regulatory Commission
Advisory Committee on Nuclear Waste
Attn: Richard Major
7920 Norfolk Avenue
Bethesda, MD 20814

STATE AGENCIES

Environmental Evaluation Group (3)
Attn: Library
Suite F-2
7007 Wyoming Blvd., N.E.
Albuquerque, NM 87109

New Mexico Bureau of Mines
and Mineral Resources (2)
Attn: F. E. Kottlowski, Director
J. Hawley
Socorro, NM 87801

New Mexico Department of Energy
and Minerals
Attn: Librarian
2040 S. Pacheco
Santa Fe, NM 87505

New Mexico Environmental Improvement
Division
Attn: Deputy Director
1190 St. Francis Drive
Santa Fe, NM 87503

LABORATORIES/CORPORATIONS

Battelle Pacific Northwest
Laboratories (6)
Attn: D. J. Bradley, K6-24
J. Relyea, H4-54
R. E. Westerman, P8-37
H. C. Burkholder, P7-41
L. Pederson, K6-47

Battelle Boulevard
Richland, WA 99352

Savannah River Laboratory (6)
Attn: N. Bibler
E. L. Albenisius
M. J. Plodinec
G. G. Wicks
C. Jantzen
J. A. Stone
Aiken, SC 29801

SAIC
Attn: George Dymmel
101 Convention Center Dr.
Las Vegas, NV 89109

INTERA Technologies, Inc. (4)
Attn: G. E. Grisak
J. F. Pickens
A. Haug
A. M. LaVenue
Suite #300
6850 Austin Center Blvd.
Austin, TX 78731

INTERA Technologies, Inc.
Attn: Wayne Stensrud
P.O. Box 2123
Carlsbad, NM 88221

IT Corporation (4)
Attn: M. Abashian
R. F. McKinney
J. Myers
J. Valdez
D. Vetter
Regional Office - Suite 700
5301 Central Avenue, NE
Albuquerque, NM 87108

Science Applications International
Corp. (12)
Attn: T. William Thompson (10)
R. G. Van Buskirk
N. C. Patti
14062 Denver West Parkway
Suite 255
Golden, CO 80401

IT Corporation (2)
Attn: D. E. Deal
P.O. Box 2078
Carlsbad, NM 88221

Arthur D. Little, Inc.
Attn: Charles R. Hadlock
Acorn Park
Cambridge, MA 02140-2390

Los Alamos National Laboratory
Attn: B. Erdal, CNC-11
P.O. Box 1663
Los Alamos, NM 87544

RE/SPEC, Inc. (2)
Attn: W. Coons
P. F. Gnirk
Suite 300
4775 Indian School Rd., NE
Albuquerque NM 87110-3927

RE/SPEC, Inc. (7)
Attn: L. L. Van Sambeek
G. Callahan
T. Pfeifle
J. L. Ratigan
P.O. Box 725
Rapid City, SD 57709

Center for Nuclear Waste
Regulatory Analysis (4)
Attn: P.K. Nair
Southwest Research Institute
6220 Culebra Road
San Antonio, TX 78228-0510

Science Applications International
Corporation
Attn: Howard R. Pratt,
Senior Vice President
10260 Campus Point Drive
San Diego, CA 92121

Science Applications International
Corporation
Attn: Michael B. Gross
Ass't. Vice President
Suite 1250
160 Spear Street
San Francisco, CA 94105

Systems, Science, and Software (2)
Attn: E. Peterson
Box 1620
La Jolla, CA 92038

Westinghouse Electric Corporation (7)
Attn: Library
L. Trego
W. P. Poirer
W. R. Chiquelin
V. F. Likar
D. J. Moak
R. F. Kehrman
P.O. Box 2078
Carlsbad, NM 88221

Weston Corporation
Attn: David Lechel
Suite 1000
5301 Central Avenue, NE
Albuquerque, NM 87108

UNIVERSITIES

University of Arizona
Attn: J. G. McCray
Department of Nuclear Engineering
Tucson, AZ 85721

University of New Mexico (2)
Geology Department
Attn: D. G. Brookins
Library
Albuquerque, NM 87131

Pennsylvania State University
Materials Research Laboratory
Attn: Della Roy
University Park, PA 16802

Texas A&M University
Center of Tectonophysics
College Station, TX 77840

G. Ross Heath
College of Ocean
and Fishery Sciences
583 Henderson Hall
University of Washington
Seattle, WA 98195

INDIVIDUALS

Dennis W. Powers
Star Route Box 87
Anthony, TX 79821

LIBRARIES

Thomas Brannigan Library
Attn: Don Dresp, Head Librarian
106 W. Hadley St.
Las Cruces, NM 88001

Hobbs Public Library
Attn: Ms. Marcia Lewis, Librarian
509 N. Ship Street
Hobbs, NM 88248

New Mexico State Library
Attn: Ingrid Vollenhofer
P.O. Box 1629
Santa Fe, NM 87503

New Mexico Tech
Martin Speere Memorial Library
Campus Street
Socorro, NM 87810

New Mexico Junior College
Pannell Library
Attn: Ruth Hill
Lovington Highway
Hobbs, NM 88240

WIPP Public Reading Room
Attn: Director
Carlsbad Public Library
101 S. Halagueno St.
Carlsbad, NM 88220

Government Publications Department
General Library
University of New Mexico
Albuquerque, NM 87131

THE SECRETARY'S BLUE RIBBON PANEL ON WIPP

Dr. Thomas Bahr
New Mexico Water Resources Research
Institute
New Mexico State University
Box 3167
Las Cruces, NM 88003-3167

Mr. Leonard Slosky
Slosky & Associates
Suite 1400
Bank Western Tower
1675 Tower
Denver, CO 80202

Mr. Newal Squyres
Holland & Hart
P.O. Box 2527
Boise, ID 83701

Dr. Arthur Kubo
Vice President
BDM International, Inc.
7915 Jones Branch Drive
McLean, VA 22102

Mr. Robert Bishop
Nuclear Management Resources Council
Suite 300
1776 I Street, NW
Washington, DC 20006-2496

**NATIONAL ACADEMY OF SCIENCES, WIPP
PANEL**

Charles Fairhurst, Chairman
Department of Civil and
Mineral Engineering
University of Minnesota
500 Pillsbury Dr. SE
Minneapolis, MN 55455

Dr. John O. Blomeke
Route 3
Sandy Shore Drive
Lenoir City, TN 37771

Dr. John D. Bredehoeft
Western Region Hydrologist
Water Resources Division
U.S. Geological Survey (M/S 439)
345 Middlefield Road
Menlo Park, CA 94025

Dr. Karl P. Cohen
928 N. California Avenue
Palo Alto, CA 94303

Dr. Fred M. Ernsberger
250 Old Mill Road
Pittsburgh, PA 15238

Dr. Rodney C. Ewing
Department of Geology
University of New Mexico
200 Yale, NE
Albuquerque, NM 87131

B. John Garrick
Pickard, Lowe & Garrick, Inc.
2260 University Drive
Newport Beach, CA 92660

John W. Healy
51 Grand Canyon Drive
Los Alamos, NMM 87544

Leonard F. Konikow
U.S. Geological Survey
431 National Center
Reston, VA 22092

Jeremiah O'Driscoll
505 Valley Hill Drive
Atlanta, GA 30350

Dr. D'Arcy A. Shock
233 Virginia
Ponca City, OK 74601

Dr. Christopher Whipple
Clement International
Suite 1380
160 Spear St.
San Francisco, CA 94105

Dr. Peter B. Myers, Staff
Director
National Academy of Sciences
Committee on Radioactive
Waste Management
2101 Constitution Avenue
Washington, DC 20418

Dr. Geraldine Grube
Board on Radioactive
Waste Management
GF456
2101 Constitution Avenue
Washington, DC 20418

Dr. Ina Alterman
Board on Radioactive Waste
Management
GF462
2101 Constitution Avenue
Washington, DC 20418

FOREIGN ADDRESSES

Studiecentrum Voor Kernenergie
Centre D'Energie Nucleaire
Attn: A. Bonne
SCK/CEN
Boeretang 200
B-2400 Mol
BELGIUM

Atomic Energy of Canada, Ltd. (4)
Whiteshell Research Estab.
Attn: Peter Haywood
John Tait
Pinewa, Manitoba, CANADA
ROE 1LO

D. K. Mukerjee
Ontario Hydro Research Lab
800 Kipling Avenue
Toronto, Ontario, CANADA
M8Z 5S4

Mr. Francois Chenevier, Director (2)
ANDRA
Route du Panorama Robert Schumann
B.P .38
92266 Fontenay-aux-Roses Cedex
FRANCE

Mr. Jean-Pierre Olivier
OECD Nuclear Energy Agency (2)
Division of Radiation Protection
and Waste Management
38, Boulevard Suchet
75016 Paris, FRANCE

Claude Sombret
Centre D'Etudes Nucleaires
De La Vallee Rhone
CEN/VALRHO
S.D.H.A. BP 171
30205 Bagnols-sur-Ceze
FRANCE

Bundesministerium fur Forschung und
Technologie
Postfach 200 706
5300 Bonn 2
FEDERAL REPUBLIC OF GERMANY

Bundesanstalt fur Geowissenschaften
und Rohstoffe
Attn: Michael Langer
Postfach 510 153
3000 Hannover 51
FEDERAL REPUBLIC OF GERMANY

Hahn-Mietner-Institut fur
Kernforschung
Attn: Werner Lutze
Glienicke Strasse 100
100 Berlin 39
FEDERAL REPUBLIC OF GERMANY

Institut fur Tieflagerung (4)
Attn: K. Kuhn
Theodor-Heuss-Strasse 4
D-3300 Braunschweig
FEDERAL REPUBLIC OF GERMANY

Kernforschung Karlsruhe
Attn: K. D. Closs
Postfach 3640
7500 Karlsruhe
FEDERAL REPUBLIC OF GERMANY

Physikalisch-Technische Bundesanstalt
Attn: Peter Brenneke
Postfach 33 45
D-3300 Braunschweig
FEDERAL REPUBLIC OF GERMANY

D. R. Knowles
British Nuclear Fuels, plc
Risley, Warrington, Cheshire WA3 6AS
1002607 GREAT BRITAIN

Shingo Tashiro
Japan Atomic Energy Research
Institute
Tokai-Mura, Ibaraki-Ken
319-11 JAPAN

Netherlands Energy Research
Foundation ECN (2)
Attn: Tuen Deboer, Mgr.
L. H. Vons
3 Westerduinweg
P.O. Box 1
1755 ZG Petten, THE NETHERLANDS

Svensk Karnbransleforsorjning AB
Attn: Fred Karlsson
Project KBS
Karnbbranslesakerhet
Box 5864
10248 Stockholm, SWEDEN

INTERNAL

1510 J. C. Cummings
1514 H. S. Morgan
1514 J. G. Arguello
1514 J. R. Weatherby
1514 C. M. Stone
3151 Supervisor (3)
3154-1 C. L. Ward, (10) for DOE/OSTI
6000 V. L. Dugan, Acting
6232 W. A. Olsson
6232 W. R. Wawersik
6300 T. O. Hunter
6310 T. E. Blejwas, Acting
6340 W. D. Weart
6340 S. Y. Pickering
6341 R. C. Lincoln
6341 Staff (9)
6341 Sandia WIPP Central Files (10)
6342 D. R. Anderson
6342 Staff (11)
6343 T. M. Schultheis
6343 Staff (2)
6344 E. Gorham
6344 Staff (10)
6345 B. M. Butcher, Acting (15)
6345 Staff (9)
6346 J. R. Tillerson
6346 Staff (7)
8524 J. A. Wackerly (SNLL Library)
9300 J. E. Powell
9310 J. D. Plimpton
9320 M. J. Navratil
9325 L. J. Keck (2)
9330 J. D. Kennedy
9333 O. Burchett
9333 J. W. Mercer
9334 P. D. Seward